AWARD NUMBER: W81XWH-12-1-0223

TITLE: Innovative Strategies for Breast Cancer Immunotherapy

PRINCIPAL INVESTIGATOR: Feng Wang-Johanning

CONTRACTING ORGANIZATION: SRI International
Menlo Park, CA 94025

REPORT DATE: September 2014

TYPE OF REPORT: Annual Report

PREPARED FOR: U.S. Army Medical Research and Materiel Command
Fort Detrick, Maryland 21702-5012

REPORT DOCUMENTATION PAGE

Form Approved
OMB No. 0704-0188

1. REPORT DATE	2. REPORT TYPE	3. DATES COVERED
Sept 2014	Annual report	1Sep2013-31Aug2014

4. TITLE AND SUBTITLE
Innovative Strategies for Breast Cancer Immunotherapy

5a. CONTRACT NUMBER

5b. GRANT NUMBER
W81XWH-12-1-0223

5c. PROGRAM ELEMENT NUMBER

6. AUTHOR(S)
Feng Wang-Johanning, MD, PhD

E-Mail: feng.wang-johanning@sri.com and fwangjoh@gamil.com

5d. PROJECT NUMBER

5e. TASK NUMBER

5f. WORK UNIT NUMBER

7. PERFORMING ORGANIZATION NAME(S) AND ADDRESS(ES)

SRI International
Menlo Park, CA 94025-3493

8. PERFORMING ORGANIZATION REPORT NUMBER

9. SPONSORING / MONITORING AGENCY NAME(S) AND ADDRESS(ES)

U.S. Army Medical Research and Materiel Command
Fort Detrick, Maryland 21702-5012

10. SPONSOR/MONITOR'S ACRONYM(S)

11. SPONSOR/MONITOR'S REPORT NUMBER(S)

12. DISTRIBUTION / AVAILABILITY STATEMENT

Approved for Public Release; Distribution Unlimited

13. SUPPLEMENTARY NOTES

14. ABSTRACT

Antitumor effects of human endogenous retrovirus type K (HERV-K) specific short hairpin RNAs (shRNAs) were determined in vitro and in vivo. We observed expression of HERV-K in breast cancer (BC) and inhibition of BC cell proliferation and induction of apoptosis in BC cells treated with anti-HERV-K antibodies. Furthermore, significantly slower growth was observed in BC cells transfected with a shRNA targeting the HERV-K env mRNA (shRNAenv) compared with a shRNA targeting a scrambled RNA sequence (shRNAc). Significantly reduced numbers of colonies formed in soft agar when HERV-K env was knocked down in BC cell lines, compared to treatment with shRNAc, and significantly reduced tumor sizes and weights were demonstrated in mice xenografted with MDA-MB-231, MDA-MB-435.eb1, and SKBR3 BC cells stably transfected with shRNAenv, compared to cells stably transfected with a shRNAc. Downregulation of HERV-K with its targeting shRNA caused an increase of BC cells in the S phase and a corresponding decrease of cells in the G1 or G2-M. HERV-K viral RNAs were found to be involved in BC tumorigenesis via effects on not only p53 signaling pathways, but also other major signaling pathways that play critically important roles in tumorigenesis.

15. SUBJECT TERMS
Breast cancer, human endogenous retroviruses, tumor associated antigen

16. SECURITY CLASSIFICATION OF:			17. LIMITATION OF ABSTRACT	18. NUMBER OF PAGES	19a. NAME OF RESPONSIBLE PERSON
a. REPORT	b. ABSTRACT	c. THIS PAGE			USAMRMC
Unclassified	Unclassified	Unclassified	Unclassified	84	19b. TELEPHONE NUMBER *(include area code)*

Table of Contents

Page

1. Introduction: Our genome harbors many endogenous retroviral sequences and some of them may continue to perform retroviral functions that contribute to disease [1]. Genome sequencing reveals that 8% of the human genome consists of human endogenous retroviruses (HERVs) and roughly half of our DNA is made up of transposable elements that include HERVs [2-4]. The integration of HERVs into the host cell happens within the context of their replication cycle [5]. HERV type K of the HML2 subtype is the most recently integrated and most intact retrovirus in the human genome [6]. These most recently acquired proviruses of the HERV-K family can express viral proteins and produce viral particles [7, 8]. In previous studies we reported that expression of HERV-K env protein in malignant BC cells was substantially higher than in normal or nonmalignant breast cells [9-11], suggesting that HERV-K might be reactivated and implicated in carcinogenesis. Monoclonal and single-chain antibodies against the HERV-K env protein recently proved capable of blocking the proliferation of human BC cells *in vitro* and inhibiting tumor growth in mice bearing xenograft tumors [12]. In addition, we found that HERV-K env protein is capable of acting as a Tumor associate antigen (TAA), activating both T-cell and B-cell responses in BC patients [13].

2. Keywords: breast cancer (BC), human endogenous retroviruses (HERVs), and Tumor associate antigen (TAA)

3. Accomplishments: Anti-HERV-K env protein monoclonal antibodies (mAbs), including the HERV-K specific 6H5 mAb, were used to evaluate HERV-K presence in breast tumors and breast cancer (BC) cells. In addition, the antitumor effects of 6H5 or shRNA were determined *in vitro* and *in vivo*.

3.1. Correlation of HERV-K viral protein presence with breast tumorigenesis: We observed 1) expression of HERV-K in BC, which verifies our earlier finding of HERV-K expression in BC; and 2) inhibition of BC cell proliferation and induction of apoptosis in BC cells exposed to 6H5, as reported previously (*JNCI, 2012*). Furthermore, short hairpin RNAs (shRNAs) targeting HERV-K *env* mRNA have been developed in our laboratory and used 1) to knock down HERV-K expression; and 2) to correlate HERV-K viral RNA presence with breast tumorigenesis. These studies were done both *in vitro* and *in vivo*.

3.2. Downregulated HERV-K inhibited BC cell proliferation: Significantly slower growth was observed in BC cells (MDA-MB-231 and Hs578T) transfected with a shRNA targeting the HERV-K *env* mRNA (shRNAenv) compared with a shRNA targeting a scrambled RNA sequence (shRNAc) (Fig. 1). The shRNA constructs expressed green fluorescent protein (GFP) that was used to track their proliferation.

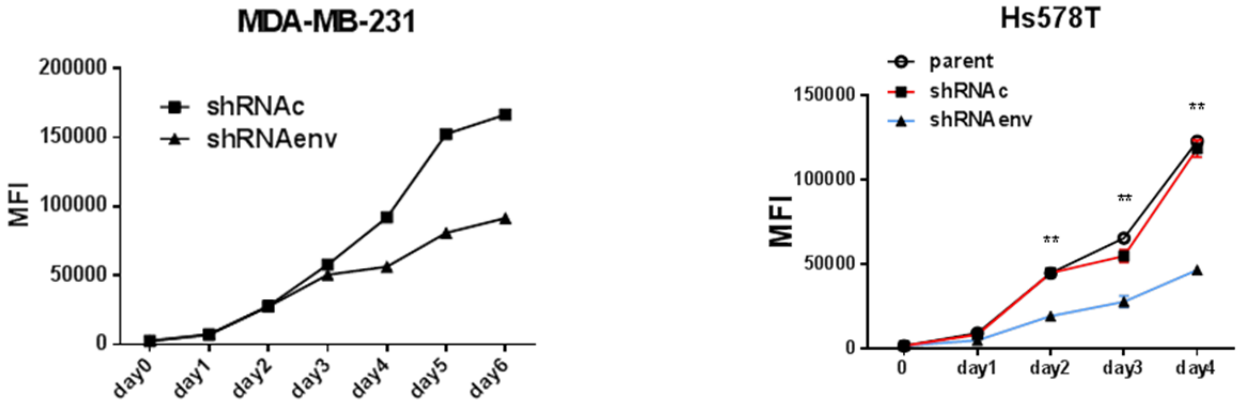

Fig. 1 Cell proliferation assays demonstrated significantly slower grow rates in MDA-MB-231 and Hs578T BC cell lines transfected with shRNAenv vs. parent cells or shRNAc. MFI=mean fluorescence intensity of GFP.

Three BC cell lines (Hs578T, MDA-MB-231, and MCF-7) were transfected with shRNAenv compared with shRNAc (Fig. 2). Smaller colony sizes and fewer numbers of colonies were detected in BC cells transfected with shRNAenv (bottom panel) compared with shRNAc (top panels).

Fig. 2 Cell growth rates were compared in BC cell lines transfected with shRNAenv vs. shRNAc. Smaller numbers of colonies and smaller colony sizes were demonstrated in three BC cell lines transfected with shRNAenv compared with cells transfected with shRNAc.

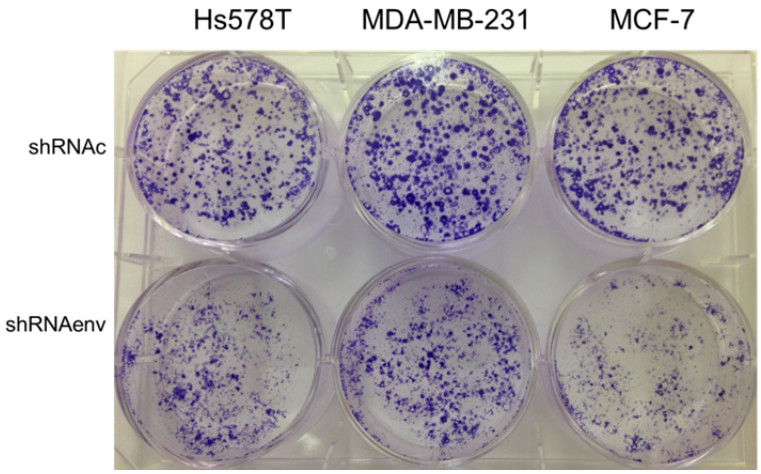

3.2 Reduced BC cell transformation: A soft agar assay was employed to determine whether HERV-K possesses a transforming capacity of BC cells. Significantly reduced numbers of colonies formed in soft agar (Fig. 3) when HERV-K env was knocked down in BC cell lines (MCF-7: p=0.001; left panel and Hs578T: p=0.006; right panel), compared to treatment with shRNAc.

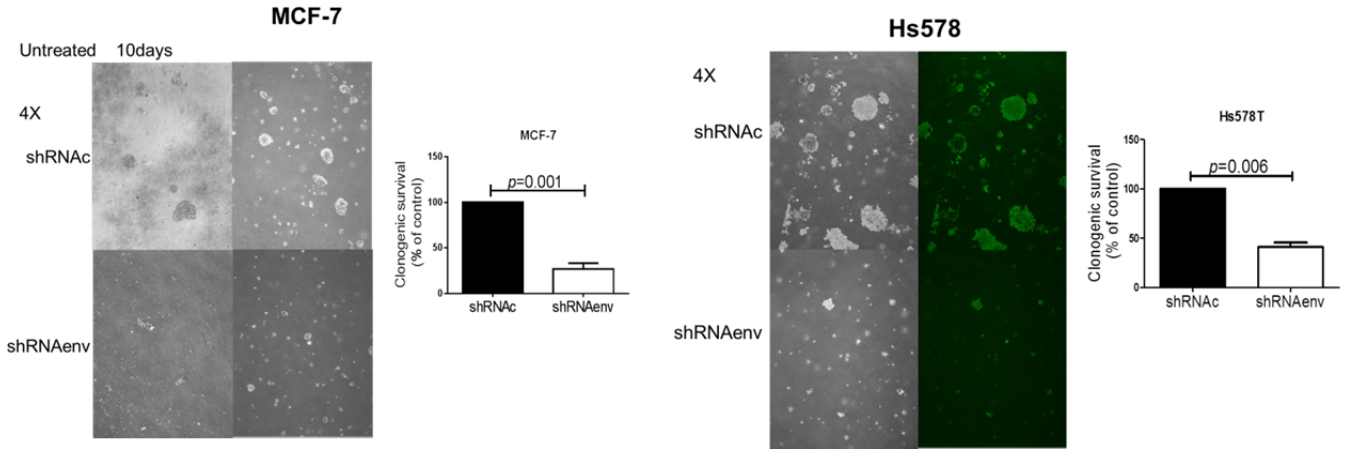

Fig. 3 Colony formation was significantly less in MCF-7 and Hs578T BC cell lines transfected with shRNAenv vs. shRNAc.

3.3 Reduced tumor sizes *in vivo*: Significantly reduced tumor sizes and weights were demonstrated in mice inoculated with MDA-MB-231, MDA-MB-435.eb1, and SKBR3 BC cells stably transfected with shRNAenv, compared to cells stably transfected with a shRNAc (Fig. 4).

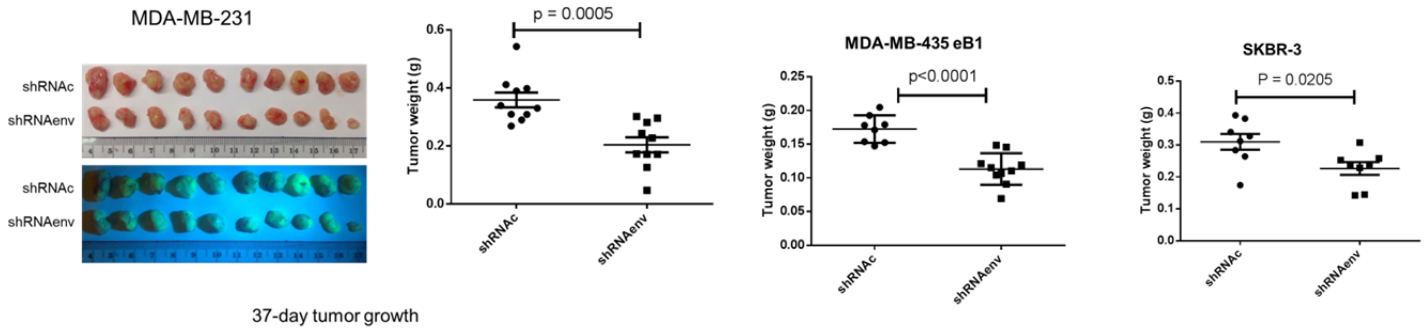

Fig. 4 Significantly reduced tumor sizes and weights were demonstrated in MDA-MB-231, MDA-MB 435 eb1, and SKBR3 BC cell lines transfected with shRNAenv vs. shRNAc.

To date, our results demonstrate that down-regulation of HERV-K has growth-inhibitory activity in several human breast cancer cell lines and reduced tumor growth in animal models. However, the precise mechanisms by which HERV-K exerts these antitumor effects are not known. To obtain insights into its mechanism of action, we examined the effects of HERV-K shRNAenv on cell proliferation, cell cycle distribution, apoptosis, and on the levels of expression of several cell cycle control proteins. Our results provide support for targeting of HERV-K with shRNAenv or other agents to block its expression, and suggest that HERV-K targeting prevents BC tumorigenesis.

3.4 Downregulated HERV-K induces S-phase cell cycle arrest in several human BC cell lines: We were also interested in examining the effects of HERV-K knockdown on cell cycle progression in exponentially dividing cultures of BC cell lines. Cell cycle analysis was done by flow cytometry using PI staining; DNA content was then analyzed using a FACScan instrument equipped with FACStation running Cell Quest software. S phase arrest was found in Hs578T and MCF-7cell lines transduced with shRNAenv, compared to these cells transduced with shRNAc or parent cells (Fig. 5). Downregulated HERV-K caused an increase of cells in the S phase and a corresponding decrease of cells in the G_1 (MCF-7, bottom panel) or G_2-M phases (Hs578T, top panel).

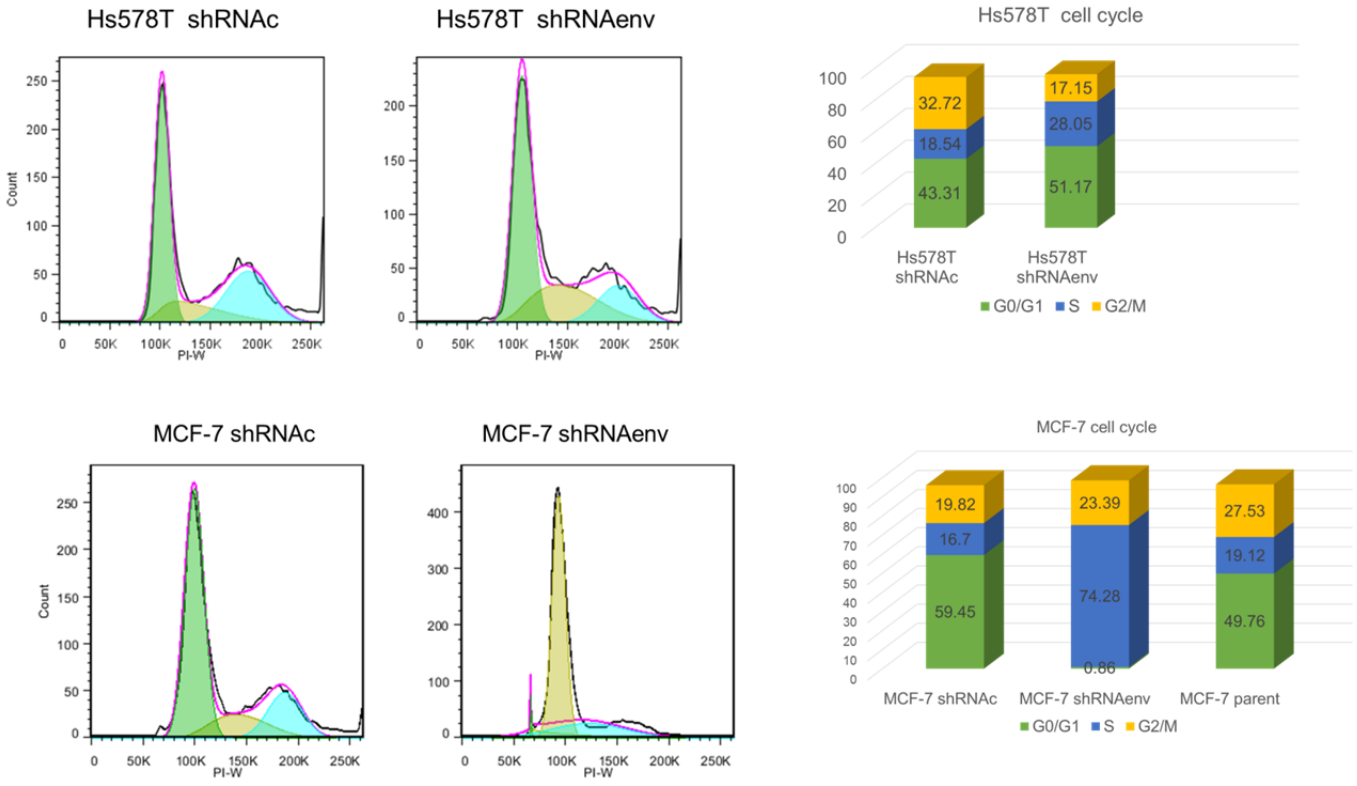

Fig. 5 Cell cycle distribution was determined in BC cell lines transduced with shRNAenv vs. shRNAc using FACS. S phase arrest was observed in MCF-7 and Hs578T BC cell lines transfected with shRNAenv compared with cells transfected with shRNAc or parent cells.

3.5 RNA-Seq: An important challenge in cancer systems biology is to uncover the complex network of interactions between genes (tumor suppressor genes and oncogenes) implicated in cancer. Next generation sequencing provides unparalleled ability to probe the expression levels of the entire set of cancer genes and their transcript isoforms. However, there are onerous statistical and computational issues in interpreting high-dimensional sequencing data and inferring the underlying genetic network. In this study, we analyzed RNA-Seq data from several BC cell lines or tumor biopsies derived from BC cell lines and implemented a probabilistic framework to construct biologically-relevant genetic networks. In particular, we employed a graphical lasso analysis, motivated by considerations of the maximum entropy formalism, to estimate the sparse inverse covariance matrix of RNA-Seq data. RNA-Seq was employed to determine the signaling pathway in BC cells transfected with shRNAenv compared with cells transfected with shRNAc (Fig. 6 to Fig. 9). One example of RNA-Seq results obtained using MCF-7 cells is shown in Fig. 6.

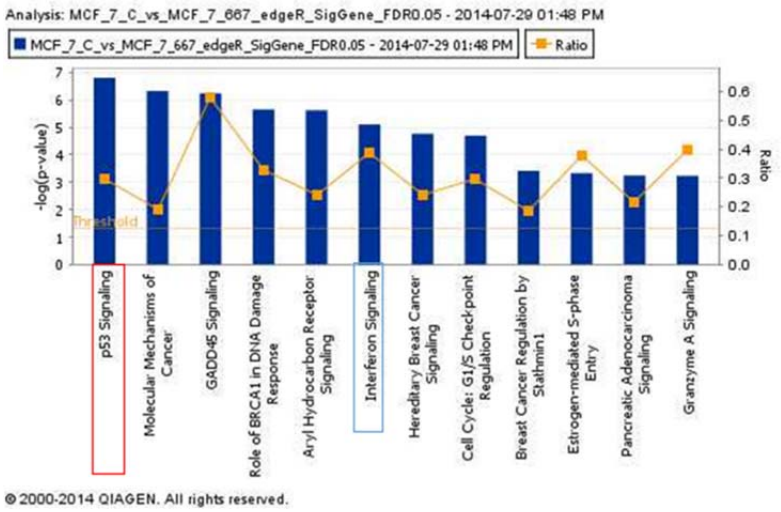

Fig. 6 Signaling pathways were determined in MCF-7 cells transduced with shRNAenv vs. shRNAc using RNA-Seq. The top three pathways are p53 Signaling, Molecular Mechanisms of Cancer and GAD45 Signaling.

p53 Signaling was the major pathway affected by HERV-K knockdown by shRNAenv, followed by Molecular Mechanisms of Cancer and GAD45 Signaling. Furthermore, signaling via the Mevalonate Pathway was strongly affected in MDA-MB-435.eb1 transfected with shRNAenv vs. shRNAc (Fig. 7). Deregulated genes in the Mevalonate Pathway (major pathway in Network 6; top left panel) and the log ratios (top middle panel) are listed. Many genes involved in the mevalonate pathway whose levels were downregulated are labeled in red for MDA-MB-435.eb1 cells transduced with shRNAenv compared with shRNAc (top right panel). qRT-PCR was further used to confirm the deregulated genes of the mevalonate pathway in MDA-MB-435.eb1 cells transduced with shRNAenv vs. shRNAc (bottom right panel). These results suggest that HERV-K may play a major and previously unknown role in cholesterol metabolism. Metabolic pathways, in turn, are becoming increasingly recognized as playing key roles in BC development and progression, and our results suggest for the first time that HERV-K expression may have an impact on metabolic pathways important in BC.

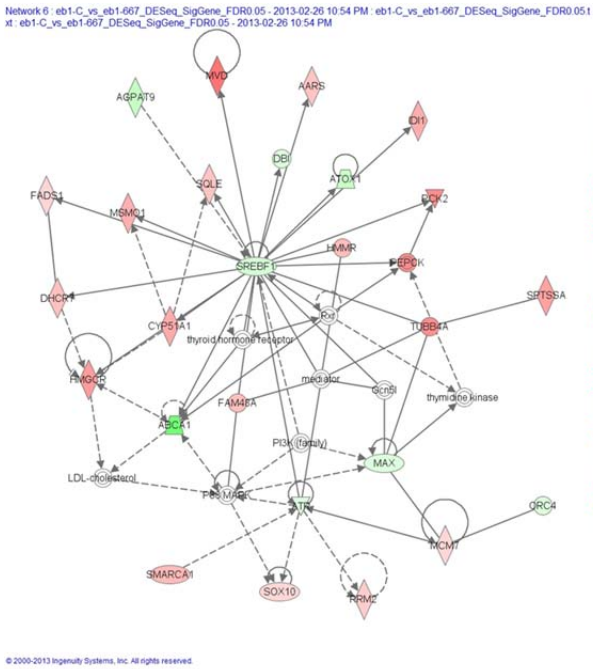

Gene symbol -- human (Hugo / HGNC, Entrez Gene)	Log Ratio	Networks
ACAT2	0.635	
HMGCS1	0.483	3
HMGCR	**0.390**	6
MVK		
PMVK		
MVD	0.547	6
IDI1	0.322	6
FDPS		
FDFT1	0.248	9
SQLE	0.231	6
LSS		
CYP51A1	0.329	6
TM7SF2		
SC4MCL		
DHCR7	0.244	6
CHCR24		

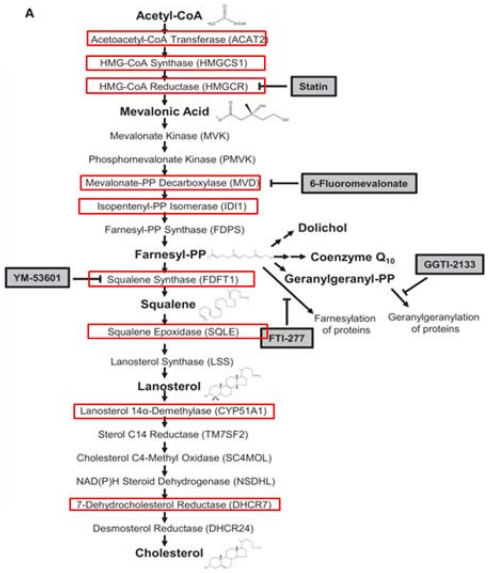

De-regulated of Mevalonate Pathway

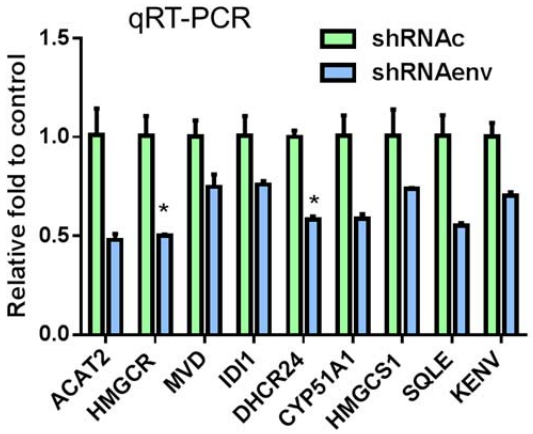

Fig. 7 Top-scoring gene network influenced by downregulated HERV-K. De-regulated genes in the mevalonate pathway were determined in MDA-MB-435.eb1 cells transduced with shRNAenv vs. shRNAc using RNA-Seq. **Top Left Panel)** Network 6 is illustrated here. Shading is in proportion to the size of the fold change. Gray nodes denote network members that did not reach false discovery rate (FDR) < 10%. **Top Middle Panel)** De-regulated genes in the mevalonate pathway (major pathway in Network 6) and log ratio are listed here. **Top Right Panel)** Many genes involved in the mevalonate pathway are labeled with red. **Bottom Right Panel)** qRT-PCR further confirmed the deregulated of the mevalonate pathway in MDA-MB-435.eb1 cells transfected with shRNAenv vs. shRNAc.

Furthermore, tumor biopsies obtained from mice xenografted with two BC cell lines (Fig. 8: MDA-MB-435.eb1, left panel; and SKBR3, right panel) that were transduced with shRNAenv compared with shRNAc share the same network centered around ERK1/2.

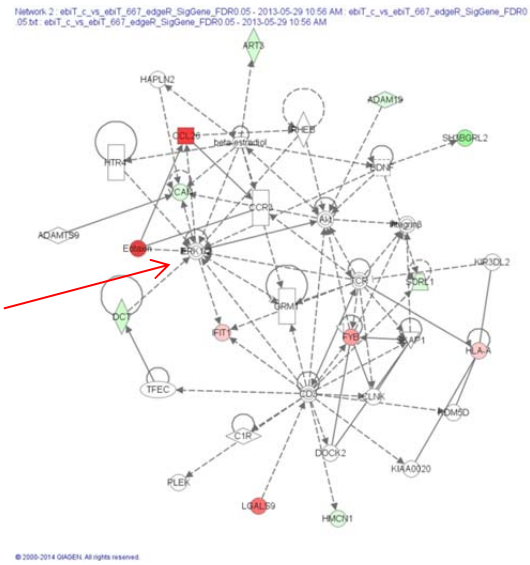

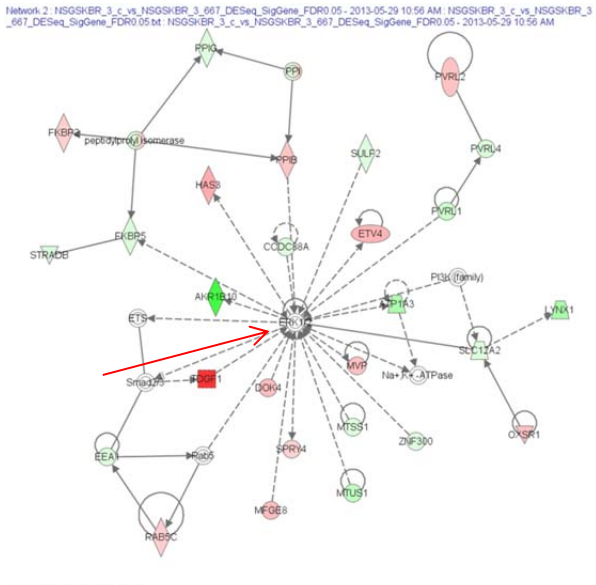

Fig. 8 Top-scoring gene network influenced by downregulated HERV-K. Networks were compared in tumor biopsies obtained from MDA-MB-435.eb1 (left panel) or SKBR3 (right panel) BC cells transfected with shRNAenv vs. shRNAc using RNA Seq. Many gene changes were centered around ERK1/2. Nodes represent genes/molecules. Shading is in proportion to the size of the fold change (red, upregulation; green, downregulation). Gray nodes denote network members that did not reach false discovery rate (FDR) < 10%.

Also, the MYC oncogene, which is frequently activated in human cancers, is downregulated in tumor biopsies (left panel) or cell lysates (right panel) obtained from SKBR3 BC cells transduced with shRNAenv, compared to cells transduced with shRNAc (Fig. 9). Downregulated MYC gene was also observed in other BC cell lines transduced with shRNAenv compared with shRNAc (data not shown). These data indicate that HERV-K viral RNAs are involved in BC tumorigenesis via effects on not only p53 signaling pathways, but also ERK and MYC pathways. All of these pathways play critically important roles in tumorigenesis.

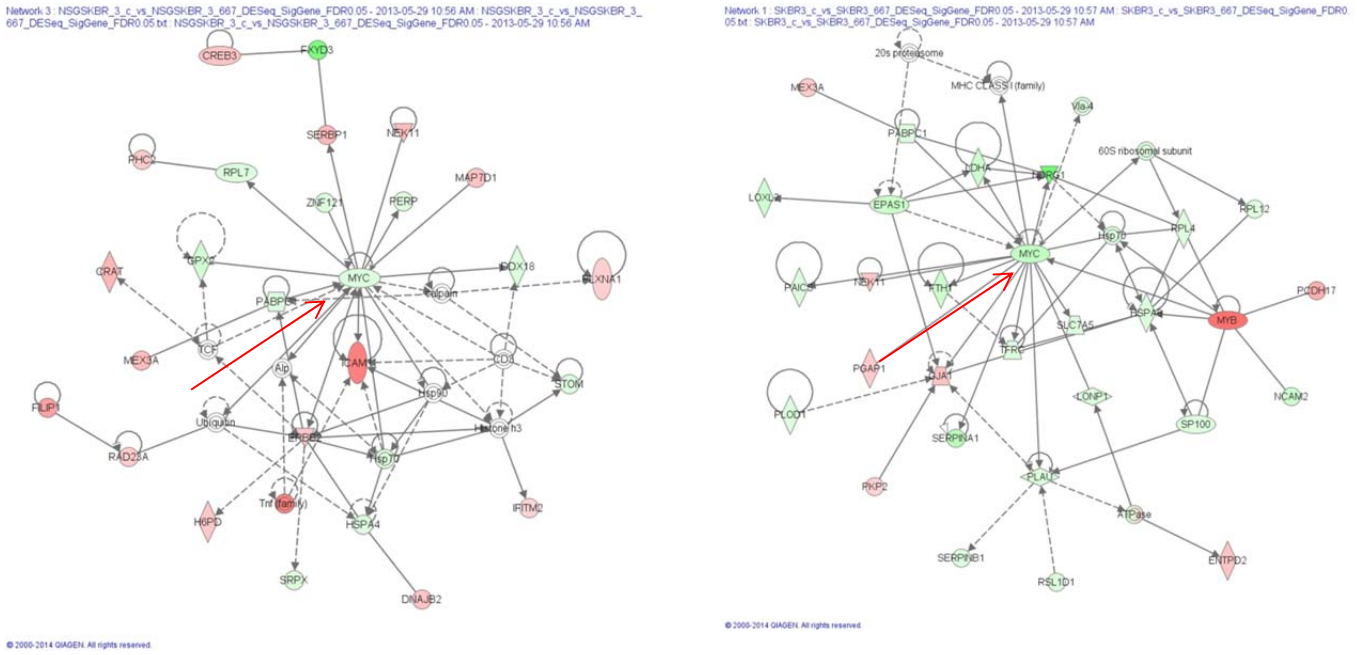

Fig. 9 Top-scoring gene networks influenced by downregulated HERV-K. Networks were compared in tumor biopsies (left panel) or cell lysates (right panel) obtained from SKBR3 BC cells transduced with shRNAenv vs. shRNAc, using RNA-Seq. Deregulated MYC gene was the central pathway affected in both cells and tumor biopsies. Nodes represent genes/molecules. Shading is in proportion to the size of the fold change (red, upregulation; green, downregulation). Gray nodes denote network members that did not reach false discovery rate (FDR) < 10%.

3.6 Protein phosphorylation arrays:

One of the most important roles of phosphate in biological systems is that of a molecular switch, turning enzyme activity on and off through the mediation of the various protein kinases and phosphatases in biological systems. Gene ontology, pathway enrichment and protein-protein path length analysis were all carried out to validate the biological context of the predicted network of interacting cancer genes described above. Since the RNA-Seq results suggested that signaling pathways involving phosphorylation might play prominent roles in response to HERV-K knockdown, phosphate binding protein arrays were employed to evaluate changes in BC cells transduced with shRNAenv compared with shRNAc (Fig. 10).

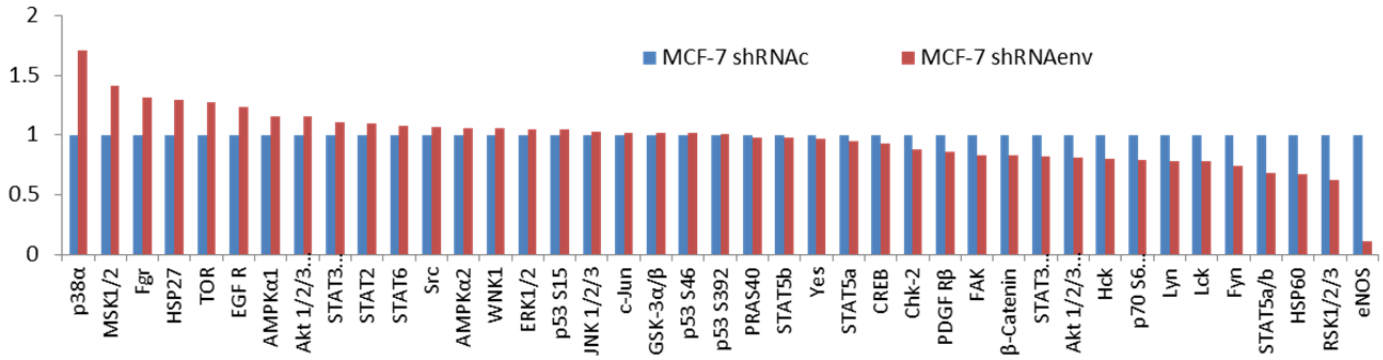

Fig. 10 Phosphate binding protein arrays were analyzed in MCF-7 BC cells transduced with shRNAenv vs. shRNAc. Phosphoprotein levels were compared in MCF-7 BC cell lines transduced with shRNAenv compared with shRNAc. P38α, MSK1/2, and Fgr were the 3 major upregulated proteins and eNOS, RSK1/2/3, and HSP60 were the 3 major downregulated proteins after HERV-K knockdown.

Expression of a variety of phosphorylated proteins important in cancer signaling transduction pathways were affected by HERV-K knockdown with shRNAenv. For example, P38α, MSK1/2, and Fgr were the most strongly upregulated proteins, and eNOS, RSK1/2/3, and HSP60 were the most strongly downregulated proteins. A potential pathway of HERV-K correlated to BC tumorigenesis is shown in Fig. 11.

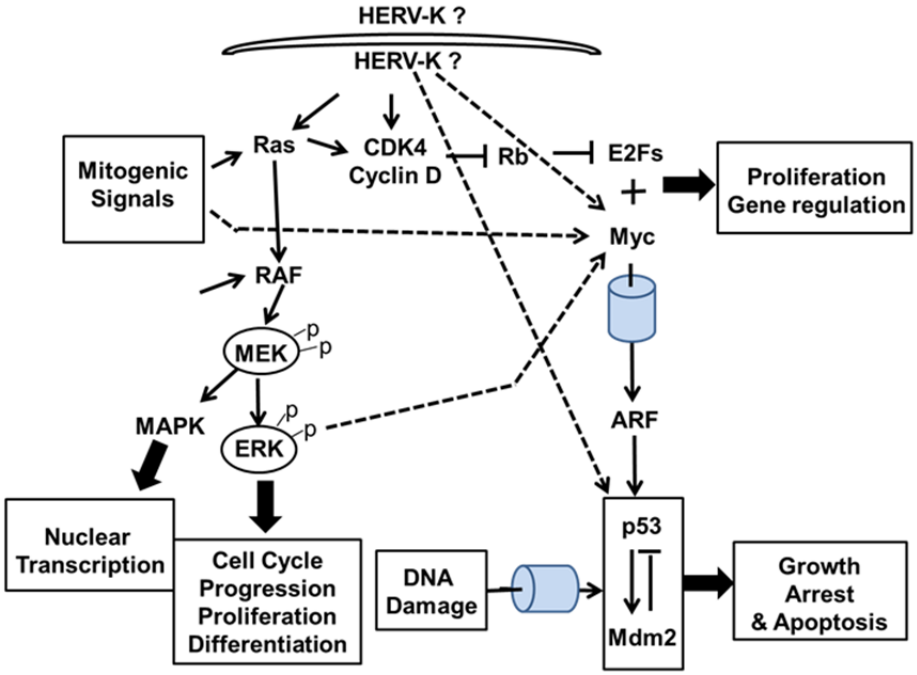

Fig. 11 Signaling pathways regulated in BC cell lines by HERV-K, based on our RNA-seq and phosphoprotein array data, as a result of transduction with shRNAenv vs. shRNAc.

In summary, our data demonstrate that HERV-K plays a very essential role in BC tumorigenesis. In the previous annual report, we explored our discovery of an effect of HERV-K on the p53 pathway in BC cell lines treated with anti-HERV-K monoclonal antibodies. Here we verified the p53 results by knockdown of HERV-K env with shRNA, and additionally discovered that the major ERK and MYC signaling pathways, which are important in BC, are affected by HERV-K knockdown. Downregulation of *H-Ras*, *MDM2* and *c-Myc* mRNAs was also demonstrated in studies in our previous annual report. c-Myc induces the tumor suppressor ARF, which inhibits MDM2 and leads to stabilization of the p53 protein [14].

In last year's report, qRT-PCR revealed changes in expression of p53, MDM2 and c-myc in cancer cell lines stably transfected with shRNA targeting the HERV-K env gene, showing that HERV-K is affecting signaling via the p14ARF/MDM2/p53 axis. Changes in the expression of these key regulatory proteins at the protein level

was also determined by flow cytometry using various antibodies and protein assay as discussed above (Fig.10). A more comprehensive description of the correlations we found between HERV-K and the above gene changes was summarized in Fig. 11.

4. Impact:

Sequences of endogenous retroviruses are commonly found in the human genome. Among them, the HERV-K family of endogenous retroviral genes, which is usually silenced, commonly becomes induced in cancer cells. Our research focus is cancer genomics, predictive biomarkers, therapeutic antibodies and cancer vaccines targeting HERV-K. Several recent publications provide evidence that endogenous retroviral-derived sequences become activated in cancer cells and contribute unique regulatory elements that have reshaped the human transcriptional landscape. This is an innovative concept because a viral etiology of BC has not yet been established, and we propose in this study to establish that HERV-K has an essential role in BC tumorigenesis. We are addressing the proposition that HERV-K is expressed in breast cells and contributes to human BC tumorigenesis. *This is the first time that a naturally-occurring virus has been identified and characterized in BC,* and our data is convincing that these retroviruses contribute to the pathology of BC. Our data will shift both current research and current clinical practice paradigms because the HERV-K viral proteins will be evaluated as a novel BC target for the first time. In addition to establishing a viral etiology of BC, our proposed study would also have an impact on BC by opening up avenues of novel treatment of BC patients, such as the immunotherapy regimen we describe below.

We recently submitted a manuscript entitled "Reduced Tumorigenesis and Metastasis of Breast Cancer by HERV-K Specific Chimeric Antigen Receptor T cells," to be considered for publication in *Science Translational Medicine* (August, 2014). The main point of the paper is to use an adoptive cell transfer approach to demonstrate antitumor and anti-metastatic effects of a chimeric antigen receptor (CAR) that allows T cells to recognize HERV-K antigen on tumor cells.

Although treatment of patients with gene-engineered T cells equipped with either CARs or T cell receptors (TCRs) has shown therapeutic successes in the treatment of some tumors, antitumor responses, especially in solid tumors, have not been forthcoming in a substantial number of patients. The main challenges for improving response are: 1. To identify tumor-specific antigens that are highly expressed in tumor tissues (on target), but not in normal tissues (off-tumor), even at low levels. 2. To endow engineered T cells with high-affinity receptors that are significantly toxic when tumor antigens are targeted. Here, we provide evidence that on-target toxicity is HERV-K directed and that no off-tumor effects were observed in animal models.

Our manuscript addresses therapy of breast cancer by identifying and characterizing a chimeric antigen receptor (K-CAR) that targets HERV-K on breast cancer cells. We first confirmed that the HERV-K envelope protein is overexpressed on the breast cancer cell lines targeted by K-CAR T cells. Artificial antigen-presenting cells expressing HERV-K env gene were used to propagate $CD3^+$ T cells expressing K-CAR (K-CAR T cells) from breast cancer patients and controls.

Several novel findings have emerged from the studies reported in this paper:

- K-CAR T cells showed efficacy against a solid tumor. CARs have shown their greatest effectiveness against hematological malignancies, but to date there has been only limited success in targeting solid tumors with CARs.
- K-CAR T cells were able to lyse artificial antigen-presenting cells and HERV-K^+ cancer cells.
- In comparison to normal controls, K-CAR T cells from BC patients had higher percentages of regulatory T cells, lower percentages of $CD8^+$ T cells, and lower proliferation rates. $CD4^+$ T cell depletion enhanced the percentage of $CD8^+$ T cells in BC patients, which provided more effective antitumor effects.
- K-CAR T cells generated from BC patients blocked growth of cultured BC cell lines and induced their lysis and release of cytokines that included IFN-γ, IL-2, TNF-α, and Grazyme B. Effects on lysis of BC

cells were reversed when HERV-K was knocked down with an shRNA, which indicated that cytotoxicity toward tumors was occurring in an antigen-dependent manner.

- Tumor biopsies of mice treated with K-CAR T cells showed changes in gene expression that were consistent with effects we have observed after therapeutic antibody treatment, further supporting the mechanism of anti-HERV therapy.
- HERV-K expression was downregulated in BC cells after K-CAR T cell treatment of female NOD/SCID mice bearing human tumor xenografts, especially after CD4 depletion. Importantly, treatment with K-CAR T cells not only blocked tumor growth in this animal model, but also significantly reduced dissemination from the primary site to form new lesions in other organs.
- These results indicate that K-CAR treatment may be capable of blocking both growth and metastasis of BC.

Our pre-clinical studies reported here could pave the way for immunotherapy regimens for clinical trials in BC patients. We feel that these observations will generate great interest in the BC immunotherapy field, because there are so few CAR therapies that are effective against solid tumors such as BC. We also believe that this paper will increase awareness of the potentially very important role of endogenous viruses in human BC.

5. Changes/Problems: Since we are in the process of moving our lab from MD Anderson Cancer Center to SRI International during the current annual reporting period, many factors have caused our research to be delayed. The DoD grant finally was transferred to SRI on May 1, 2014. However, we have had to wait for DoD approval for using human subjects; this approval was granted on Sept. 12, 2014. Therefore, in this reporting period, no patient samples have been collected for our study. When these patient samples become available, we will make a strong effort to complete the analyses of these samples, as proposed in the grant. In addition, many materials, including crucial antibodies and other materials essential for completing our studies, have been held at MD Anderson because MTAs have not been executed to date. The only thing MD Anderson has released is "HERV-K shRNAenv and shRNAc," and the availability of these key reagents is the reason we have so many new results for this annual report. We used all reagents available to finish or continue our ongoing projects, and are hopeful that MTAs at MD Anderson will be finalized as soon as possible. Another achievement during this reporting period is that we completed our HERV-K chimeric antigen receptor (CAR) study in BC patients (see below for the summary of this study, and the attachment containing the manuscript). Ours is among the first reports of a CAR to treat solid tumors, and we were successful in reducing tumor burden and preventing metastasis of BC to the lung, liver, and other organs.

6. Products: The products we generated during this reporting period are underlined and highlighted in boldface type below. We have previously reported the antitumor effects of anti-human endogenous retrovirus-K (HERV-K) monoclonal antibodies, as well as vaccines for BC based on HERV-K envelope (env) protein as a tumor-associated antigen. Here, **a chimeric antigen receptor (CAR) specific for HERV-K env protein (K-CAR)** was generated using the Sleeping Beauty system. K-CARs from peripheral blood mononuclear cells of 9 BC patients and 12 normal female donors were able to inhibit growth of, and to exhibit significant cytotoxicity toward, BC cells but not MCF-10A normal breast cells. The antitumor effects were significantly reduced when the expression of HERV-K in BC cells was knocked down by **shRNAs targeting HERV-K**. Secretion of multiple cytokines, including IFN-γ, TNF-α, and IL-2, was significantly enhanced in culture media of BC cells treated with K-CARs. Significantly reduced tumor growth and tumor weight was observed in xenograft models bearing MDA-MB-231 or MDA-MB-435.eB1 cells. Importantly, the K-CAR prevented tumor metastasis to other organs. Moreover, downregulation of HERV-K expression in tumors of mice treated with K-CAR correlated with upregulation of TP53 and downregulation of MDM2 and p-ERK. Our results indicate that CARs directed toward HERV-K may play an important role in immunotherapy of BC, and that K-CAR shows potential for use in clinical trials involving BC patients.

7. Participants &Other Collaborating Organizations

8. Special Reporting Requirements

9. Appendices

9.1 References:

1. Kassiotis G. Endogenous retroviruses and the development of cancer. J Immunol 2014;192(4): 1343-9.
2. Kazazian HH, Jr. Mobile elements: drivers of genome evolution. Science 2004;303(5664): 1626-32.
3. Lander ES. Initial impact of the sequencing of the human genome. Nature 2011;470(7333): 187-97.
4. Ahn K, Kim HS. Structural and quantitative expression analyses of HERV gene family in human tissues. Mol Cells 2009;28(2): 99-103.
5. Stoye JP. Studies of endogenous retroviruses reveal a continuing evolutionary saga. Nat Rev Microbiol 2012;10(6): 395-406.
6. Reus K, Mayer J, Sauter M, Zischler H, Muller-Lantzsch N, Meese E. HERV-K(OLD): ancestor sequences of the human endogenous retrovirus family HERV-K(HML-2). J Virol 2001;75(19): 8917-26.
7. Hohn O, Hanke K, Bannert N. HERV-K(HML-2), the Best Preserved Family of HERVs: Endogenization, Expression, and Implications in Health and Disease. Front Oncol 2013;3: 246.
8. Contreras-Galindo R, Kaplan MH, Leissner P, et al. Human endogenous retrovirus K (HML-2) elements in the plasma of people with lymphoma and breast cancer. J Virol 2008;82(19): 9329-36.
9. Wang-Johanning F, Frost AR, Jian B, Epp L, Lu DW, Johanning GL. Quantitation of HERV-K env gene expression and splicing in human breast cancer. Oncogene 2003;22(10): 1528-35.
10. Zhao J, Rycaj K, Geng S, et al. Expression of Human Endogenous Retrovirus Type K Envelope Protein is a Novel Candidate Prognostic Marker for Human Breast Cancer. Genes Cancer 2011;2(9): 914-22.
11. Wang-Johanning F, Li M, Esteva FJ, et al. Human endogenous retrovirus type K antibodies and mRNA as serum biomarkers of early-stage breast cancer. Int J Cancer 2014;134(3): 587-95.
12. Wang-Johanning F, Rycaj K, Plummer JB, et al. Immunotherapeutic potential of anti-human endogenous retrovirus-K envelope protein antibodies in targeting breast tumors. J Natl Cancer Inst 2012;104(3): 189-210.
13. Wang-Johanning F, Radvanyi L, Rycaj K, et al. Human endogenous retrovirus K triggers an antigen-specific immune response in breast cancer patients. Cancer Res 2008;68(14): 5869-77.
14. Pomerantz J, Schreiber-Agus N, Liegeois NJ, et al. The Ink4a tumor suppressor gene product, p19Arf, interacts with MDM2 and neutralizes MDM2's inhibition of p53. Cell 1998;92(6): 713-23.

9.2 Manuscript for CAR paper:

Title: Specific Chimeric Antigen Receptor T cells that target HERV-K Inhibits Breast Cancer Development and Metastasis

One sentence summary: This study is the first to demonstrate antitumor effects and metastasis prevention by a human endogenous retrovirus-specific chimeric antigen receptor in breast cancer.

Authors: *Fuling Zhou,[1,6] *Janani Krishnamurthy,[2,5] Yongchang Wei,[1,6] Ming Li,[1,5,6] Kelly Hunt,[4] Gary L. Johanning,[1,5,6] Laurence J.N. Cooper,[2,5] and Feng Wang-Johanning[1,3,5,6]*

Affiliations: [1]Department of Veterinary Sciences, [2]Division of Pediatrics, [3]Department of Immunology, [4]Department of Surgical Oncology, University of Texas M. D. Anderson Cancer Center, Houston, TX, USA, [5]Graduate School of Biomedical Sciences, 6767 Bertner Avenue Mitchell BSRB S3.8344, Houston, Texas. [6]Viral Oncology Program, SRI International, 333 Ravenswood Avenue, Menlo Park, CA, USA

*FZ and JK are co-first authors.

Corresponding author: Feng Wang-Johanning, MD, PhD, SRI International, 333 Ravenswood Avenue, Menlo Park, CA, USA, 650-859-3271, feng.wang-johanning@SRI.com

Abstract:

We have previously reported the antitumor effects of anti-human endogenous retrovirus-K (HERV-K) monoclonal antibodies, as well as vaccines for breast cancer (BC) based on HERV-K envelope (env) protein as a tumor-associated antigen. Here, a chimeric antigen receptor (CAR) specific for HERV-K env protein (K-CAR) was generated using the Sleeping Beauty system. K-CARs from peripheral blood mononuclear cells of 9 BC patients and 12 normal female donors were able to inhibit growth of, and to exhibit significant cytotoxicity toward, BC cells but not MCF-10A normal breast cells. The antitumor effects were significantly reduced when the expression of HERV-K in BC cells was knocked down by an shRNA. Secretion of multiple cytokines, including IFN-γ, TNF-α, and IL-2, was significantly enhanced in culture media of BC cells treated with K-CARs. Significantly reduced tumor growth and tumor weight was observed in xenograft models bearing MDA-MB-231 or MDA-MB-435.eB1 cells. Importantly, the K-CAR prevented tumor metastasis to other organs. Moreover, downregulation of HERV-K expression in tumors of mice treated with K-CAR correlated with upregulation of TP53 and downregulation of MDM2 and p-ERK. Our results indicate that CARs directed toward HERV-K may play an important role in immunotherapy of BC, and that K-CAR shows potential for use in clinical trials involving BC patients.

Main Text:

INTRODUCTION

Clinical trials for a variety of malignant diseases have shown that T-cell therapy may be effective and even curative for some patients (*1*). Many tumor-associated antigens (TAAs) have been identified, and their ability to induce antitumor T-cell immunity has been documented in clinical studies (*2*). A promising approach in cancer treatment is adoptive immunotherapy using chimeric antigen receptor (CAR)-engineered T cells to redirect specificity toward a particular TAA (*3-5*) in a manner independent of the major histocompatibility complex. The efficacy and safety of adoptive CAR-engineered T cells have been evaluated in multiple clinical studies. Early-phase clinical trials reported that adoptively transferred CAR^+ T cells have efficacy in treating hematological malignancies and some solid tumors. The most encouraging results have been achieved in patients with chronic lymphocytic leukemia and lymphoma who were treated with CD19 CAR^+ T cells (*6-8*). CAR-based therapy of solid tumors has also been attempted, including the use of CARs targeting HER2 for colorectal cancer (*9*), folate receptor-α for ovarian cancer (*10*), carcinoembryonic antigen for colorectal cancer and breast cancer (BC) (*11*), prostate-specific membrane antigen for prostate cancer (*12*), and carbonic anhydrase IX for metastatic renal cell carcinoma (*13*). A primary challenge using CARs in solid tumors will thus be to target TAAs with CARs that are able to penetrate the tumor microenvironment and provoke on-target cytotoxicity toward tumor cells.

Our genome harbors many endogenous retroviral sequences and some of them may continue to perform retroviral functions that contribute to disease (*14*). Genome sequencing reveals that 8% of the human genome consists of human endogenous retroviruses (HERVs) and roughly half of our DNA is made up of transposable elements that include HERVs (*15-17*). The integration of

HERVs into the host cell happens within the context of their replication cycle (*18*). HERV type K of the HML2 subtype is the most recently integrated and most intact retrovirus in the human genome (*19*). These most recently acquired proviruses of the HERV-K family can express viral proteins and produce viral particles (*20, 21*). In previous studies we reported that expression of HERV-K env protein in malignant BC cells was substantially higher than in normal or nonmalignant breast cells (*22-24*), suggesting that HERV-K might be reactivated and implicated in carcinogenesis. Monoclonal and single-chain antibodies against the HERV-K env protein recently proved capable of blocking the proliferation of human BC cells *in vitro* and inhibiting tumor growth in mice bearing xenograft tumors (*25*). In addition, we found that HERV-K env protein is capable of acting as a TAA, activating both T-cell and B-cell responses in BC patients (*26*).

Here we genetically modified T cells using the Sleeping Beauty (SB) system to stably introduce a single-chain variable fragment (scFv: G11D10) (*25*) generated from an anti-HERV-K monoclonal antibody (mAb: 6H5) (*26*) to produce an HERV-K specific CAR (K-CAR). Antitumor effects of K-CAR were demonstrated *in vitro* and *in vivo*.

RESULTS

Expression of HERV-K env protein in breast cancer cells

The expression of HERV-K env protein on the BC cell membrane and cytoplasm was observed in MDA-MB-231, MDA-MB-435.eB1, and MCF-7 BC cells to a greater extent than in MCF-10A or MCF-10AT non-malignant breast cells by flow cytometry (fluorescence-activated cell sorting, or FACS; Fig. S1A), immunofluorescence (Fig. S1B), immunohistochemistry (IHC; Fig. S1C), and immunoblot (Fig. S1D) using anti-HERV-K mAb 6H5 (*26*) , confirming our findings

from previous studies (*22-27*). Expression of HERV-K env protein was increased in MDA-MB-231 (~6-fold), MDA-MB-435.eB1 (~5-fold), MCF-7 (~4-fold), and SKBR3 (~4-fold; data not shown) BC cells, compared to the level of expression in MCF-10A (1-fold) or MCF-10AT (~1.5-fold) nonmalignant breast cell lines, as assessed by immunoblot, using the ImageJ program to estimate band intensity, with normalization to β-actin. Based on their degree of overexpression, MDA-MB-231 and MDA-MB-435.eB1 BC cells were used as targets for adoptive T therapy in subsequent studies.

HERV-K specific CAR construction and propagation

6H5 mAb and its scFv were previously shown to exhibit specificity and sensitivity in detecting and binding HERV-K env protein on BC cell lines (*25*), and these antibodies were used for generation of K-CAR. In this construct (Fig. S2A), the 6H5 scFv is fused to the IgG4Fc region by a flexible linker, followed by the CD28 transmembrane and CD28 and CD3ζ intracellular domains, as described previously (*28*). K562 cells expressing HERV-K *env* gene in a lentiviral vector (Fig. S2B) were used as artificial antigen-presenting cells (aAPCs) to propagate $CD3^+$ T cells expressing K-CAR. The expression of HERV-K env in K562 cells was demonstrated by RT-PCR (Fig. S2C, left panel), immunoblot (Fig. S2C, right panel), and FACS using 6H5 mAb (Fig. S2D).

***In vitro* expansion of K-CAR T cells originating from BC patients and normal female donors**

Peripheral blood mononuclear cells (PBMCs) from 9 BC patients (Table 1) and 12 normal female donors (NDs) were electroporated with HERV-KCD28MZ SB transposon (pSBSO) along

with pCMV-SB11 transposase and cultured with IL-2 to expand $CD3^+$ T cells expressing K-CAR. scFv expression in K-CAR T cells from various donors (BC: n=9 and ND: n=12) was further confirmed by RT-PCR using primers specific to the 6H5 scFv (Fig. 1A), and growth of T cells was monitored over time by microscopy (Fig. S3A, top panel). The percentage of K-CAR T cells generated from PBMCs was determined post-electroporation by FACS using anti-CD3 and anti-Fc antibodies. Sample FACS results from a BC patient (#157, diagnosed with ductal carcinoma *in situ*, or DCIS; see Table 1 for detail) and a normal donor (ND1) are shown in Fig. 1B. K-CAR T cells from patient #157 had a significantly lower proliferation rate than cells from ND1 (Fig. S3A, bottom panel). Nearly all cells from BC patients as well as NDs expressed the K-CAR scFv on day 28 post-electroporation, as measured by expression of the Fc backbone (Fig. S3B). Specific lysis of K562-HERV-K cells by K-CAR T cells obtained from two normal donors was observed, as determined by a cytotoxic T lymphocyte (CTL) assay (Fig. S3C). Since the proliferation of CAR T cells was decreased relative to normal donors, percentages of $CD4^+$ and $CD8^+$ T cells as well as T regulatory cells (Tregs: FOXP3 and CD25 positive) were determined in K-CAR T cells obtained from BC patients or normal female donors, since Tregs are a component of the immune system that suppresses immune responses of other cells. A sample from a BC patient (#243, diagnosed with DCIS) revealed a higher percentage of FOXP3 in $CD4^+$ T cells than in $CD8^+$ T cells (Fig. 1C, left panel), and increased percentages of $CD8^+$ T cells were observed after $CD4^+$ depletion (Fig. 1C, right panel). Higher percentages of both $FOXP3^+$ and $CD25^+$ T cells were demonstrated in K-CAR obtained from a BC patient than from ND1 control (Fig. S3D). Higher percentages of $CD4^+$ than $CD8^+$ T cells were observed in BC patients (n=7) compared with NDs (n=12), but the differences were not significant (Fig. 1D, top panel). $CD4^+$ cell T depletion resulted in significantly enhanced percentages of $CD8^+$ and significantly

decreased percentages of $CD4^+$ T cells in K-CAR T cells from BC patients (Fig. 1D, bottom panel).

Antitumor effects of K-CAR *in vitro*

Antitumor effects were evaluated in MDA-MB-231 and MDA-MB-435.eB1 BC cells treated *in vitro* with K-CAR^+ T cells or control T cells generated, respectively, from BC patients #157 or #108 (diagnosed with metastatic invasive ductal carcinoma), with a ratio of K-CAR T cells to tumor cells of 10:1. Significantly reduced growth was observed in MDA-MB-231 cells treated with K-CAR T cells from patient #157, and in MDA-MB-435.eB1 treated with K-CAR T cells from patient #108 (Fig. 2A).

CTL assays were further employed to analyze the cytotoxicity of K-CAR T cells. Specific lysis was significantly greater in BC cell lines treated with K-CAR T cells when compared to treatment with control (wild-type) T cells generated from patient #108 (Fig. 2B). Enhanced specific lysis was observed in BC cell lines treated with K-CAR T cells with depletion of $CD4^+$ T cells when compared to treatment without depletion from cells derived from a triple negative IDC patient #233. To further test the specificity for HERV-K, the HERV-K *env* RNA was knocked down in both cell lines using an shRNA targeted to HERV-K env (shRNAenv) using a pGreenPuro vector (System Biosciences; Fig. S4A). An immunoblot analysis showed about 70 to 80% knockdown in HERV-K protein levels of shRNAenv treated cells compared to cells stably transduced with scrambled shRNAc (Fig. 2C). The specific lysis of MDA-MB-231 and MDA-MB-435.eB1 BC cells by K-CAR T cells from BC patients #108 and #257 was significantly reduced after knockdown of HERV-K env RNA (Fig. 2D, top panel). Reduced cytotoxicity of K-CAR toward BC cell lines was also observed after shRNA knockdown in K-CARs generated

from normal female donors ND8 and ND10 (Fig. 2D, bottom panel). These results suggest that the potency of K-CAR T cells in eliminating tumors *in vitro* depends on antigen being specifically expressed on the surface of BC cells.

The specific killing capability of K-CAR was further tested on various breast cell lines using the co-stained Live/Dead Viability Assay, using 5:1 or 20:1 ratios of K-CAR T cells to target cells that included BC cell lines MDA-MB-231, MDA-MB-435eB1, and MCF-7 as well as MCF-10A breast cells (Fig. 3A, quantitated in Fig. 3B). Dead cells stained with CYTOX appear as a red color, while live cells stain green (Fig. 3A). Larger ratios of K-CAR T cells to target cells resulted in significantly higher deaths of target cells, with the exception of non-malignant MCF-10A cells (Fig. S4B). A significantly larger percentage of dead cells was observed for BC cell lines than for MCF-10A cells. The specific killing of BC cells by patient-generated K-CAR T cells was further compared by FACS using the cell-impermeant viability indicator ETHD1. Significantly increased killing of BC cells was observed for K-CAR from a BC patient (#257, diagnosis of invasive lobular carcinoma) in comparison to the patient's autologous PBMC cells, with a higher ratio of K-CAR cells to target cells leading to a higher percentage of target cell death (Fig. 3C). Significantly increased killing of BC cells was also observed for K-CAR from a normal donor (ND8) in comparison to her autologous T cells, with a higher ratio of K-CAR cells to target cells leading to a higher percentage of target cell death (Fig. 3D). HERV-K-CAR redirected T cells mediated potent effector activity against HERV-K^+ BC cell lines as well as a primary patient sample cultured as tumorspheres from a biopsy (patient 78, diagnosis of IDC).

Quantification of cytokine release

In order to further evaluate the functionality of these HERV-K specific CAR^+ T cells, cytokine release was assessed by enzyme-linked immunosorbent assay (ELISA) or FACS assays. Release of IFN-γ, TNF-α, and Granzyme B, assessed by ELISA (Fig. 4A), was greater from BC target cells mixed with K-CAR T cells from a BC patient (#157) than when mixed with control T cells obtained from the same patient. Released intracellular cytokine levels, determined using flow cytometry, were greater after 4-hour stimulation of MDA-MB-231 target cells at a 20:1 ratio with K-CAR T cells from BC patient 243 or from a normal female donor (ND1) than after stimulation with the corresponding T cells from these subjects (Fig. S4C). Significantly increased levels of IFN-γ (Fig. 4B), TNF-α (Fig. 4C) and IL-2 (Fig. 4D) were released by target cells after K-CAR T cell stimulation compared with control T cells, but there was not a significant difference in cytokine stimulation when K-CAR T cells obtained from BC patients were compared with K-CAR T cells from normal female donors. These data strengthen the previous observation that K-CAR T cells stimulate Th1 cytokine secretion, which may promote killing of target cells.

Antitumor effects of K-CAR T cells *in vivo*

Antitumor effects of K-CAR^+ T cells were evaluated using human tumor xenograft mouse models. After tumor cell engraftment, K-CAR^+ T cells with $CD4^+$ T depletion were infused intravenously in one group of mice on days 5, 13, and 20, along with IL-2 and IL-21. Control T cells from the same donors were infused in the same manner to serve as controls. Significantly reduced tumor growth (Fig. 5A), tumor sizes (Fig. 5B, top panel) and tumor weights (Fig. 5B, bottom panel) were observed in mice bearing MDA-MB-231 or MDA-MB-435.eB1 cells treated with K-CAR T cells compared to control T or no treatment (blank). Tumor sizes and weights in

mice bearing MDA-MB-435.eB1 cells without any treatment, or treated with IL-2, T cells+IL-2, PBMC, and PBMC+IL-2 were determined. Significantly reduced tumor sizes and tumor weights were observed in mice bearing MDA-MB-435.eB1 cells treated with K-CAR, compared to treatment with PBMCs with or without IL-2, or IL-2 treatment only (Fig. S4D).

The profiles of gene expression in tumor biopsies

In a previous study we reported that treatment of BC cells with an anti-HERV mAb impacted p53 signaling pathways, and wanted to determine whether K-CAR affected tumorigenesis by a similar mechanism. We observed significantly reduced expression of HERV-K in tumor biopsies obtained from mice treated with K-CAR compared with T cell treatment, as assessed by qRT-PCR (Fig. 5C), immunoblot (Fig. 5D), or FACS (Figs. S5A to S5C). Of interest, TP53 or P53-AIP1 was upregulated (Fig. 5C, Fig. 5D, and Fig. S5D), and oncogenes including MDM2 (Fig. 5C, Fig. 5D, and Fig. S5D) and p-ERK (Fig. 5D) were downregulated in BC cells treated with K-CAR.

Reduced tumor metastasis after K-CAR treatment

BC cells in this study were stably transfected with green fluorescent protein (GFP; pGreenPuro; System Biosciences; Fig. S4A), and imaging was used to assess metastasis of tumor cells from the primary xenograft tumor to other organs. The appearance of GFP in various organs was used for evaluating metastasis. Whole mouse images were compared in control, T cell–treated, and K-CAR–treated xenografts (Fig. S6A). Intense green fluorescent areas were found in untreated mice, compared with mice treated with T cells or with K-CAR. A complete absence of fluorescent signal was observed in some mice treated with K-CAR. Significantly reduced

numbers of metastases to organs were found in mice treated with K-CAR compared with the other treatments, including T cells with or without IL-2, PBMC cells with or without IL-2, or IL-2 only (Fig. 6A). Images of various organs revealed that metastases were present in untreated mice but not in mice treated with K-CAR (Fig. 6B).

Weights of body, liver, lung, and brain revealed no change of body weight in mice bearing either cell line (data not shown) and reduced lung tissue weights in both cell models treated with K-CAR compared with T cell treatment or other groups (Fig. S6B). Brain weights were reduced in mice bearing MDA-MB-435.eB1 cells treated with K-CAR compared with T cell treatment or other treatment groups. Tissues including lung, liver, and brain were minced, and no GFP^+ human cancer cells were observed in mice treated with K-CAR T cells compared with other groups (Fig. S6C, top panel). In addition, GFP^+ metastatic cells harvested from pleural lavage fluid were observed in mice treated with T cells, but not with K-CAR T cells (Fig. S6C, bottom panel). Cells from minced tissues were cultured and GFP^+ human BC cells were seen at 2 weeks post-culture only in cells from groups not treated with K-CAR (Fig. S6D). Hematoxylin and eosin (H&E) staining was further used to assess morphological features of tumor tissues and tissues from other organs (Fig. 6C). Tumors from mice treated with K-CAR showed greatly reduced volumes and sizes in comparison to tumors obtained from mice treated with T cells or other treatments. K-CAR treatment resulted in smaller tumor volumes, less tumor focality and number, less infiltrative borders, and decreased mitotic activities. Also, tumor cells from the K-CAR group were more uniform with less pleomorphic nuclei and smaller nucleoli, and tumor-infiltrating lymphocytes were significantly increased in number. Metastasis of BC cells was observed in many tissues, including liver and lung tissues from mice treated with T cells (Fig. 6C) compared with K-CAR treated mice. Only one small metastatic area was observed in liver

from mice treated with K-CAR compared to mice treated with T cells, which had many more metastatic foci (Fig. 6A). Small nuclei with more regular contour, little variation in size and with more uniform chromatin were observed when comparing K-CAR–treated mice with mice treated with T cells; the T cell–treated group had marked variation in sizes and shapes of nuclei.

Immunohistochemistry revealed the expression of HERV-K and H-Ras in tumor and metastatic cells in several tissues obtained from mice treated with control T cells, but not in K-CAR–treated mice (Fig. 6D, Fig. S6E). K-CAR–treated tumors showed minimal IHC reactivity to HERV-K env protein or H-Ras protein, in contrast to tumors harvested from the mice treated with T cells, with the latter group showing strong immune reactivity against 6H5 mAb and H-Ras antibody. In summary, there was dramatically reduced tumor burden after treatment with K-CAR T cells, mostly due to the prevention of tumor metastasis to multiple tissues.

DISCUSSION

Adoptive immunotherapy is a promising approach for the treatment of cancer, and observations from preclinical and clinical studies have revealed a very encouraging therapeutic efficacy of CAR-mediated immunotherapy, especially for hematological malignancies. These promising clinical observations provide an indication that adoptive immunotherapy may become a mainstream therapy in the clinical oncology field in the near future. However, targeting solid tumors is more challenging than treatment of hematological malignancies because solid tumors may have rare target antigens, poor T-cell trafficking to the tumor site, and lower agent cytotoxicity due to the immunosuppressive environment of the local tumor. In addition, although clinical trials with CARs have given positive results, some adverse reactions have been reported (*9, 29*). The primary challenge to the field is to identify tumor-specific targets and avoid off-

tissue toxicity. Appropriate candidate target antigen selection is thus essential for improving efficacy and safety of the CAR-based immunotherapy. Collectively, an optimal design of the CAR and a careful choice of the TAA are indispensable for CAR-mediated therapy to attain a significant response.

We and others have previously reported that the expression of HERV-K env protein is unique to BC cells and tissues, and we have successfully used the protein as a TAA for development of a BC vaccine (*22, 26, 27*). Furthermore, we generated an anti-HERV-K mAb 6H5 and its scFv and tested their ability to bind to BC cells and tissues. Our data indicate that these antibodies not only have specificity and sensitivity in binding to BC cell lines, but also exhibit anti-tumor effects against BC *in vitro* and *in vivo* (*25*). Our accumulated data thus provide strong evidence that HERV-K env protein may be an ideal target for BC immunotherapy, suggesting that 6H5 scFv can be used for CAR-based therapy against BC.

To date, most studies of CAR-related therapy have utilized retroviruses or lentiviruses for gene delivery. The SB system we employed here is frequently used for gene delivery and long-term transgene expression due to its lower cost and better safety profile (*30-32*). We used the SB system to transfer HERV-K-CAR into PBMCs from BC patients and normal female donors to propagate K-CAR T cells, and showed that these cells display CAR-dependent effector function and anti-proliferative effects. Both BC patients and normal donors can produce K-CAR T cells. The overall population of K-CAR$^+$ T cells obtained from BC patients was significantly expanded compared to those from NDs, as analyzed 21 days after culture with aAPC and IL-2, suggesting that there may be increased memory T cells in this group. However, a slower proliferation rate was observed for K-CAR T cells generated from BC patients than from NDs. A higher percentage of CD4$^+$ T cells and a lower percentage of CD8$^+$ T cells were noted in BC patients

compared with NDs, but there was no significant difference in the percentage of $CD8^+$ or $CD4^+$ T cells from K-CAR T cells obtained from BC patients or NDs. Of interest, a significantly enhanced percentage of $CD8^+$ T cells were found in K-CAR T cells after CD4 depletion. Significantly enhanced specific lysis of target cells was observed in BC patient K-CAR T cells with $CD4^+$ T cell depletion, compared to those without depletion. Tumor escape from immune-mediated destruction has been associated with immunosuppressive mechanisms that inhibit T cell activation (*33*). Suppression of $CD8^+$ effector cells by $CD4^+CD25^+FoxP3^+$ regulatory T cells (Tregs) plays a key role in this immunosuppression (*34*). Our results indicate that K-CAR T cells from BC patients contain a high presence of $CD4^+CD25^+FOXP3^+$ Tregs, compared with K-CAR T cells from normal female donors. Our data thus support the concept that Treg depletion from K-CAR T cells provides synergy for improved immune-mediated tumor control *in vitro* and *in vivo*.

K-CAR-dependent effector function and cytotoxicity against HERV-K^+ BC cells was demonstrated in many of our assays, which showed inhibition of BC cell proliferation, increased specific lysis in CTL assays, and increased cell death. Anti-tumor effects were also greater with K-CAR T cells than T cells from the same donors. Inhibition of proliferation and enhanced cytotoxicity toward BC cells was observed to increase upon exposure to a larger number of K-CAR T cells. The specific killing occurred in an antigen-dependent manner, because no killing was observed if target cells such as MCF-10A breast cells did not express HERV-K, or if the expression of HERV-K was knocked down by shRNA in BC cells.

Enhanced release of cytokines, including IFN-gamma, IL-2, TNF-alpha, and Granzyme B, was detected in culture media of BC cells treated with K-CAR T cells versus T cells obtained from BC patients and NDs. No significant difference in cytokine production was found in K-

CAR obtained from BC patients and controls. Release of these Th1 cytokines may assist in K-CAR T cell killing of BC cells.

Anti-tumor effects were also demonstrated in xenograft models inoculated with two BC cell lines. Significantly reduced tumor growth of K-CAR$^+$ T cell treatment groups was observed in both models compared with mice treated with T cells. The expression of HERV-K was concomitantly significantly reduced in tumor biopsies treated with K-CAR in both mouse models. Interestingly, upregulation of P53 and downregulation MDM2 was detected in tumor biopsies treated with K-CAR compared with T cell treatment. These changes were observed not only at the RNA level but also at the level of protein expression. TP53-inducible genes play crucial roles in cell cycle control, DNA repair, and apoptosis. The tumorigenic potential of MDM2, the principal cellular antagonist of p53, is closely linked to its repressive function of p53.

The RAS–ERK pathway is known to play a pivotal role in differentiation, proliferation and tumor progression. HERV-K env protein downregulation correlated with downregulation of p-ERK protein in most of the mice treated with K-CAR T cells. In an earlier study, knockdown of wild-type p53 led to activation of p-ERK1/2 (*35*), showing a reciprocal relationship similar to what we observed in the current study. The RAS-RAF-MEK-ERK signaling pathway has been proposed to play an important role in HERV-K activation (*36*). These observations may thus provide a mechanistic explanation of the role(s) HERV-K plays in breast tumorigenesis.

Another important finding in this study is the anti-metastatic role of K-CAR. We observed significantly reduced or no metastasis to lung, liver, brain, and lymph nodes in mice treated with K-CAR compared with mice treated with T cells and the other treatments tested. These tumor cells present in tumor biopsies, as well as those that metastasized to other organs, were HERV-

K^+ BC cells. It will be of interest to determine the mechanism by which K-CAR prevents metastasis to distant sites, and whether p53, H-RAs, and MAPK signaling pathways are also involved in K-CAR mediation of metastasis suppression in this model.

Since RAS–ERK and MDM2 signaling have been demonstrated to play important roles in cell growth and tumorigenesis, our results may explain mechanistically how K-CAR treatment induces inhibition of cell proliferation *in vitro* and tumorigenesis *in vivo*.

In summary, our data provide strong evidence that K-CAR is very effective for immunotherapy against BC. The K-CAR blocked BC proliferation both *in vitro* and *in vivo* in xenograft models. A significant finding from this study is that the K-CAR prevented metastasis from the site of tumor implantation to a variety of other organs. K-CAR thus appears to be effective in blocking both primary tumor growth and metastasis to distant sites. This study demonstrated antitumor efficacy in murine models; antitumor effects in in BC patients will need to be evaluated in future studies.

One limitation of this study is that only the HERV-K(HML-2) family was evaluated. There are multiple other HERV families that could potentially be used for CAR-based adoptive immunotherapy. Another limitation is that metastasis was evaluated from primary xenograft tumors generated from cancer cell lines. Clinical trials are needed to determine the efficacy of K-CARs in humans.

MATERIALS AND METHODS

Study Design

Patient cells and samples were analyzed for various aspects of immune response, and data were analyzed in a blinded fashion. Samples were analyzed at least in triplicate, and experiments in

mice (n=5 per group) were independently replicated at least twice. Animal studies that gave similar results were used to arrive at conclusions.

Ethics Statement

Peripheral blood mononuclear cells (PBMCs) were obtained from cancer patients and NDs at MD Anderson Cancer Center according to an approved Institutional Review Board protocol (LAB04-0083) and written informed consent was provided by study participants and/or their legal guardians. Animal studies were carried out in accordance with the recommendations in the Guide for the Care and Use of Laboratory Animals of MD Anderson Cancer Center. The procedures employed herein were performed according to the Declaration of Helsinki.

Plasmids

The scFv sequence from mAb clone 6H5 (*25*) against HERV-K envelope protein was codon optimized (CoOp) (Invitrogen, Carlsbad, CA) and cloned into the SB transposon driven by the human elongation factor-1α (hEF-1α) promoter, flanked by SB inverted repeats forming $_{CoOp}$6H5CD28/pSBSO (a gift from Dr. Laurence Cooper, MD Anderson Cancer Center). The HERV-K full-length env sequence obtained from BC patient 37 (diagnosis of IDC; Fig. S2B), containing the viral surface and transmembrane domains of HERV-K *env*, was cloned into a pLVX-DsRed-Monomer-C1 vector (Clontech Laboratories, Inc).

Cell lines

MCF-7, SKBR3, MDA-MB-231 and MDA-MB-435.eB1 BC cell lines as well as HEK293, K562, and MCF-10A (immortalized breast epithelial cells) were obtained from the American

Type Culture Collection (Manassas, VA). MCF-10AT cells were a gift from Dr. Fred Miller at the Michigan Cancer Foundation. Cell lines were cultured in Roswell Park Memorial Institute medium (RPMI) or Dulbecco's modified eagle medium (DMEM; Thermo Scientific, Rockford, IL) with 10% fetal bovine serum (FBS; Thermo Scientific) and 5% GlutaMAX (Gibco Life Technologies, Grand Island, NY). All cell lines were tested and found to be mycoplasma free.

In vitro proliferation of HERV-K-specific CAR T cells

Peripheral blood mononuclear cells were isolated by Ficoll-Paque density gradient centrifugation as described previously (*26*) and electroporated with the SB system as described previously with some minor modifications (*28*). Briefly, PBMCs ($1x10^7$ per cuvette) were resuspended in 100 µl of Amaxa Nucleofector solution (Human T-cell Kit), mixed with 8 µg of 6H5scFvCD28mZ (CoOp/pSBSO) and 5 µg of pCMV-SB11, and electroporated using the U-14 program in an Amaxa Nucleofector® (Lonza, Allendale, NJ). K562 cells stably transduced with pLVX-Kenv to express HERV-K env protein were used as aAPC to propagate and generate K-CAR^+ T cells. After 4 hours of culture, the electroporated T cells were split to maintain suitable density and co-cultured with γ-irradiated (100 Gy) aAPC at a 1:2 T cell:aAPC ratio. The aAPCs were added twice weekly. Soluble IL-21 (eBioscience) and IL-2 (Chiron) cytokines were supplemented every other day at a concentration of 30 ng/mL and 50 U/ml, respectively, to complete RPMI media in the presence of OKT3 (0.5 µg/ml), as described previously (*28*). CAR^+ T cells were quantified weekly by FACS and were identified as those positive for both Fc and $CD3^+$ markers, as described previously (*28*). The PE-conjugated $F(ab')_2$ fragment of goat anti-human Fcγ was used for assessing Fc positivity. Control T cells were mock transfected without added DNA or GFP, as negative controls.

FACS analysis

6H5 mAb (1 μg/10^6 cells) was used to detect the expression of HERV-K in breast cell lines as described previously (*25*). Antibodies including PE-conjugated F(ab′)$_2$ fragment of goat anti-human Fcγ, Alexa Fluor® 647-anti-CD3, anti–CD4 PerCPCy5.5, anti–CD8 APC, anti–IFN-γ PE, anti–IL-2 PE, anti–TNF-α PE, anti-CD25 APC, and anti-FOXP3 PE (BD Biosciences) were used for FACS assays, as described previously (*25, 26*). Cells were washed twice, followed by blocking of nonspecific binding using FACS wash buffer (2% FBS and 0.1% sodium azide in phosphate-buffered saline). Flow cytometry was done multiple times on each sample to ascertain reproducibility of the results. FlowJo_V10 software (BD Biosciences) was used for the analysis of flow cytometry data.

Immunohistochemistry

Immunohistochemistry was carried out using a VECTASTAIN kit (Vector Laboratories) as described previously (*25, 26*). Briefly, slides were stained with 6H5 mAb or Ras Rabbit mAb (Cell Signaling Technology, 10 μg/ml; 100 μl per slide) at room temperature for 30 minutes, followed by diluted biotinylated secondary antibody and universal ABC Reagent. Freshly prepared DAB substrate-chromogen solution (DAKO) was applied until the desired stain intensity was achieved. Sections were rinsed in tap water, followed by counterstaining with giemsa, clearing and mounting.

$CD4^+$ lymphocyte depletion

$CD4^+$ lymphocyte depletion was carried out using $CD4^+$ beads (Miltenyi Biotech Inc., Auburn, CA) on an autoMACS Pro Separator (Miltenyi Biotech) according to the manufacturer's instructions. K-CAR T cells were depleted of CD4 T cells at 30 days post-electroporation and used for *in vivo* experiments. The percentage of $CD8^+$ and $CD4^+$ T cells in K-CAR T population was assessed by FACS.

Detection of K-CAR

Total RNA was isolated and purified from K-CAR^+ T cells as described previously (*22, 27*). Primers specific for 6H5 scFv [forward (5'- GAGGGCAACGTCTTTAGCTG-3') and reverse (5'-GATGATGAAGGCCACTGTCA-3')] were used for RT-PCR and the reaction conditions were as described previously (*26*). The 6H5 scFv plasmid served as the positive control.

Cytotoxic T lymphocyte (CTL) assay Cytolytic activity was measured using target cells labeled with the fluorescence-enhancing ligand DELFIA EuTDA, according to the manufacturer's instruction (Perkin-Elmer Life Sciences, Norwalk, CT). Fluorescence was measured using a Wallac Victor 2 Multilabel Counter (Perkin-Elmer). Percent specific release was calculated according to the following formula: %specific lysis = 100 × [(experimental release - spontaneous release) / (maximum release - spontaneous release)].

Cytokine release assay

HERV-K specific CAR T cells were co-cultured with tumor cells at various concentrations for 4 hours in a round-bottomed 96-well plate with 200 μl of complete RPMI culture medium. BD

Golgi Plug (1 μl/ml) was added to all wells to trap cytokines inside the cell. The cells were then washed, fixed and permeabilized with 100 μl of Cytofix/Cytoperm buffer (BD Biosciences) for 20 minutes at 4°C. Release of the intracellular cytokines that included IFN-γ, TNF-α and IL-2 was determined. The permeabilized cells were stained with PE-conjugated anti-IFN-γ, TNF-α, and IL-2 antibodies, and analyzed by FACS. PMA (10 ng/ml) plus ionomycin (200 ng/ml; BD Biosciences) treated T cells were used as positive controls for this assay. In addition, a cell-release capture ELISA was introduced to detect cellular production of IFN-γ, TNF-α, and Granzyme B as described previously (*26*). Absorbance was measured after 10 minutes of incubation in the dark, and the plate was read on a Wallac Victor 2 V Microplate Reader (PerkinElmer).

HERV-K *env* shRNA lentiviral packaging

shRNAs targeting the HERV-K *env* gene (shRNAenv; GenBank No. M14123.1) and matched scrambled shRNA sequences serving as negative controls (shRNAc) were designed using the Invitrogen RNAi Designer program, and cloned into the pGreenPuro™ vector (System Biosciences). Lentiviral particles expressing shRNA were then packaged and titered according to the manufacturer's instructions. RT-PCR, qRT-PCR, FACS, and immunoblot were subsequently performed to determine the expression of HERV-K env RNA or protein in cell lines.

Immunoblot analysis

Total protein lysates of cells or tissues were used for immunoblot analysis as described previously (*37, 38*). Anti-HERV-K mAb 6H5, anti-human tumor protein p53 (TP53, 1 μg/mL

final concentration), phospho-p44./p\42 MAP kinase (Erk1/2) and p44./p\42 MAP kinase (Erk1/2) (137F5) (Cell Signaling Technology), TP53-regulated apoptosis–inducing protein-1 (TP53AIP1, 1 μg/mL) (Abcam), MDM2 (1:1,000 dilution; Sigma-Aldrich), and β-Actin antibodies (1:1,000 dilution; University of Iowa) were used as primary antibodies. β-Actin was used as the internal positive control for all immunoblots. Immunoreactive bands were detected with anti-mIgG-horseradish peroxidase (1:5,000 dilution; Sigma-Aldrich, St. Louis, MO), which served as the secondary antibody. The protein levels were quantified by ImageJ software (NIH, Bethesda, MD; http://rsb.info.nih.gov/ij).

Alamar Blue Assay of Cell Viability

Cells were seeded in flat-bottomed 96-well culture plates at a density of 1×10^4 cells/well. Ten μl of Alamar Blue (AbD Serotec, U.K.) was then added to each well and cells were co-cultured with HERV-K specific CAR T cells at various ratios. The plates were incubated and the fluorescence intensity was measured at different time points using a Victor 1402 multilabel counter (Wallac). The cell viability was proportional to the amount of fluorescence.

Cancer Stem Cell Culture

For growing tumorspheres in suspension, trypsinized cells (MDA-MB-435.eB1) and patients' tumor cells were cultured on ultra-low attachment tissue culture plates with stem cell culture medium under 5% CO_2 at 37°C, as described previously (*39-41*).

Live/Dead Viability/Cytotoxicity tests

To assess the cytotoxicity of CAR T cells toward targets, cell viability was investigated using a live/dead viability/cytotoxicity kit (Invitrogen, Carlsbad, CA). Nonfluorescent cell-permeant calcein acetoxymethyl ester AM is converted to intensely fluorescent calcein in the presence of intracellular esterase activity; the calcein is well retained within live cells and produces green fluorescence. Ethidium homodimer-1 penetrates cells with membrane damage and binds to nucleic acids to produce red fluorescence in dead cells. Staining was performed according to the manufacturer's instructions. Adequate negative (cells without treatment) and positive (cells treated with 0.3% Triton X-100 detergent; Serva, Heidelberg, Germany) controls for cell death were run with each set of experiments. Cell viability was also analyzed by fluorescence microscopy after 24 hours of incubation. Green and red cells were counted per eight fields at 200-fold magnification for calculation of the percentage of dead cells.

In vivo antitumor activity of HERV-K-CAR T cells

Eight-week-old female NOD/SCID mice were injected with 1×10^6 BC cells subcutaneously in both flanks. Another model was created by subcutaneous injection of 2×10^6 MDA-MB-435.eB1 cells in both flanks. Mice (n=5) received $1x10^6$ K-CAR cells by intravenous infusion starting on days 5 and 13 post-injection. On day 20 post-injection of BC cells, $1x10^7$ K-CAR cells were infused, followed by 600 U of IL-2 (eBioscience), which was injected intraperitoneally and intravenously once a week during the treatment period. One cohort of mice (n=5) bearing the tumor received no treatment as a blank control group. The other four cohorts were treated with IL-2, PBMC, PBMC plus IL-2, and control T cells, respectively. When tumors became measurable, tumor size was calculated and growth rates measured twice weekly. Mice were euthanized when tumor volumes exceeded 1000 mm^3. Fresh lung, liver, bone, brain, pleural lavage fluid, and axillary lymph nodes were then extracted, weighed, and evaluated for

metastases. RNA and protein were isolated from both groups and the expression of HERV-K env RNA was determined by qRT-PCR and immunoblot. qRT-PCR was carried out using the TaqMan® One-Step RT-PCR Master Mix Reagents Kit (Applied Biosystems, CA). The expression level of GAPDH gene was used as an internal control. The relative gene expression levels were quantified by the $2^{(-\Delta\Delta CT)}$ method as described (*42*).

Statistical Analysis

Data are expressed as means ± SD, and were analyzed by Student's t test when only two groups were examined or by using one-way analysis of variance when more than two groups were examined. All statistical tests were two-sided, and all *P* values less than 0.05 were considered statistically significant, as determined using Graph Pad Prism software (GraphPad Software Inc., San Diego, CA) or IBM SPSS Statistics software, release 19.0.0 (2010, IBM Corporation).

References and Notes

1. G. Dotti *et al.*, Adenovector-induced expression of human-CD40-ligand (hCD40L) by multiple myeloma cells. A model for immunotherapy. *Experimental hematology* **29**, 952 (Aug, 2001).
2. F. Mami-Chouaib, H. Echchakir, G. Dorothee, I. Vergnon, S. Chouaib, Antitumor cytotoxic T-lymphocyte response in human lung carcinoma: identification of a tumor-associated antigen. *Immunological reviews* **188**, 114 (Oct, 2002).
3. D. M. Davies, J. Maher, Adoptive T-cell immunotherapy of cancer using chimeric antigen receptor-grafted T cells. *Archivum immunologiae et therapiae experimentalis* **58**, 165 (Jun, 2010).
4. M. Sun *et al.*, Construction and evaluation of a novel humanized HER2-specific chimeric receptor. *Breast cancer research : BCR* **16**, R61 (Jun 11, 2014).
5. E. Lanitis *et al.*, Chimeric antigen receptor T Cells with dissociated signaling domains exhibit focused antitumor activity with reduced potential for toxicity in vivo. *Cancer immunology research* **1**, 43 (Jul, 2013).

6. H. Singh, H. Huls, P. Kebriaei, L. J. Cooper, A new approach to gene therapy using Sleeping Beauty to genetically modify clinical-grade T cells to target CD19. *Immunological reviews* **257**, 181 (Jan, 2014).
7. B. Jena *et al.*, Chimeric antigen receptor (CAR)-specific monoclonal antibody to detect CD19-specific T cells in clinical trials. *PloS one* **8**, e57838 (2013).
8. M. Kalos *et al.*, T cells with chimeric antigen receptors have potent antitumor effects and can establish memory in patients with advanced leukemia. *Science translational medicine* **3**, 95ra73 (Aug 10, 2011).
9. R. A. Morgan *et al.*, Case report of a serious adverse event following the administration of T cells transduced with a chimeric antigen receptor recognizing ERBB2. *Molecular therapy : the journal of the American Society of Gene Therapy* **18**, 843 (Apr, 2010).
10. L. E. Kandalaft, D. J. Powell, Jr., G. Coukos, A phase I clinical trial of adoptive transfer of folate receptor-alpha redirected autologous T cells for recurrent ovarian cancer. *Journal of translational medicine* **10**, 157 (2012).
11. C. Schlimper, A. A. Hombach, H. Abken, I. G. Schmidt-Wolf, Improved activation toward primary colorectal cancer cells by antigen-specific targeting autologous cytokine-induced killer cells. *Clinical & developmental immunology* **2012**, 238924 (2012).
12. C. C. Kloss, M. Condomines, M. Cartellieri, M. Bachmann, M. Sadelain, Combinatorial antigen recognition with balanced signaling promotes selective tumor eradication by engineered T cells. *Nature biotechnology* **31**, 71 (Jan, 2013).
13. C. H. Lamers *et al.*, Treatment of metastatic renal cell carcinoma with CAIX CAR-engineered T cells: clinical evaluation and management of on-target toxicity. *Molecular therapy : the journal of the American Society of Gene Therapy* **21**, 904 (Apr, 2013).
14. G. Kassiotis, Endogenous retroviruses and the development of cancer. *J Immunol* **192**, 1343 (Feb 15, 2014).
15. H. H. Kazazian, Jr., Mobile elements: drivers of genome evolution. *Science* **303**, 1626 (Mar 12, 2004).
16. E. S. Lander, Initial impact of the sequencing of the human genome. *Nature* **470**, 187 (Feb 10, 2011).
17. K. Ahn, H. S. Kim, Structural and quantitative expression analyses of HERV gene family in human tissues. *Mol Cells* **28**, 99 (Aug 31, 2009).
18. J. P. Stoye, Studies of endogenous retroviruses reveal a continuing evolutionary saga. *Nat Rev Microbiol* **10**, 395 (Jun, 2012).
19. K. Reus *et al.*, HERV-K(OLD): ancestor sequences of the human endogenous retrovirus family HERV-K(HML-2). *J Virol* **75**, 8917 (Oct, 2001).
20. O. Hohn, K. Hanke, N. Bannert, HERV-K(HML-2), the Best Preserved Family of HERVs: Endogenization, Expression, and Implications in Health and Disease. *Front Oncol* **3**, 246 (2013).
21. R. Contreras-Galindo *et al.*, Human endogenous retrovirus K (HML-2) elements in the plasma of people with lymphoma and breast cancer. *J Virol* **82**, 9329 (Oct, 2008).
22. F. Wang-Johanning *et al.*, Quantitation of HERV-K env gene expression and splicing in human breast cancer. *Oncogene* **22**, 1528 (Mar 13, 2003).
23. J. Zhao *et al.*, Expression of Human Endogenous Retrovirus Type K Envelope Protein is a Novel Candidate Prognostic Marker for Human Breast Cancer. *Genes & cancer* **2**, 914 (Sep, 2011).

24. F. Wang-Johanning *et al.*, Human endogenous retrovirus type K antibodies and mRNA as serum biomarkers of early-stage breast cancer. *International journal of cancer. Journal international du cancer* **134**, 587 (Feb 1, 2014).
25. F. Wang-Johanning *et al.*, Immunotherapeutic potential of anti-human endogenous retrovirus-K envelope protein antibodies in targeting breast tumors. *Journal of the National Cancer Institute* **104**, 189 (Feb 8, 2012).
26. F. Wang-Johanning *et al.*, Human endogenous retrovirus K triggers an antigen-specific immune response in breast cancer patients. *Cancer research* **68**, 5869 (Jul 15, 2008).
27. F. Wang-Johanning *et al.*, Expression of human endogenous retrovirus k envelope transcripts in human breast cancer. *Clinical cancer research : an official journal of the American Association for Cancer Research* **7**, 1553 (Jun, 2001).
28. S. N. Maiti *et al.*, Sleeping beauty system to redirect T-cell specificity for human applications. *J Immunother* **36**, 112 (Feb, 2013).
29. J. N. Kochenderfer *et al.*, B-cell depletion and remissions of malignancy along with cytokine-associated toxicity in a clinical trial of anti-CD19 chimeric-antigen-receptor-transduced T cells. *Blood* **119**, 2709 (Mar 22, 2012).
30. H. Torikai *et al.*, A foundation for universal T-cell based immunotherapy: T cells engineered to express a CD19-specific chimeric-antigen-receptor and eliminate expression of endogenous TCR. *Blood* **119**, 5697 (Jun 14, 2012).
31. P. Kebriaei *et al.*, Infusing CD19-directed T cells to augment disease control in patients undergoing autologous hematopoietic stem-cell transplantation for advanced B-lymphoid malignancies. *Human gene therapy* **23**, 444 (May, 2012).
32. H. Singh *et al.*, Redirecting specificity of T-cell populations for CD19 using the Sleeping Beauty system. *Cancer research* **68**, 2961 (Apr 15, 2008).
33. S. Spranger *et al.*, Up-regulation of PD-L1, IDO, and T(regs) in the melanoma tumor microenvironment is driven by CD8(+) T cells. *Science translational medicine* **5**, 200ra116 (Aug 28, 2013).
34. J. Kline *et al.*, Homeostatic proliferation plus regulatory T-cell depletion promotes potent rejection of B16 melanoma. *Clinical cancer research : an official journal of the American Association for Cancer Research* **14**, 3156 (May 15, 2008).
35. A. P. Gulati *et al.*, Mutant human tumor suppressor p53 modulates the activation of mitogen-activated protein kinase and nuclear factor-kappaB, but not c-Jun N-terminal kinase and activated protein-1. *Molecular carcinogenesis* **45**, 26 (Jan, 2006).
36. G. Huang, Z. Li, X. Wan, Y. Wang, J. Dong, Human endogenous retroviral K element encodes fusogenic activity in melanoma cells. *Journal of carcinogenesis* **12**, 5 (2013).
37. Y. Pan, F. Zhou, R. Zhang, F. X. Claret, Stat3 inhibitor Stattic exhibits potent antitumor activity and induces chemo- and radio-sensitivity in nasopharyngeal carcinoma. *PLoS One* **8**, e54565 (2013).
38. Y. Pan, Q. Zhang, V. Atsaves, H. Yang, F. X. Claret, Suppression of Jab1/CSN5 induces radio- and chemo-sensitivity in nasopharyngeal carcinoma through changes to the DNA damage and repair pathways. *Oncogene* **32**, 2756 (May 30, 2013).
39. F. Yu *et al.*, Kruppel-like factor 4 (KLF4) is required for maintenance of breast cancer stem cells and for cell migration and invasion. *Oncogene* **30**, 2161 (May 5, 2011).
40. P. B. Gupta *et al.*, Identification of selective inhibitors of cancer stem cells by high-throughput screening. *Cell* **138**, 645 (Aug 21, 2009).

41. X. Yang, S. K. Sarvestani, S. Moeinzadeh, X. He, E. Jabbari, Effect of CD44 binding peptide conjugated to an engineered inert matrix on maintenance of breast cancer stem cells and tumorsphere formation. *PLoS One* **8**, e59147 (2013).
42. K. J. Livak, T. D. Schmittgen, Analysis of relative gene expression data using real-time quantitative PCR and the 2(-Delta Delta C(T)) Method. *Methods* **25**, 402 (Dec, 2001).

Acknowledgments:

This work was supported in part by grant BC113114 from the United States Department of Defense, grant ES007784 from the National Institute of Environmental Health Sciences, and grants 07-2007-070 01 (GLJ) and 02-2011-104 (FWJ) from the Avon Foundation for Women. We thank Dr. Perry Hackett for his permission to use SB system in our study, Dr. Danielle Lu for pathologic analysis of mouse tumors, and Dr. Nathalie Scholler for reviewing the manuscript. No potential conflicts of interest were disclosed by any of the authors.

Author contributions: LJNC and FWJ conceptualized the study. FWJ designed the overall study, provided advice, interpreted data, and participated in writing the manuscript. FZ participated in study design, performed the major experiments involving K-CAR and *in vitro* and *in vivo* experiments, and participated in writing the manuscript. JK initiated and optimized the study design of some experiments. ML designed and cloned the shRNA and the pLVX-K env plasmids, and performed experiments involving these plasmids; YW contributed to immune assays and *in vivo* experiments. KH provided breast cancer patient samples and clinical information. GLJ assisted in designing experiments and interpreting data, and participated in writing the manuscript.

After publication, all data necessary to understand, assess, and extend the conclusions of the manuscript will be made available in the body of the paper, in the Supplementary Materials, or archived in an approved database.

Figure Legends:

Fig. 1A

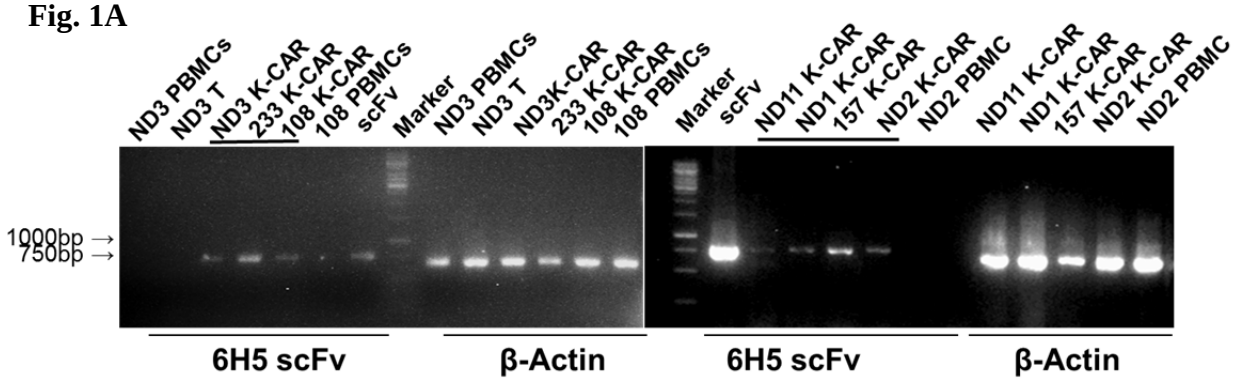

Fig. 1B

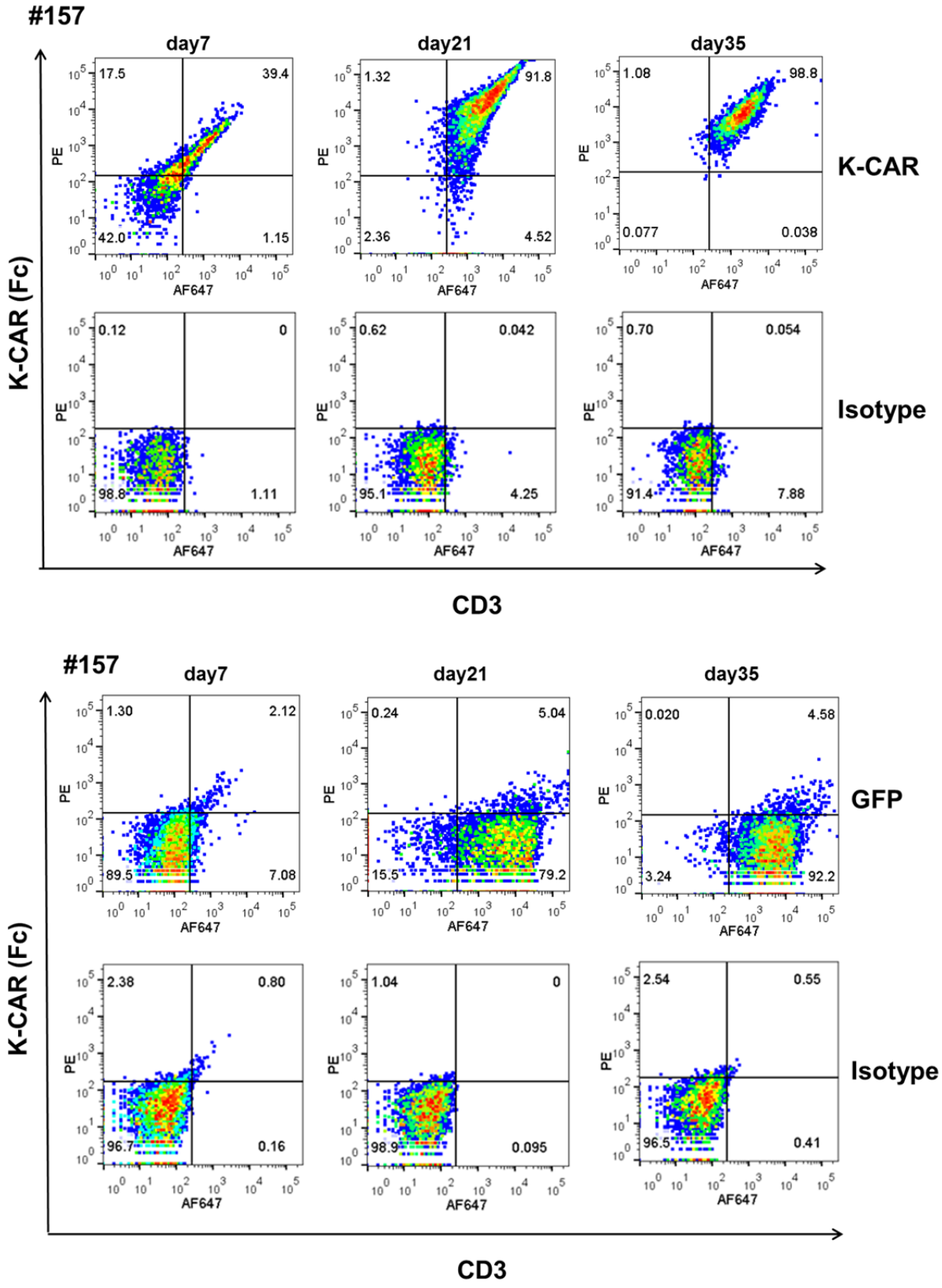
#157
day7
day21
day35
K-CAR
Isotype
K-CAR (Fc)
CD3
PE
AF647
17.5
39.4
42.0
1.15
1.32
91.8
2.36
4.52
1.08
98.8
0.077
0.038
0.12
0
98.8
1.11
0.62
0.042
95.1
4.25
0.70
0.054
91.4
7.88
#157
day7
day21
day35
GFP
Isotype
K-CAR (Fc)
CD3
PE
AF647
1.30
2.12
89.5
7.08
0.24
5.04
15.5
79.2
0.020
4.58
3.24
92.2
2.38
0.80
96.7
0.16
1.04
0
98.9
0.095
2.54
0.55
96.5
0.41

Fig. 1C

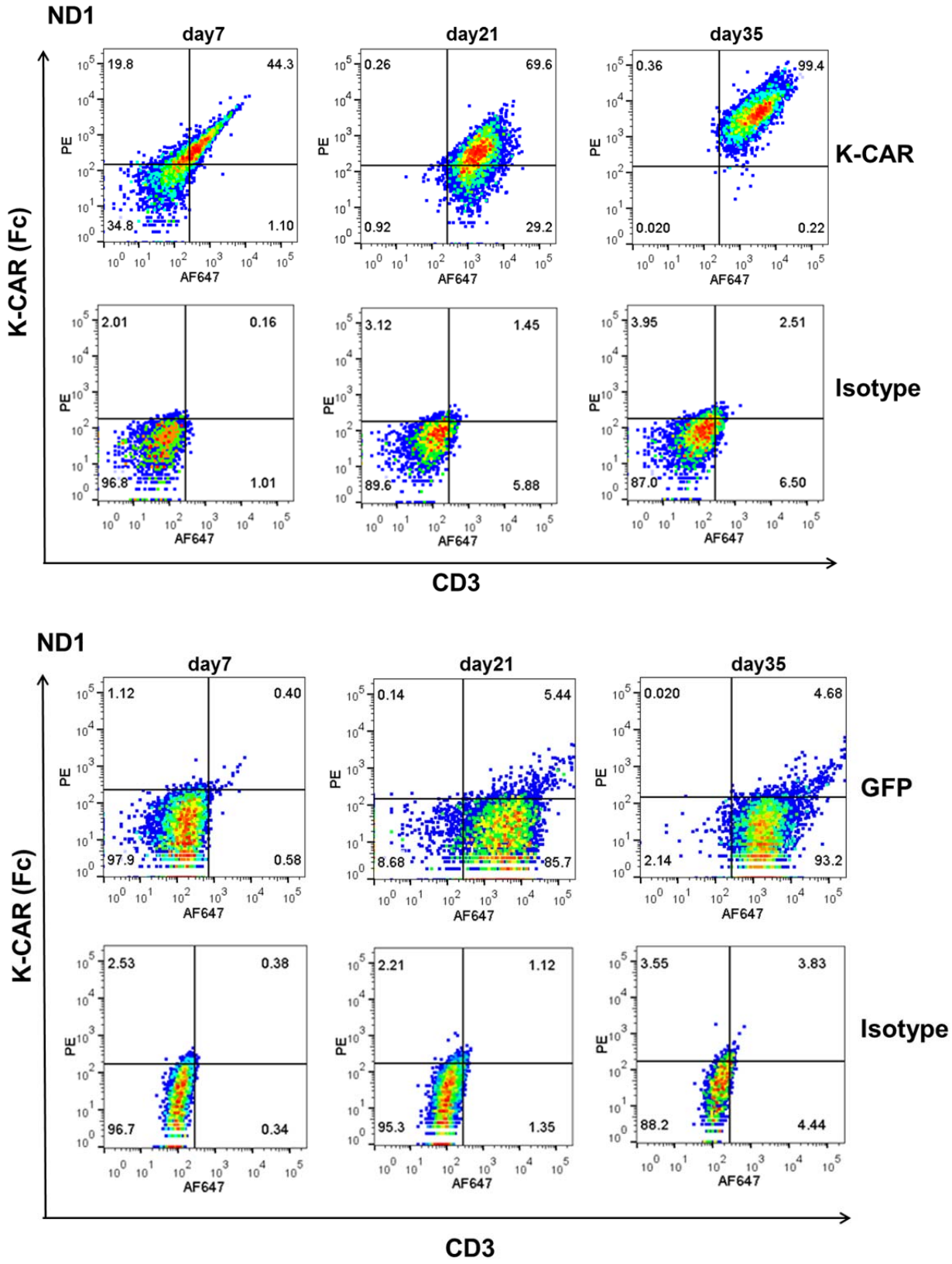
ND1
day7
day21
day35
K-CAR
Isotype
K-CAR (Fc)
CD3
PE
AF647
19.8
44.3
34.8
1.10
0.26
69.6
0.92
29.2
0.36
99.4
0.020
0.22
2.01
0.16
96.8
1.01
3.12
1.45
89.6
5.88
3.95
2.51
87.0
6.50
ND1
day7
day21
day35
GFP
Isotype
K-CAR (Fc)
CD3
1.12
0.40
97.9
0.58
0.14
5.44
8.68
85.7
0.020
4.68
2.14
93.2
2.53
0.38
96.7
0.34
2.21
1.12
95.3
1.35
3.55
3.83
88.2
4.44

Fig. 1C

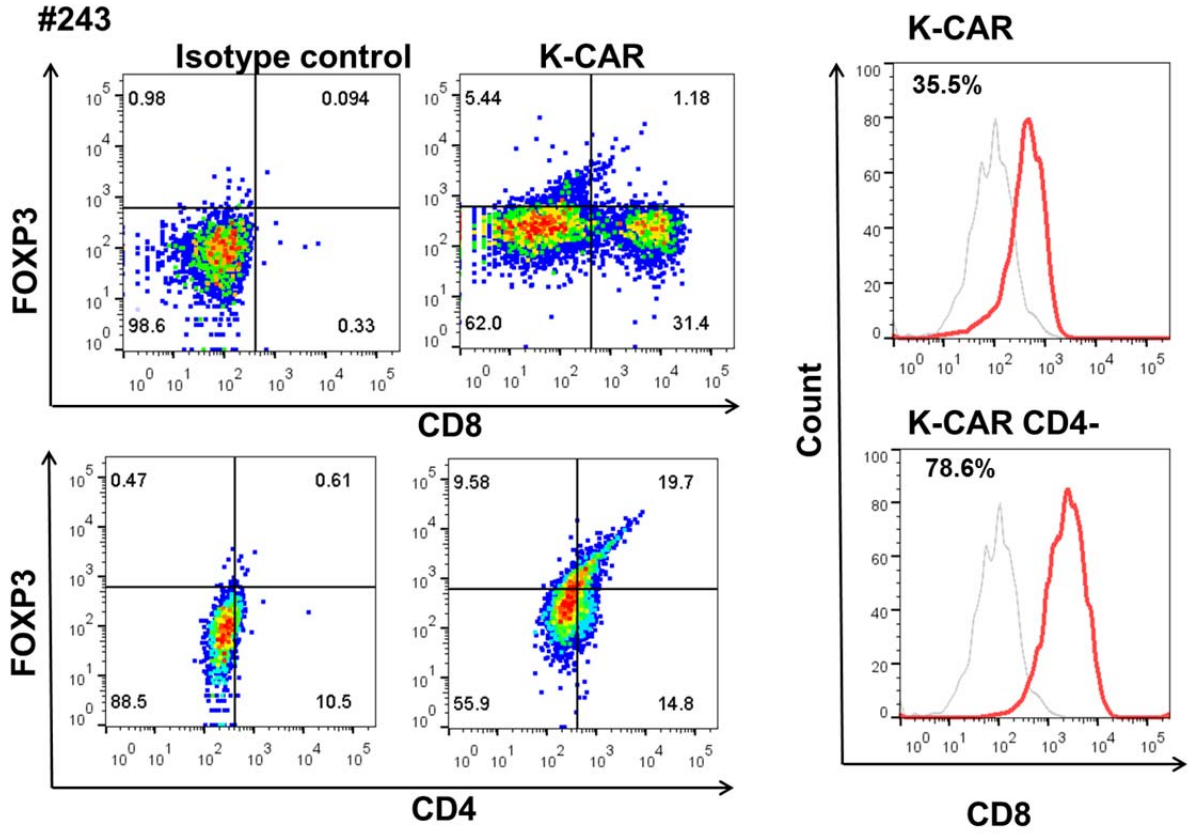
#243
Isotype control
K-CAR
0.98
0.094
98.6
0.33
5.44
1.18
62.0
31.4
FOXP3
CD8
0.47
0.61
88.5
10.5
9.58
19.7
55.9
14.8
FOXP3
CD4
K-CAR
35.5%
K-CAR CD4-
78.6%
Count
CD8

Fig. 1D

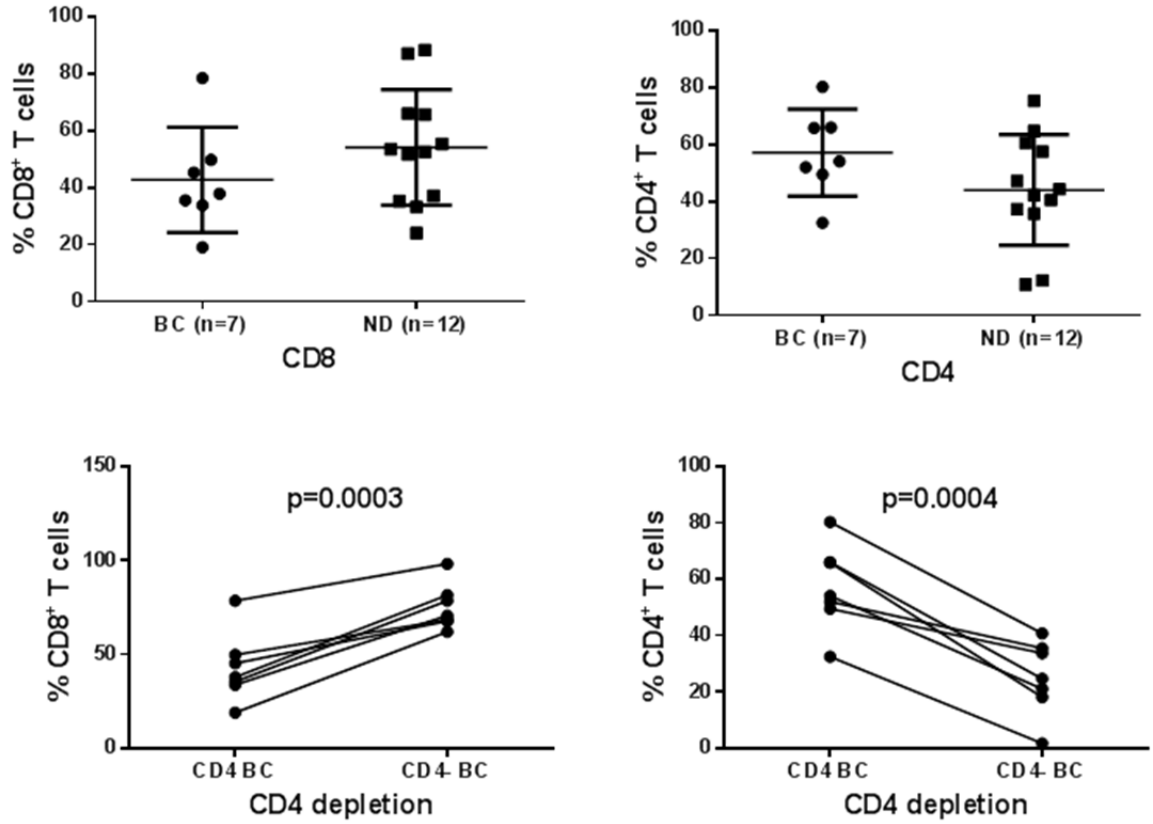
% CD8+ T cells
100
80
60
40
20
0
BC (n=7)
ND (n=12)
CD8
% CD4+ T cells
100
80
60
40
20
0
BC (n=7)
ND (n=12)
CD4
% CD8+ T cells
150
100
50
0
p=0.0003
CD4 BC
CD4- BC
CD4 depletion
% CD4+ T cells
100
80
60
40
20
0
p=0.0004
CD4 BC
CD4- BC
CD4 depletion

Fig. 1 Characterization of K-CAR in various donors. A) RT-PCR was employed to detect the expression of 6H5 scFv (700 bp) using scFv specific primers. Amplified β-actin was used as a loading control, and scFv plasmid was used as a positive control. Expression of 6H5 scFv was demonstrated in K-CAR T cells obtained from BC patients and NDs. No scFv expression was detected in control T cells or PBMCs. B) Both Fc^+ and $CD3^+$ T cell populations were determined in T cells transfected with K-CAR or GFP from patient 157 (top panel) and ND1 (bottom panel) by FACS using anti-Fc and CD3 antibodies on days 7, 21 and 35 post-transfection. The isotype alone was used as control. C) Both $FOXP3^+$ and $CD8^+$ or $CD4^+$ T cells from BC patient 243 were determined by FACS (left panel). The percentage of $CD8^+$ T cells was increased in K-CAR T cells after CD4 depletion (right panel). D) Lower percentages of $CD8^+$ and higher percentages of $CD4^+$ T cells were demonstrated in K-CAR T cells obtained from BC patients than from NDs (top panel). Significantly enhanced $CD8^+$ (P=0.0003) and reduced $CD4^+$ (P=0.0004) T cell populations were demonstrated in T cells from BC patients (n=7) after CD4 depletion.

Fig. 2A

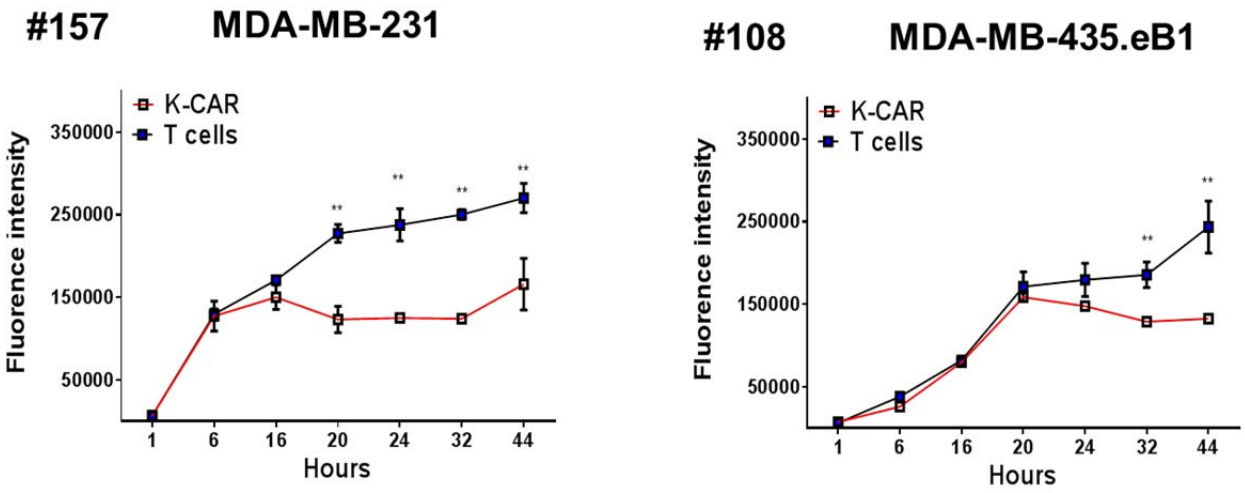
#157
MDA-MB-231
K-CAR
T cells
Fluorence intensity
350000
250000
150000
50000
1
6
16
20
24
32
44
Hours
#108
MDA-MB-435.eB1
K-CAR
T cells
Fluorence intensity
350000
250000
150000
50000
1
6
16
20
24
32
44
Hours

Fig. 2B

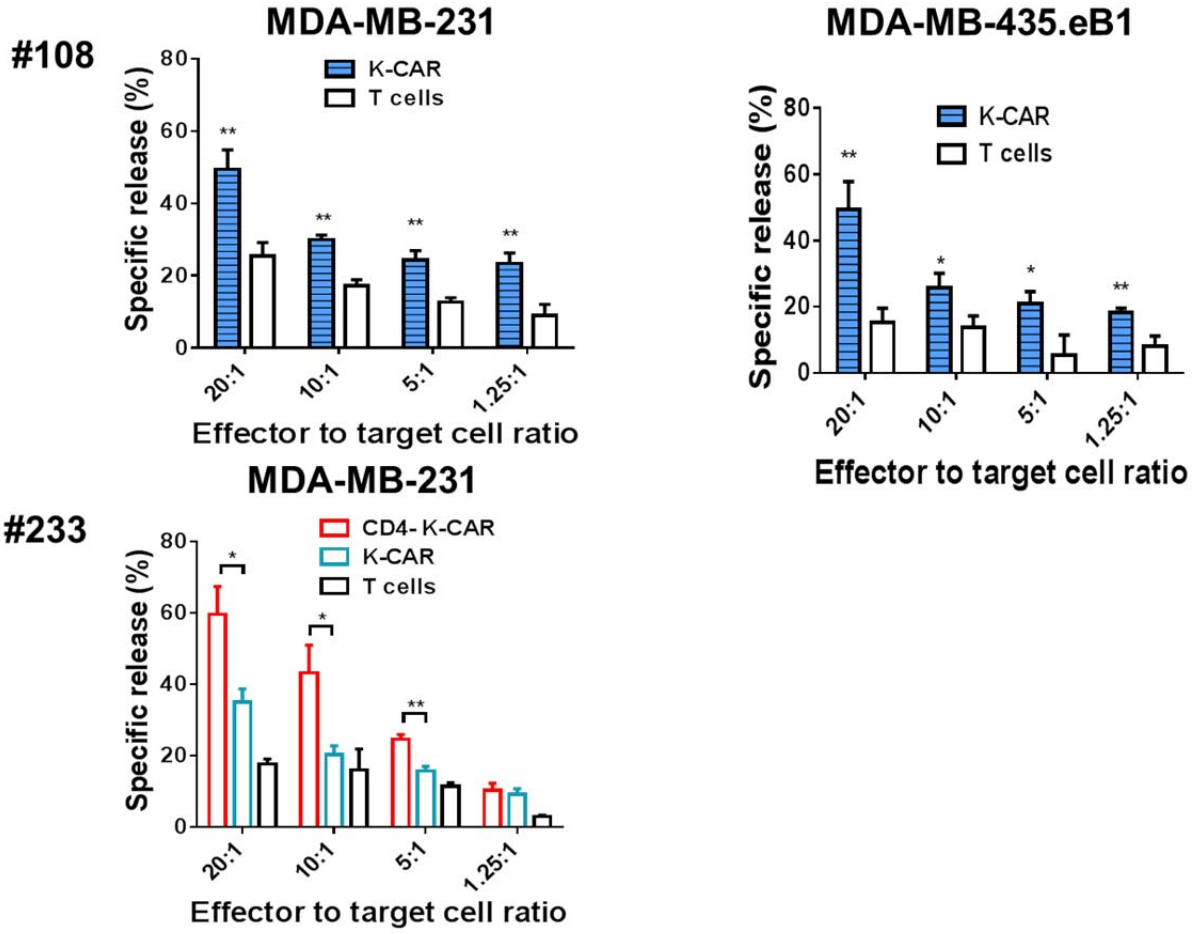
#108
MDA-MB-231
K-CAR
T cells
Specific release (%)
80
60
40
20
0
20:1
10:1
5:1
1.25:1
Effector to target cell ratio
MDA-MB-435.eB1
K-CAR
T cells
Specific release (%)
Effector to target cell ratio
#233
MDA-MB-231
CD4- K-CAR
K-CAR
T cells
Specific release (%)
Effector to target cell ratio

Fig. 2C

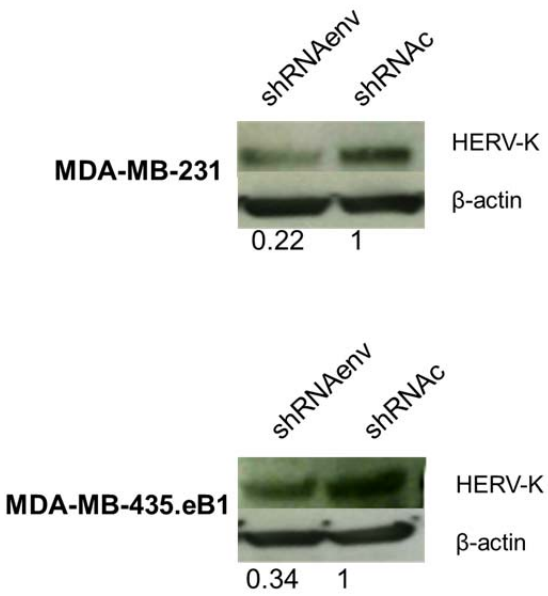
shRNAenv
shRNAc
MDA-MB-231
HERV-K
β-actin
0.22 1
shRNAenv
shRNAc
MDA-MB-435.eB1
HERV-K
β-actin
0.34 1

Fig. 2D

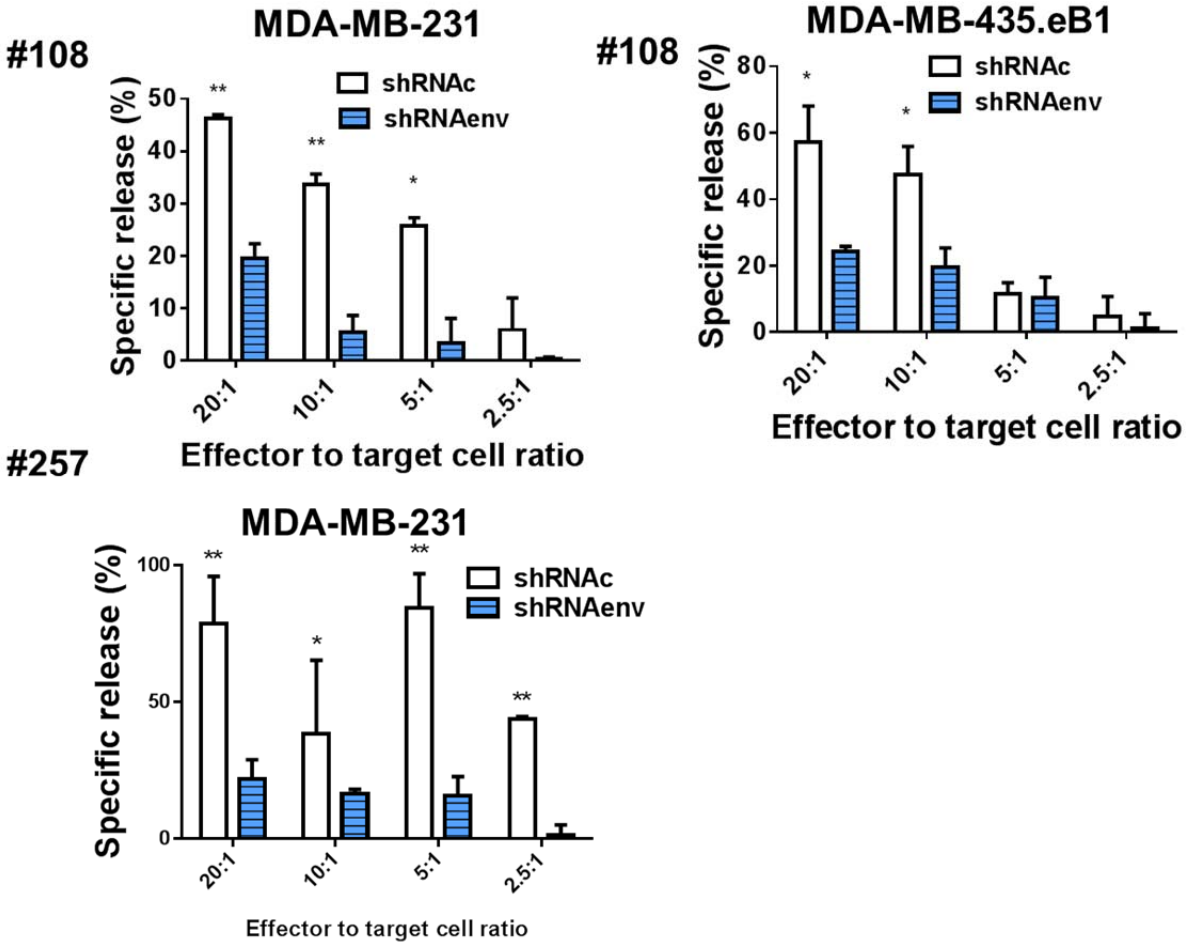
#108
MDA-MB-231
shRNAc
shRNAenv
Specific release (%)
Effector to target cell ratio
20:1
10:1
5:1
2.5:1
#108
MDA-MB-435.eB1
shRNAc
shRNAenv
Specific release (%)
Effector to target cell ratio
#257
MDA-MB-231
shRNAc
shRNAenv
Specific release (%)
Effector to target cell ratio

Fig. 2 Detection of anti-tumor effects *in vitro*: A) Inhibition of BC cell growth was observed when these cells were treated with K-CARs from patients (157 and 108), using the Alamar Blue assay. B) CTL assays were employed to determine the cytotoxicity of K-CAR toward BC cells at various ratios of effector to target. Significantly greater lysis was demonstrated in both cell lines using K-CAR from patient 108 (top panel). Enhanced specific lysis was observed in MDA-MB-231 cells using K-CAR from patient 233 with $CD4^+$ T depletion (CD4-K-CAR), compared to no depletion of $CD4^+$ T cells (K-CAR; bottom panel). C) The expression of HERV-K was determined in BC cell lines transduced with a shRNAenv or control shRNAc by immunoblot assays using 6H5 mAb. Expression of HERV-K protein was downregulated by approximately 70 to 80%, compared to the expression level of shRNAc transduced cells. D) The specific lysis of K-CAR T cells from patients 108 and 257 or NDs (ND8 or ND10) was reduced in BC target cells stably transduced with shRNAenv compared with shRNAc. This result indicates that specific lysis is antigen-dependent.

Fig. 3A

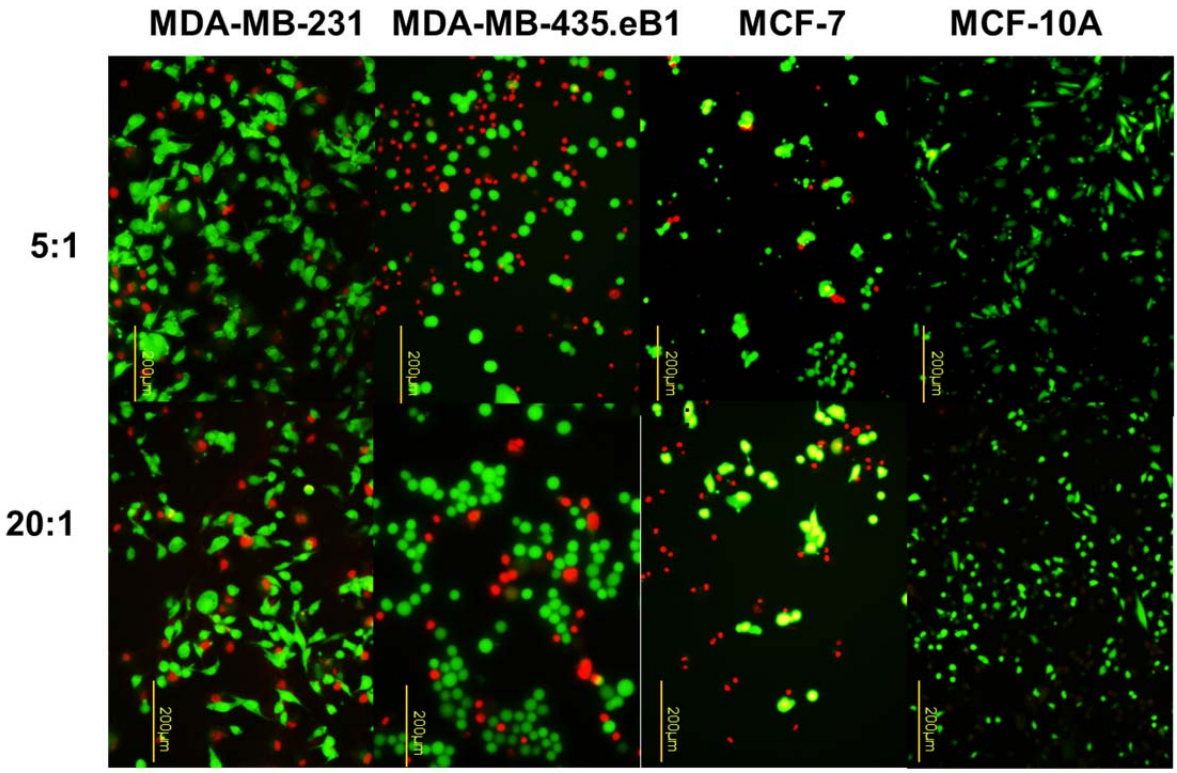
MDA-MB-231
MDA-MB-435.eB1
MCF-7
MCF-10A
5:1
20:1
200µm

Fig. 3B

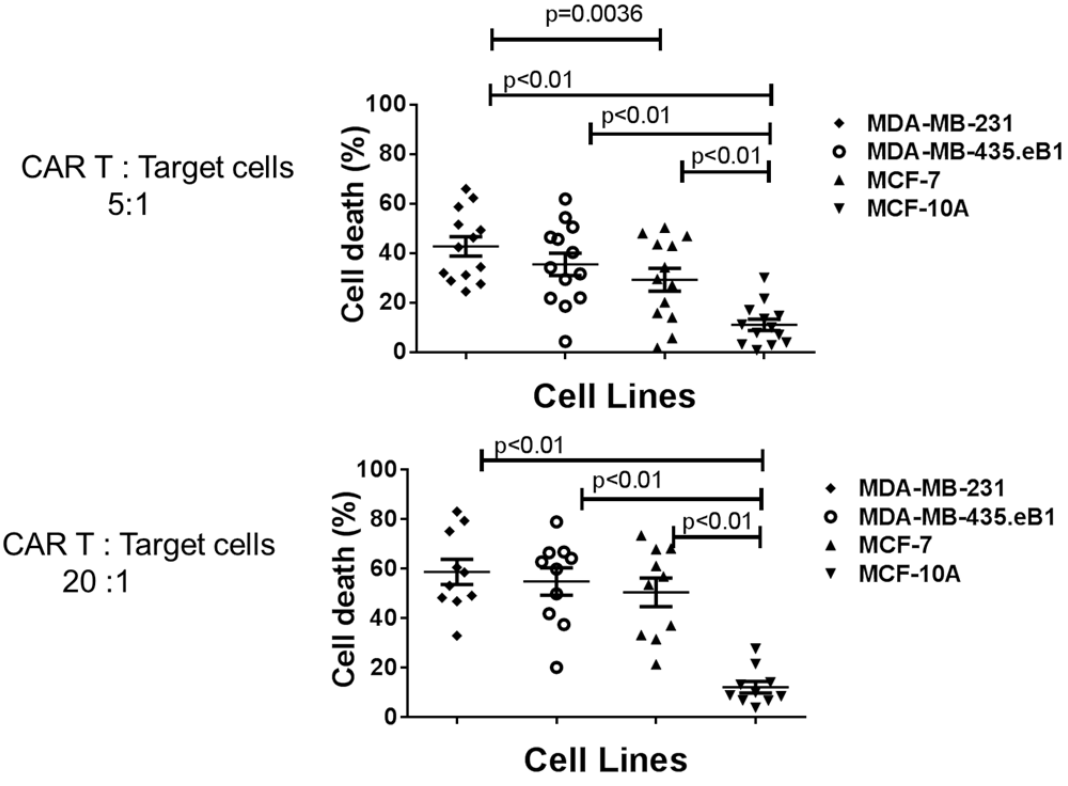
CAR T : Target cells
5:1
p=0.0036
p<0.01
p<0.01
p<0.01
Cell death (%)
100
80
60
40
20
0
Cell Lines
MDA-MB-231
MDA-MB-435.eB1
MCF-7
MCF-10A
CAR T : Target cells
20 :1
p<0.01
p<0.01
p<0.01
Cell death (%)
100
80
60
40
20
0
Cell Lines
MDA-MB-231
MDA-MB-435.eB1
MCF-7
MCF-10A

Fig. 3C

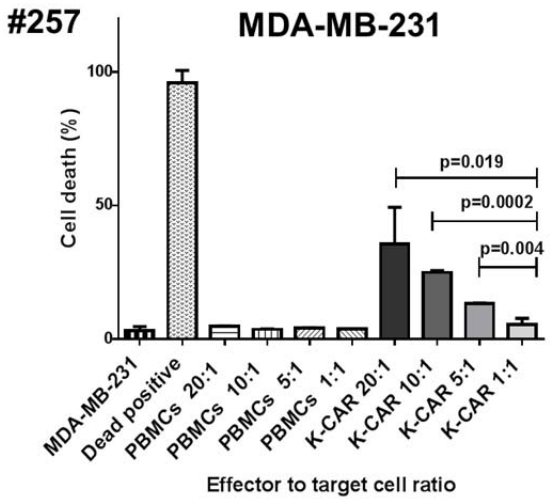
#257
MDA-MB-231
Cell death (%)
100
50
0
p=0.019
p=0.0002
p=0.004
MDA-MB-231
Dead positive
PBMCs 20:1
PBMCs 10:1
PBMCs 5:1
PBMCs 1:1
K-CAR 20:1
K-CAR 10:1
K-CAR 5:1
K-CAR 1:1
Effector to target cell ratio

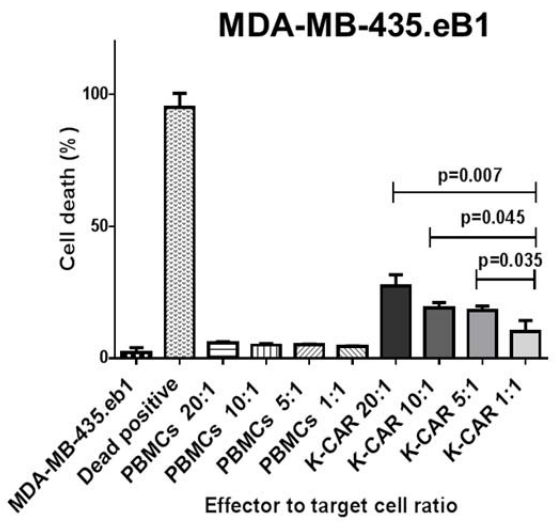
MDA-MB-435.eB1
Cell death (%)
100
50
0
p=0.007
p=0.045
p=0.035
MDA-MB-435.eb1
Dead positive
PBMCs 20:1
PBMCs 10:1
PBMCs 5:1
PBMCs 1:1
K-CAR 20:1
K-CAR 10:1
K-CAR 5:1
K-CAR 1:1
Effector to target cell ratio

Fig. 3D

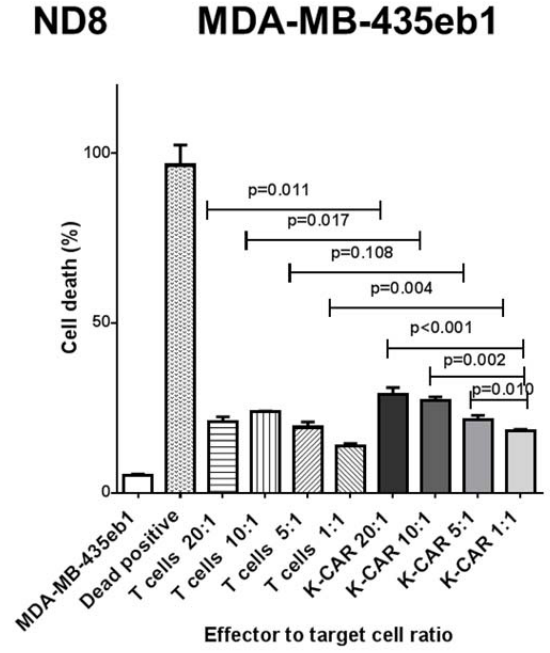
ND8
MDA-MB-435eb1
Cell death (%)
100
50
0
p=0.011
p=0.017
p=0.108
p=0.004
p<0.001
p=0.002
p=0.010
MDA-MB-435eb1
Dead positive
T cells 20:1
T cells 10:1
T cells 5:1
T cells 1:1
K-CAR 20:1
K-CAR 10:1
K-CAR 5:1
K-CAR 1:1
Effector to target cell ratio

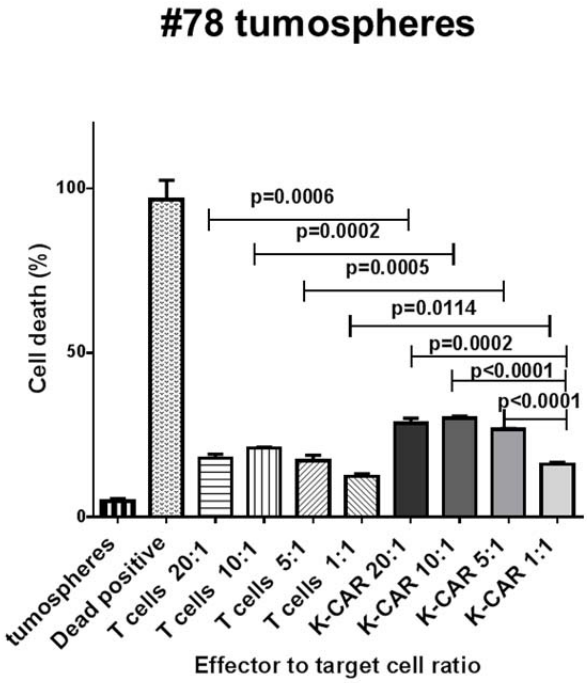
#78 tumospheres
Cell death (%)
100
50
0
p=0.0006
p=0.0002
p=0.0005
p=0.0114
p=0.0002
p<0.0001
p<0.0001
tumospheres
Dead positive
T cells 20:1
T cells 10:1
T cells 5:1
T cells 1:1
K-CAR 20:1
K-CAR 10:1
K-CAR 5:1
K-CAR 1:1
Effector to target cell ratio

Fig. 3 Specificity of cell death assay of K-CAR: A) Target cells were loaded with K-CAR (5:1 ratio of K-CAR T cells to target cells, top panel; or 20:1 ratio, bottom panel) for 4 hours. Live cells (green color) and putative dead cells (red color) were identified using the co-stained Live/Dead Viability Assay. EthD-1 penetrates cells with membrane damage and binds to nucleic acids to produce red fluorescence in dead cells. B) Significantly greater numbers of dead cells were found in K-CAR-treated BC cells compared with MCF-10A after random counts of eight fields per well. Cell death was greatest in BC cells that had higher expression of HERV-K env protein (MDA-MB-231>MDA-MB-435.eB1>MCF-7>MCF-10A). C) Cell viability was also analyzed by FACS. The percentage of dead target cells increased with the ratio of K-CAR T cells to target cells for patient 257 (Fig. 3C) or ND8 (Fig. 3D), but not with the ratio of PBMC (Fig. 3C) or control T cells (Fig. 3D) to target cells. Primary tumorspheres grown from a tumor biopsy of patient 78 were used as target cells in Fig. 3D (right panel). Target cells treated with 0.3% Triton X-100 detergent were used as positive controls for cell death.

Fig. 4A

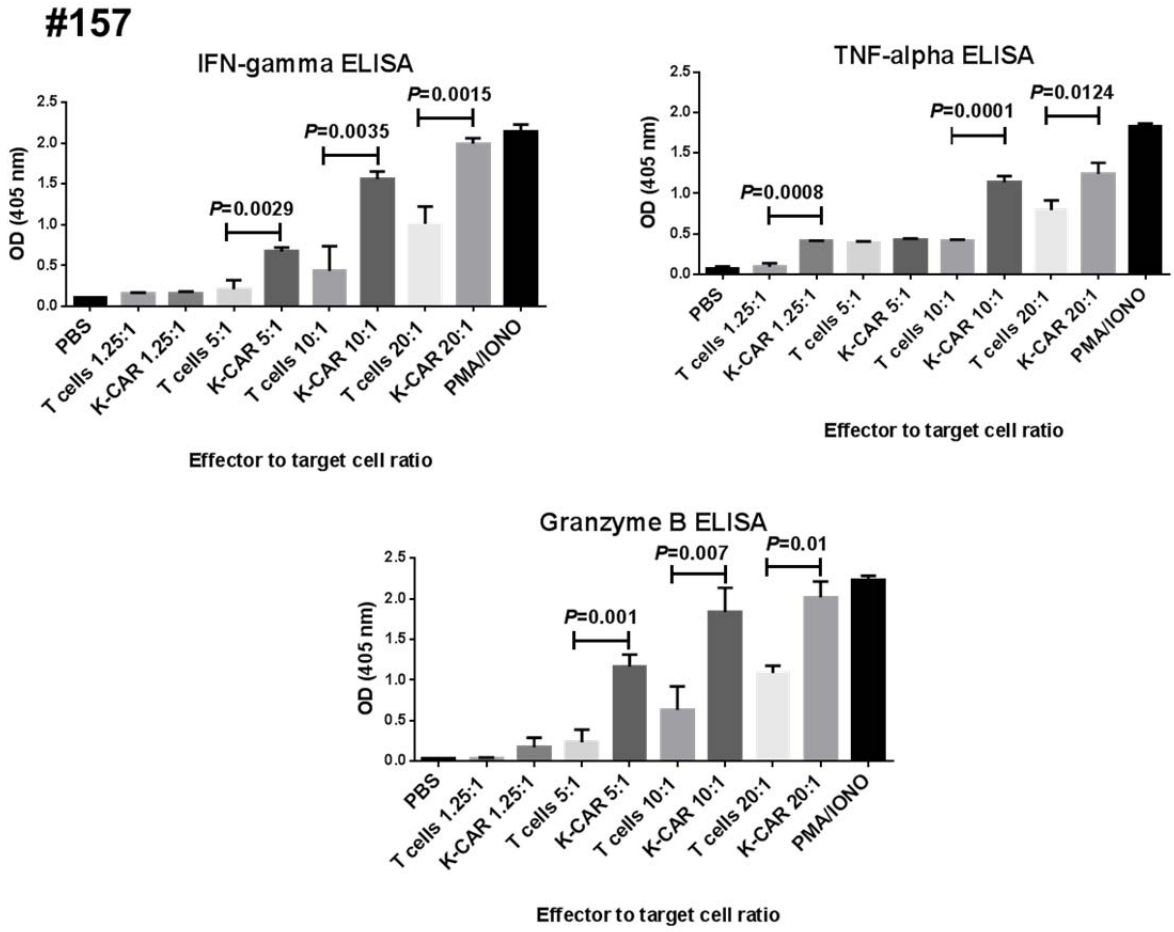
#157
IFN-gamma ELISA
OD (405 nm)
P=0.0029
P=0.0035
P=0.0015
PBS
T cells 1.25:1
K-CAR 1.25:1
T cells 5:1
K-CAR 5:1
T cells 10:1
K-CAR 10:1
T cells 20:1
K-CAR 20:1
PMA/IONO
Effector to target cell ratio
TNF-alpha ELISA
OD (405 nm)
P=0.0008
P=0.0001
P=0.0124
Effector to target cell ratio
Granzyme B ELISA
OD (405 nm)
P=0.001
P=0.007
P=0.01
Effector to target cell ratio

Fig. 4B

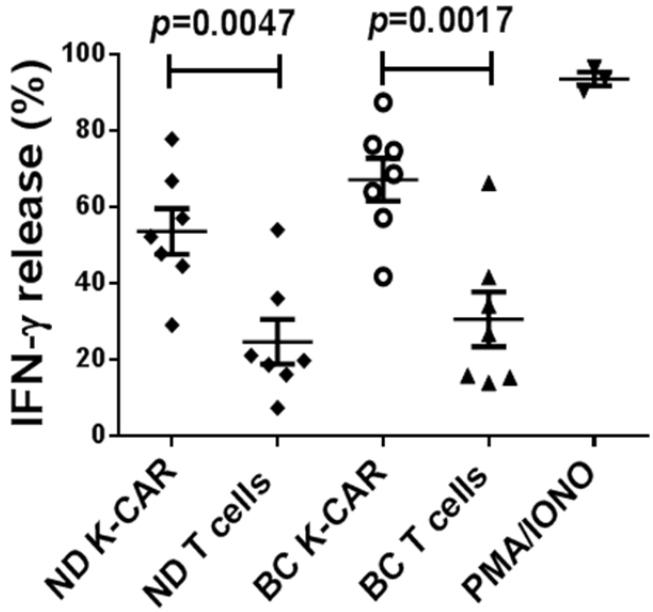
p=0.0047
p=0.0017
IFN-γ release (%)
ND K-CAR
ND T cells
BC K-CAR
BC T cells
PMA/IONO

Fig. 4C

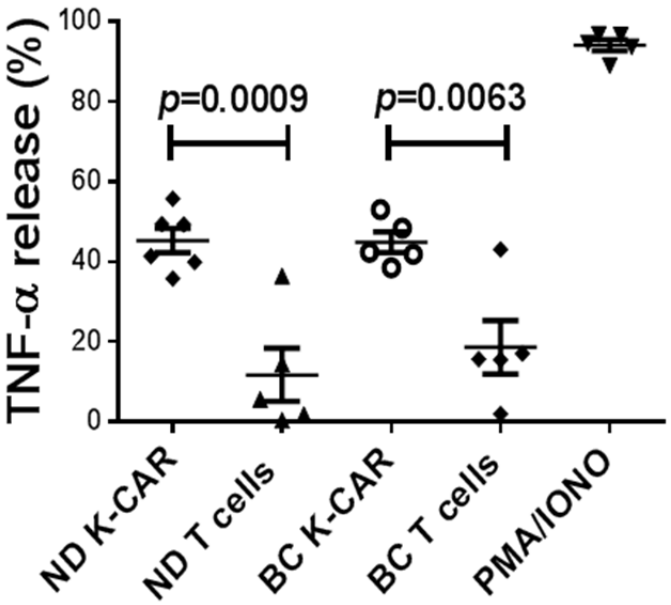
TNF-α release (%)
100
80
60
40
20
0
p=0.0009
p=0.0063
ND K-CAR
ND T cells
BC K-CAR
BC T cells
PMA/IONO

Fig. 4D

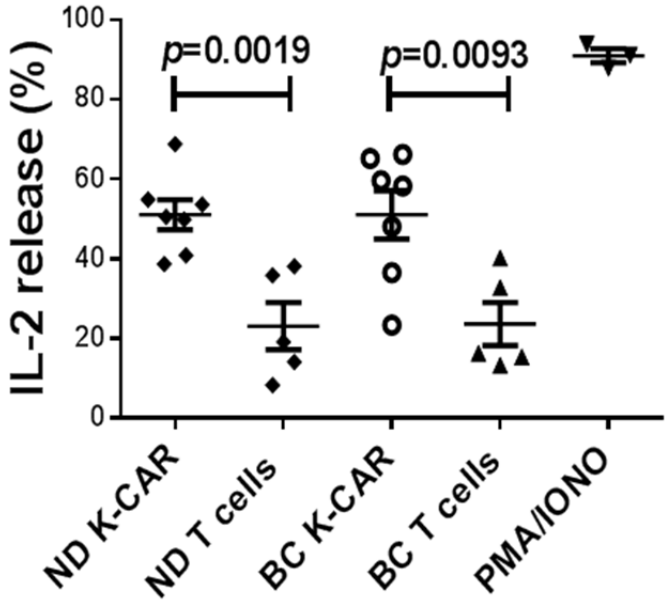
IL-2 release (%)
100
80
60
40
20
0
p=0.0019
p=0.0093
ND K-CAR
ND T cells
BC K-CAR
BC T cells
PMA/IONO

Fig. 4 Cytokine release: A) An ELISA assay was used to detect cytokine release from BC cells treated with K-CAR or control T cells. Significantly enhanced IFN-gamma, TNF-alpha, and Granzyme B release into the culture media was demonstrated in target cells treated with K-CAR compared to treatment with control T cells generated from BC patient 157. A greater release of cytokine was detected as the ratio of target to effector increased. PMA/IONO was used as a positive control to stimulate maximal cytokine release. The percentage of cytokine release in target cells treated with K-CAR from BC patients or from normal female donors was determined by FACS assays using antibodies for various cytokines. Significantly enhanced release of IFN-gamma (B), TNF-alpha (C), and IL-2 (D) was observed from target cells treated with K-CAR T cells compared with control T cells. No significant difference was found between target cells treated with K-CAR T cells from BC patients or normal female donors.

Fig. 5A

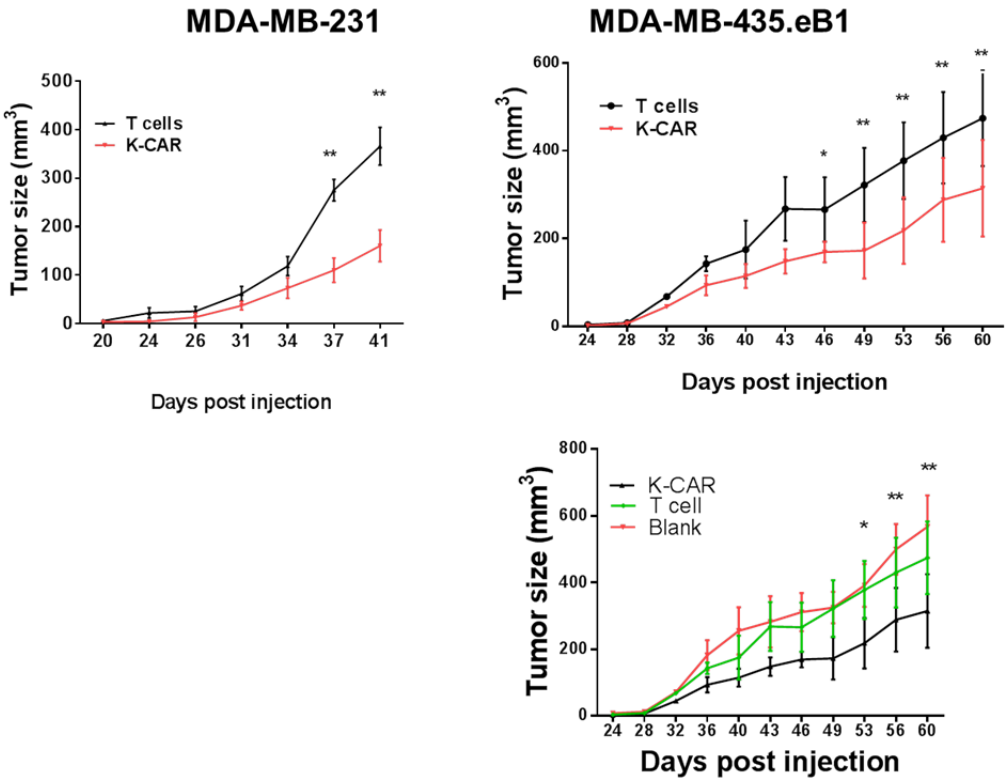
MDA-MB-231
Tumor size (mm3)
T cells
K-CAR
Days post injection
MDA-MB-435.eB1
Tumor size (mm3)
T cells
K-CAR
Days post injection
Tumor size (mm3)
K-CAR
T cell
Blank
Days post injection

Fig. 5B

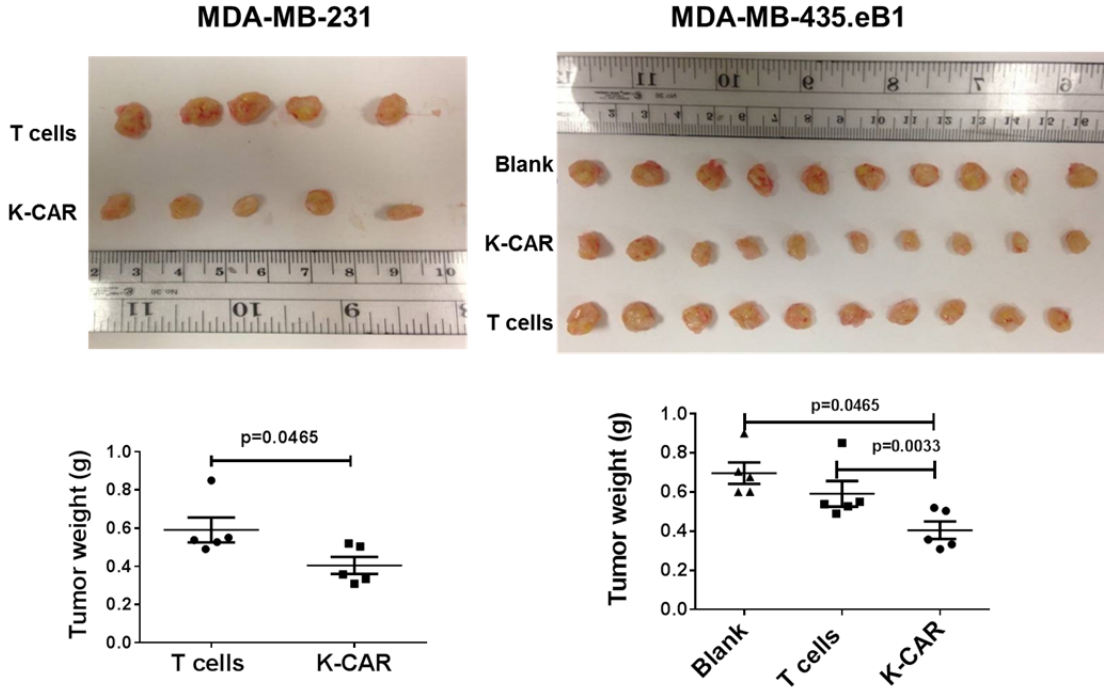
MDA-MB-231
T cells
K-CAR
MDA-MB-435.eB1
Blank
K-CAR
T cells
Tumor weight (g)
p=0.0465
T cells
K-CAR
Tumor weight (g)
p=0.0465
p=0.0033
Blank
T cells
K-CAR

Fig. 5C

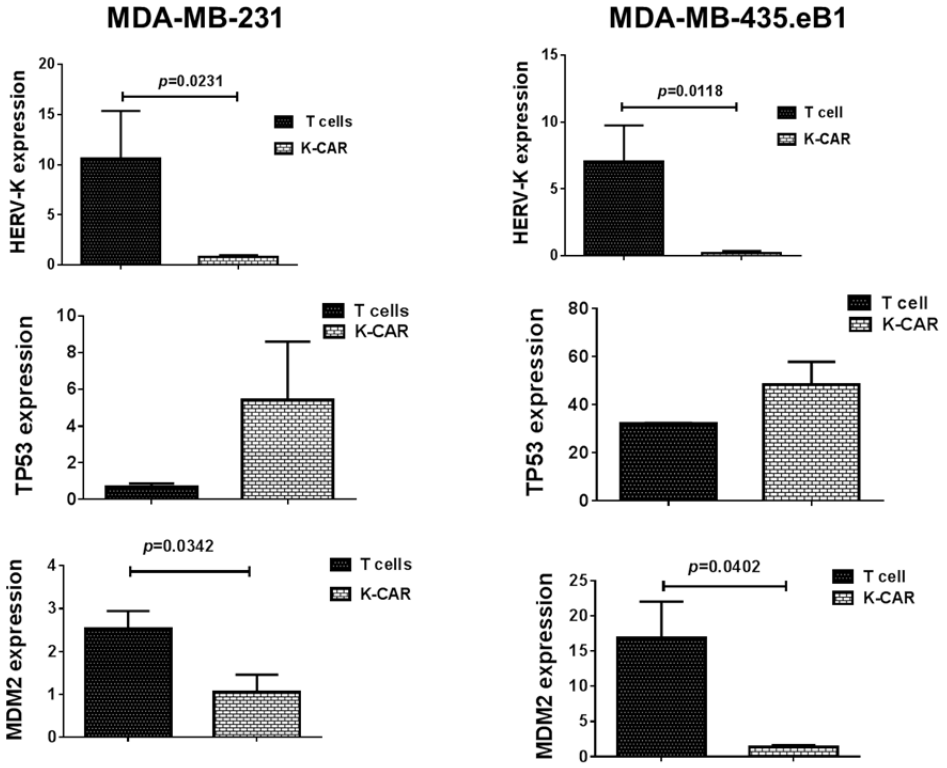
MDA-MB-231
MDA-MB-435.eB1
HERV-K expression
p=0.0231
T cells
K-CAR
p=0.0118
T cell
TP53 expression
MDM2 expression
p=0.0342
p=0.0402

Fig. 5D

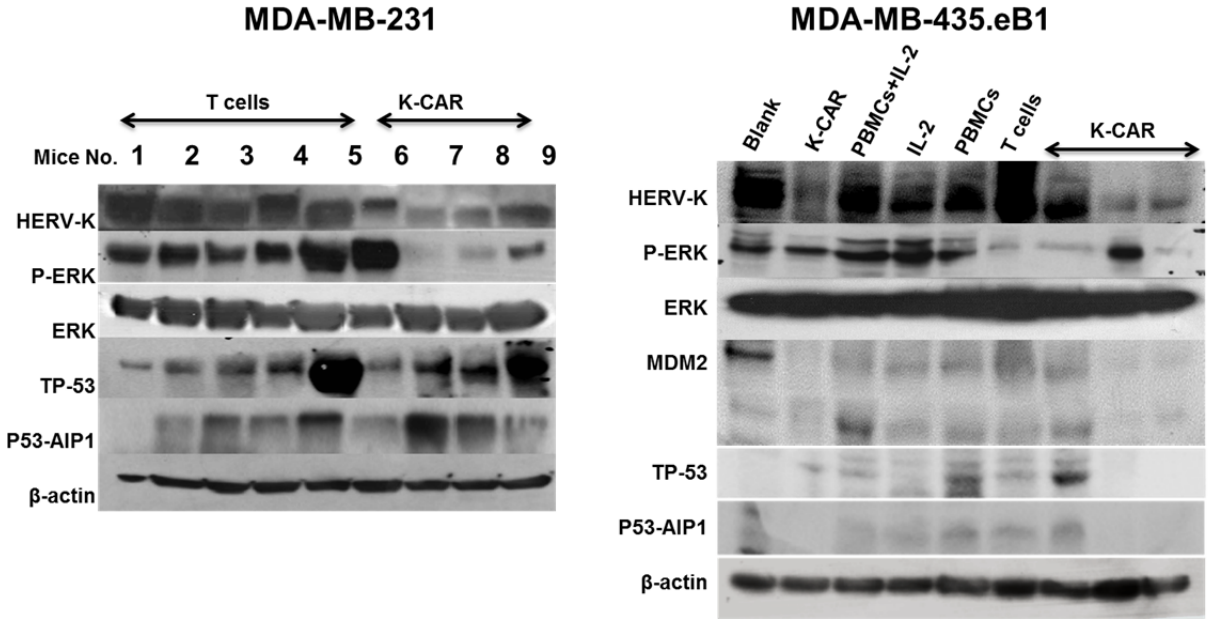
MDA-MB-231
MDA-MB-435.eB1
T cells
K-CAR
Mice No. 1 2 3 4 5 6 7 8 9
HERV-K
P-ERK
ERK
TP-53
P53-AIP1
β-actin
Blank
PBMCs+IL-2
IL-2
PBMCs
MDM2

Fig. 5 Antitumor effect *in vivo* and mechanism: A) Mice were inoculated with BC cells and were untreated (black tracing), or treated with control T cells (T cells) or K-CAR T cells (K-CAR) on post-injection days 5, 13 and 21. Significantly reduced tumor growth was demonstrated in mice treated with K-CAR compared to treatment with control T cells or no treatment. B) Tumor weights were significantly reduced in mice treated with K-CAR compared to treatment with other controls. C) The expression of various genes in the treatment groups was detected by qRT-PCR. Significantly reduced expression of HERV-K in tumor biopsies was observed in mice treated with K-CAR in both BC cell xenograft models. K-CAR treatment downregulated expression of HERV-K, and this was accompanied by upregulation of TP53 and downregulation of MDM2 expression. D) These profiles of gene expression were confirmed at the protein level by immunoblot assays. In addition to effects on p53 and MDM2 expression, K-CAR T cell treatment of mice produced tumors that had decreased expression of p-ERK but not of ERK, compared with controls.

Fig. 6A

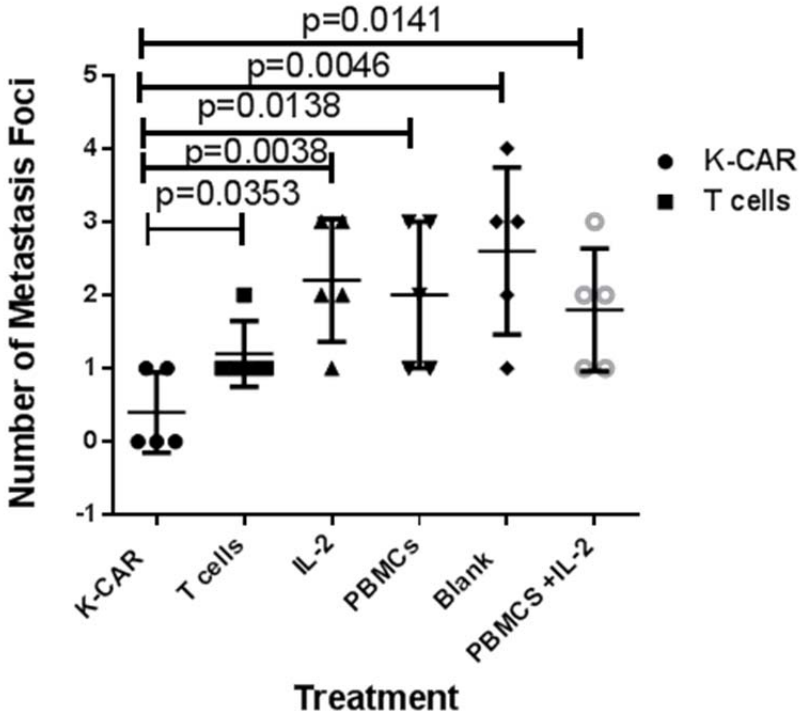
p=0.0141
p=0.0046
p=0.0138
p=0.0038
p=0.0353
Number of Metastasis Foci
5
4
3
2
1
0
-1
K-CAR
T cells
IL-2
PBMCs
Blank
PBMCS+IL-2
Treatment
K-CAR
T cells

Fig. 6B

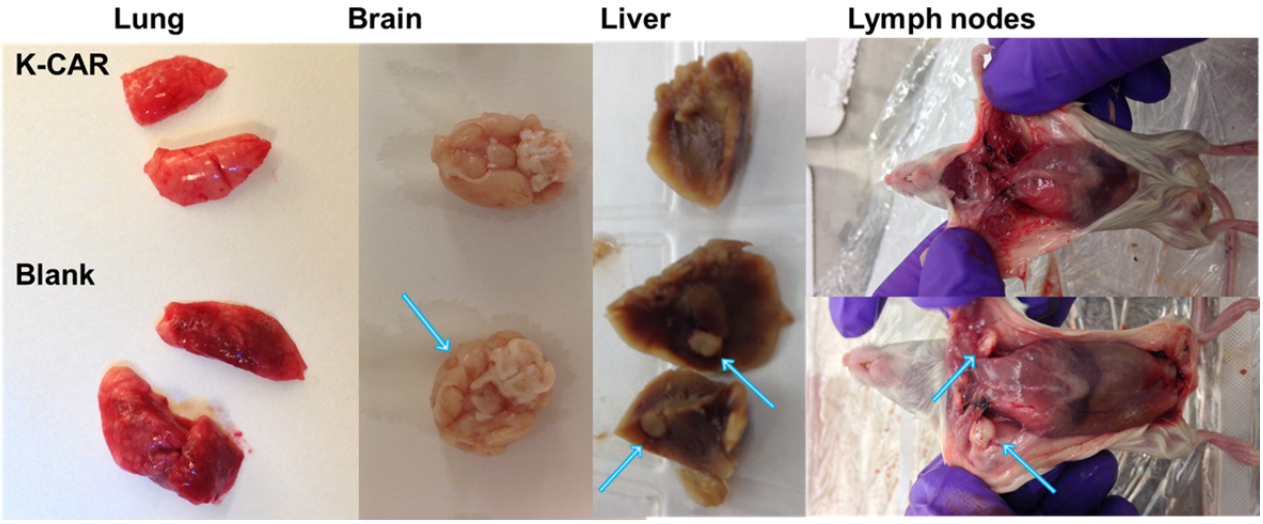
Lung
Brain
Liver
Lymph nodes
K-CAR
Blank

Fig. 6C

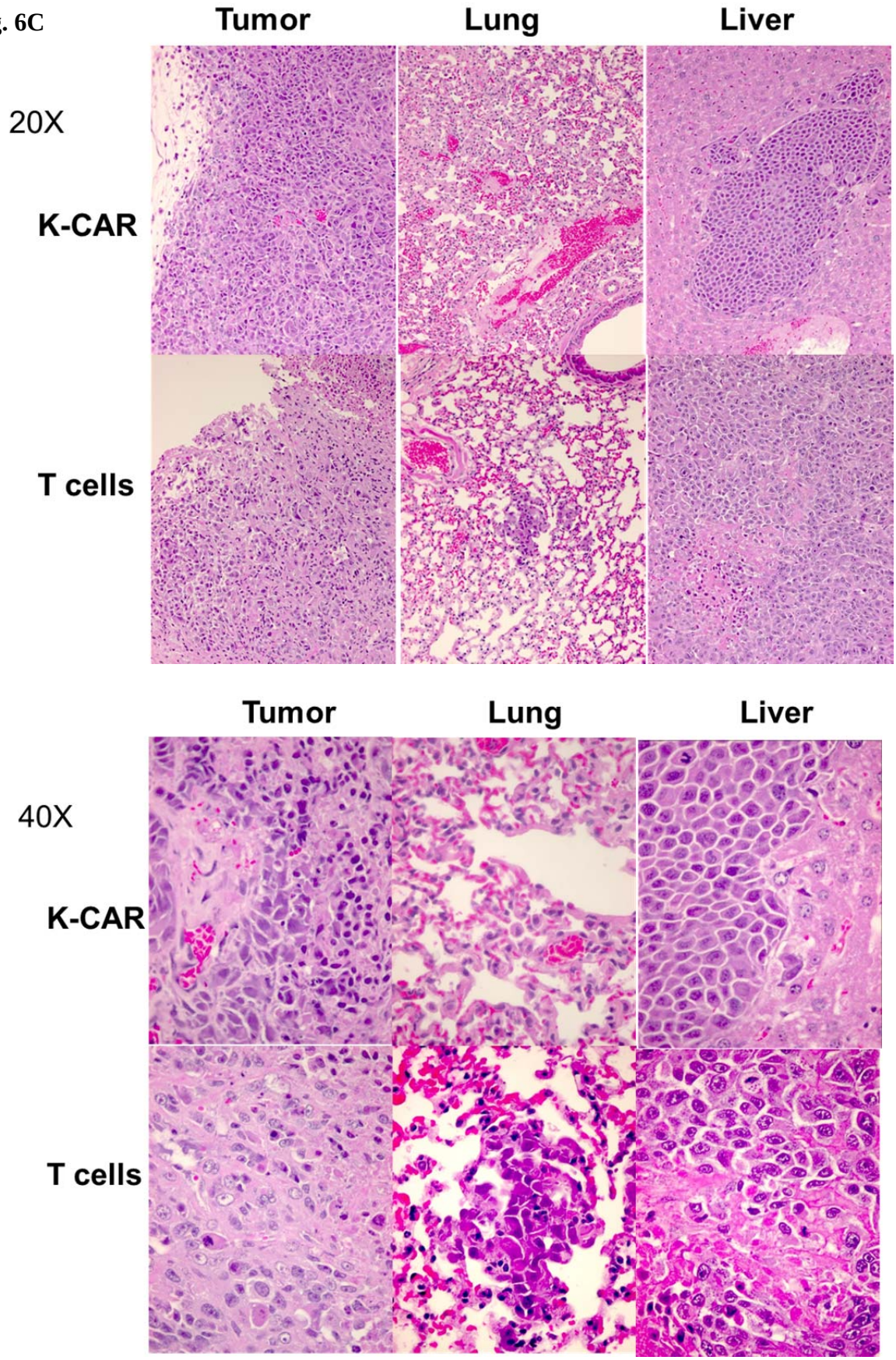
Tumor
Lung
Liver
20X
K-CAR
T cells
Tumor
Lung
Liver
40X
K-CAR
T cells

Fig. 6D

6H5

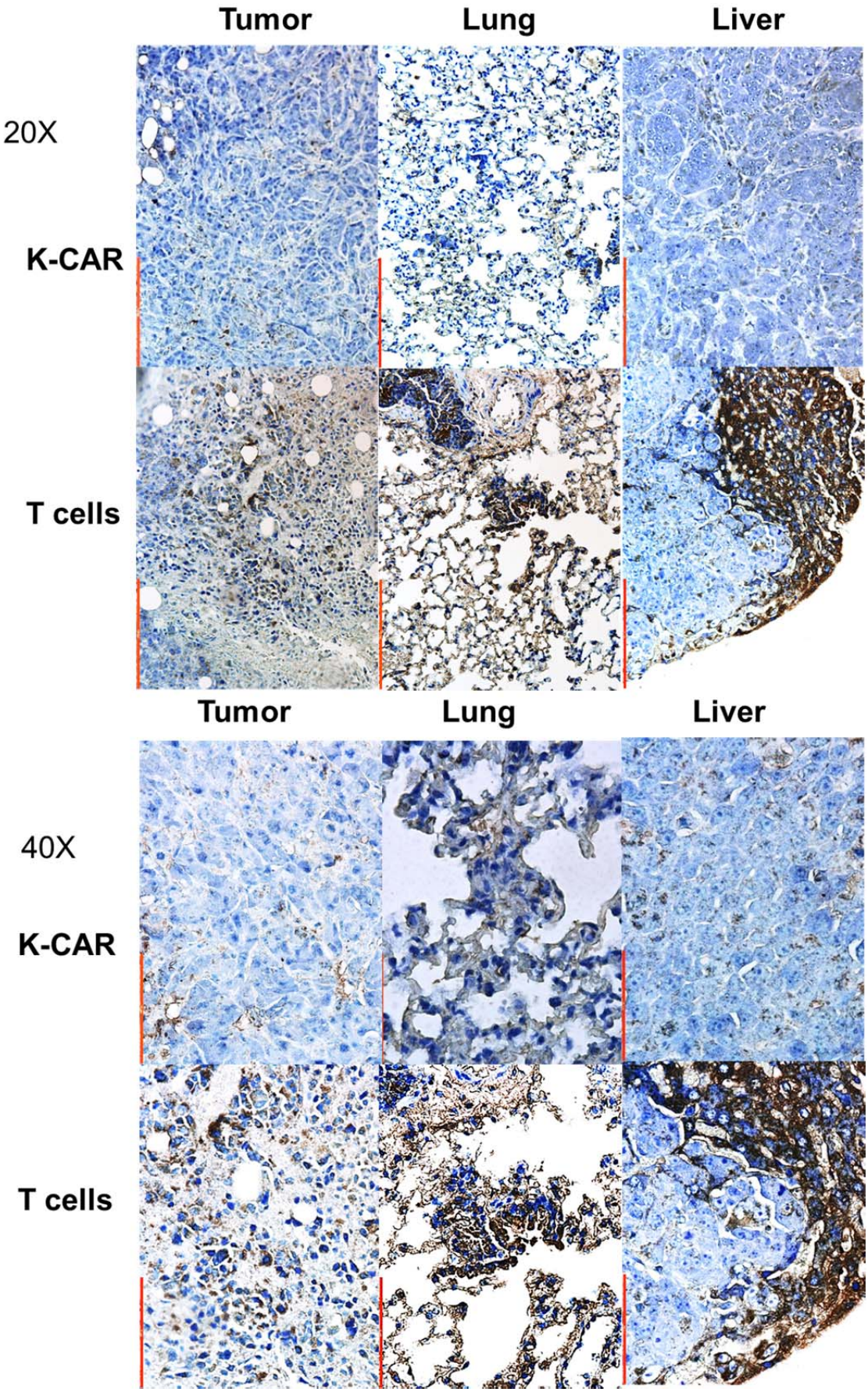
Tumor
Lung
Liver
20X
K-CAR
T cells
Tumor
Lung
Liver
40X
K-CAR
T cells

H-Ras

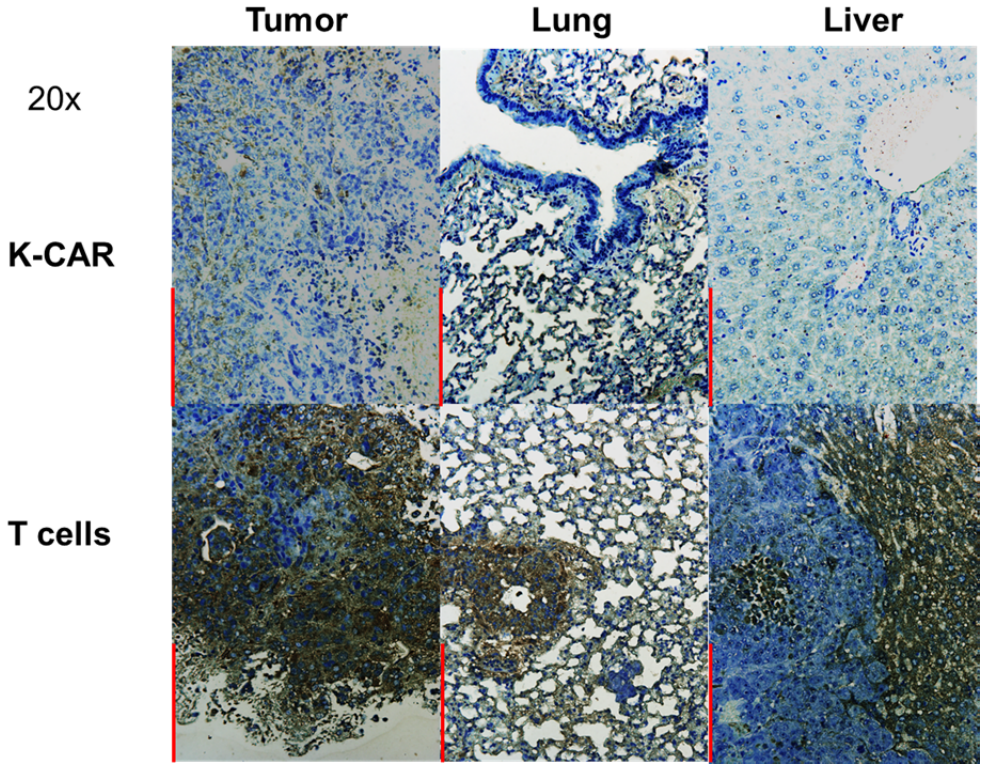
Tumor
Lung
Liver
20x
K-CAR
T cells

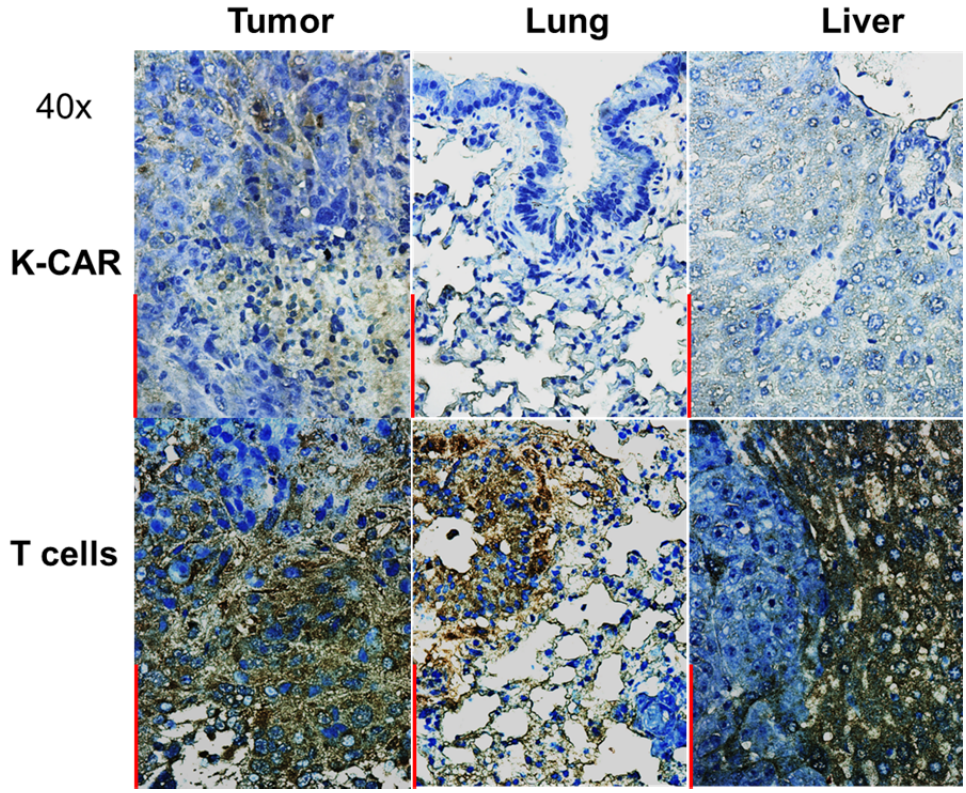
Tumor
Lung
Liver
40x
K-CAR
T cells

Fig. 6 *In vivo* anti-metastatic effect of K-CAR treatment: A) Mice inoculated with MDA-MB-435.eB1 cells and treated with K-CAR, vs. mice treated with control T cells, had metastases to organs that included axillary lymph node (1 metastatic focus in K-CAR T cell treatment group vs. 1 metastatic focus in the control T cell treatment group), lung (0 vs.1), liver (0 vs.1), brain (0 vs.1), and pleural lavage fluid (1 vs. 2). Thus, mice treated with K-CAR had 2 total metastatic foci to these organs, while mice treated with control T cells had 6 total foci. IL-2, PBMC, blank, and PBMCs + IL-2 treatment groups also had significantly more metastases than the K-CAR T cell treatment group. B) Metastases that formed in other organs) after K-CAR treatments or no treatment (blank) are pictured here. C) Biopsies of tumors as well as metastases to lung and liver from K-CAR and T cell treatment groups were stained with H&E and samples are shown here in 20X and 40X. D) The expression of HERV-K and H-Ras in biopsies from the same tissues as in (C) was determined by IHC using 6H5 mAb and H-Ras antibody. The expression of HERV-K or H-RAs was demonstrated in the tumor areas identified by H&E staining.

Supplemental Figure Legends:

Fig. S1A

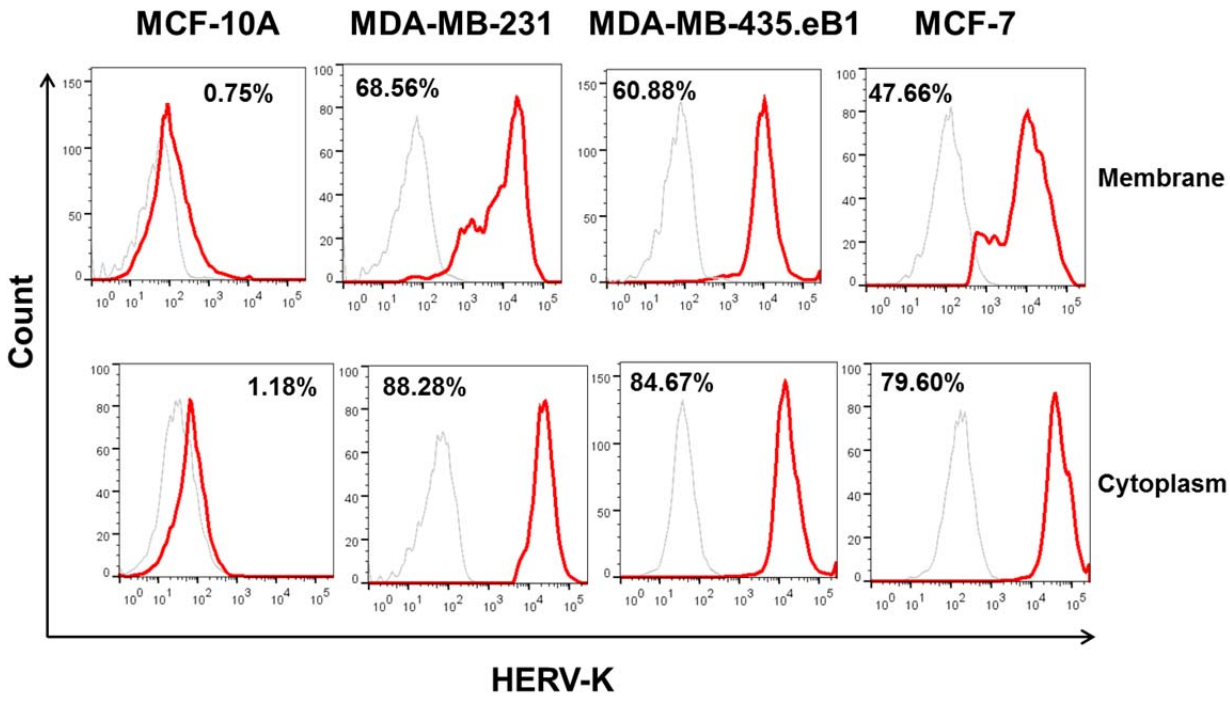

Fig. S1B

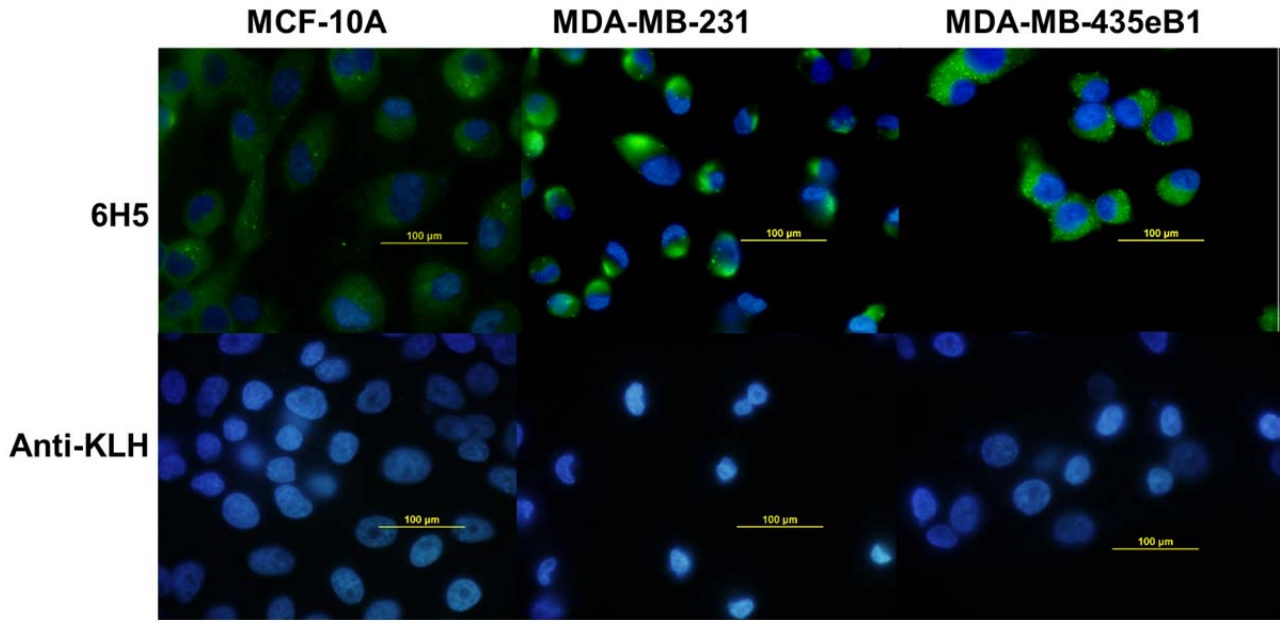

Fig. S1C

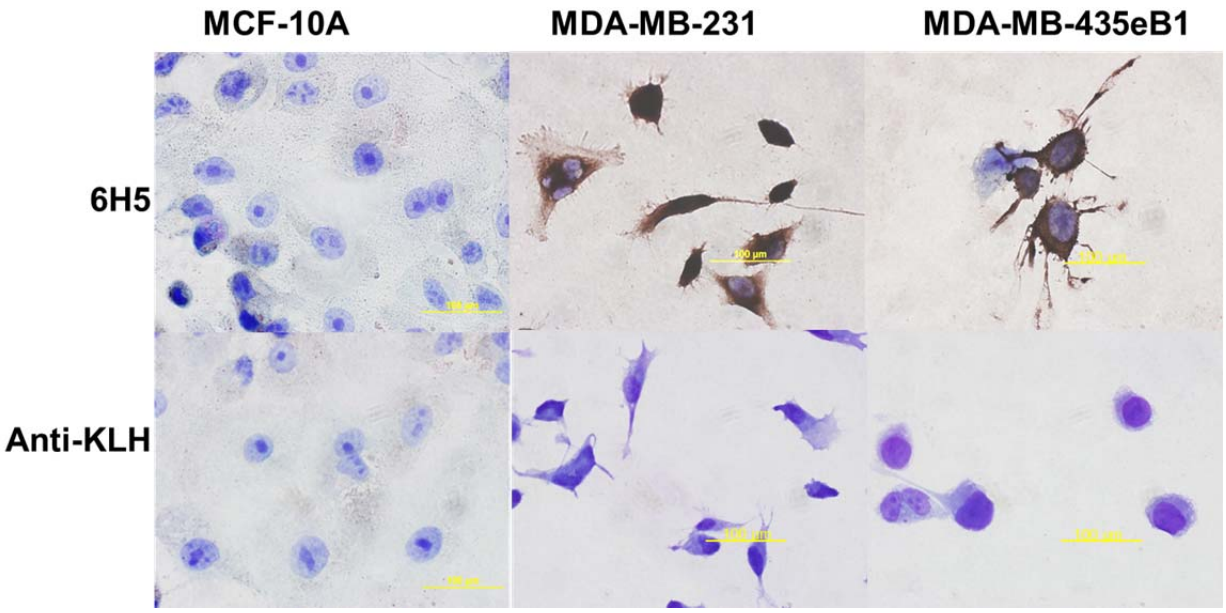

Fig. S1D

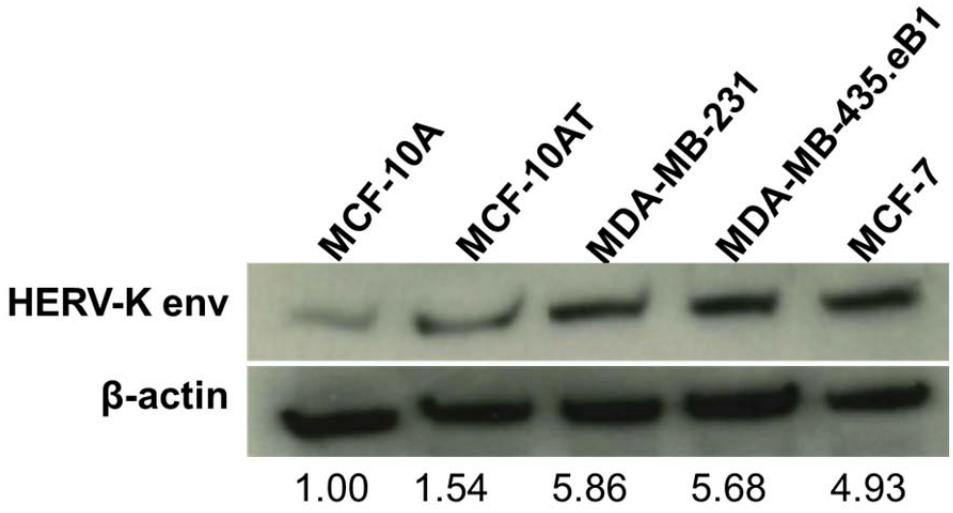

Fig. S1 The expression of HERV-K env protein in various breast cell lines: A) FACS was used to determine the expression of HERV-K env protein in various breast cell lines using 6H5 mAb. A higher percentage of membrane and cytoplasmic expression of viral protein was demonstrated in BC cells lines compared with MCF-10A transformed breast cells. B) Immunofluorescence staining was employed to detect the expression of viral protein in breast cell lines. Higher HERV-K expression was demonstrated in BC cell lines than in MCF-10A breast cells. Anti-KLH mIgG was used as a control. C) Immunocytochemistry was employed to detect the expression of viral protein; only BC cells stained HERV-K positive but not MCF-10A non-tumorigenic breast cells. D) Immunoblot assays were used to detect the expression of HERV-K protein, using β-actin as a control. Enhanced viral protein expression was observed in BC cells compared to the expression in MCF-10A.

Fig. S2A

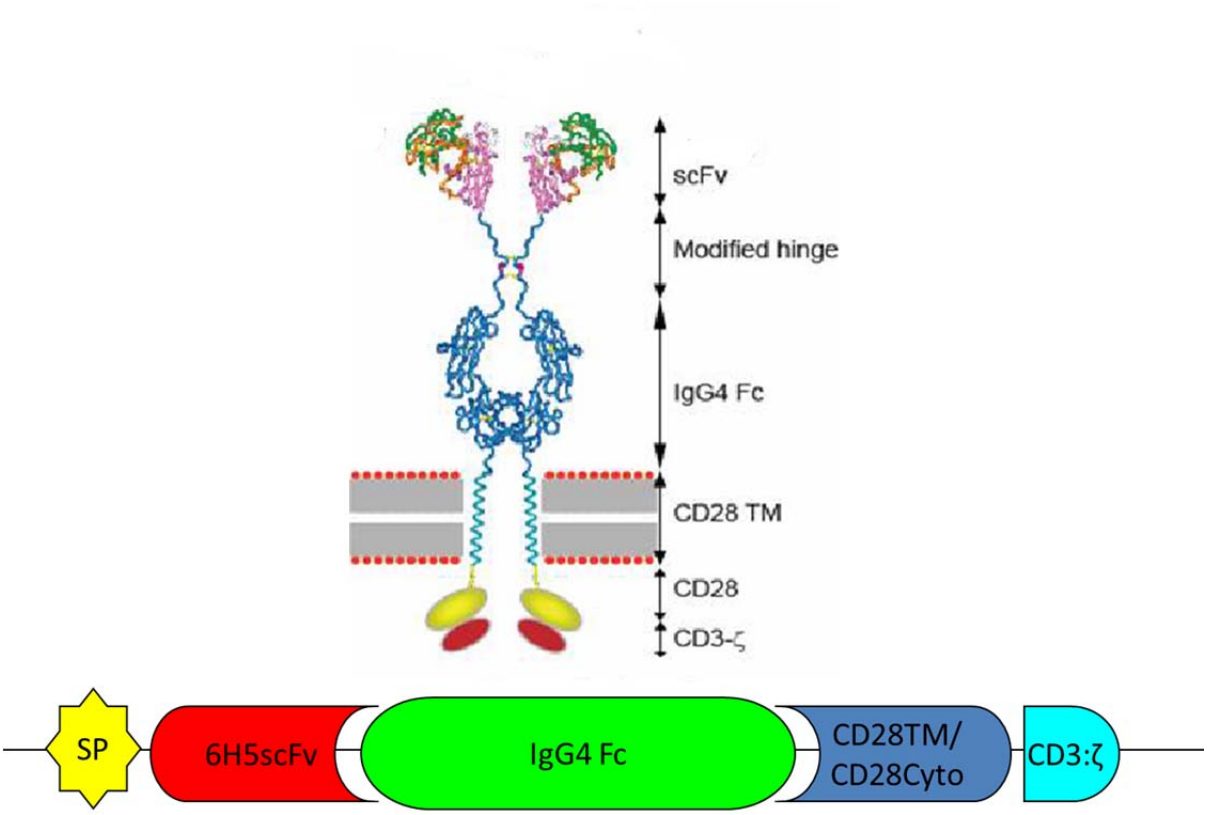

Fig. S2B

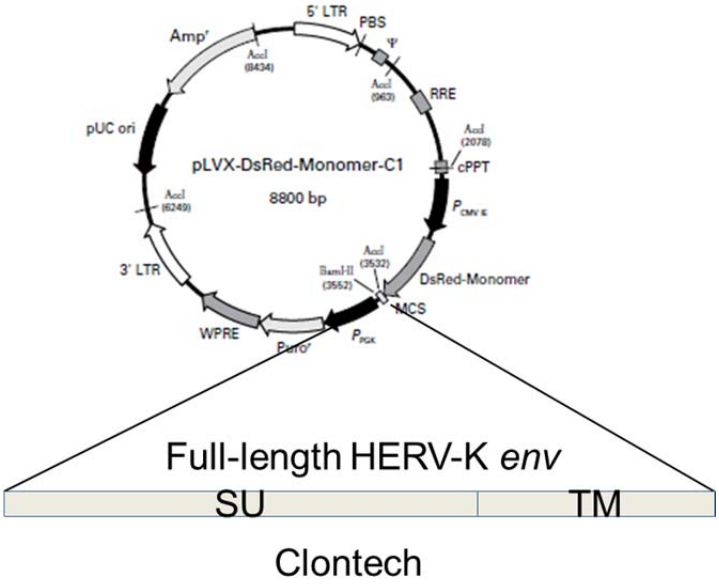

Fig. S2C

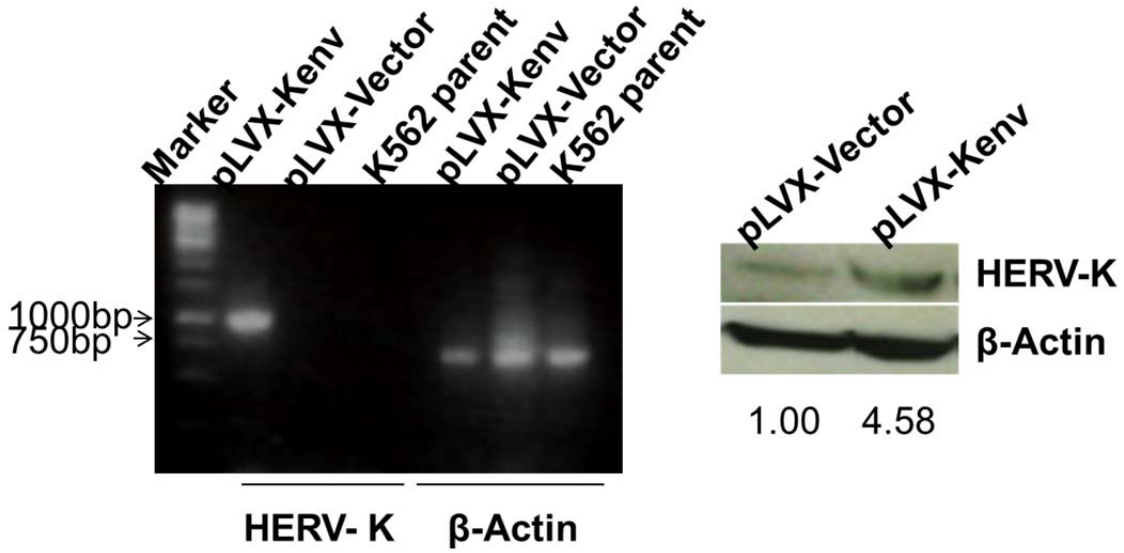

Fig. S2D

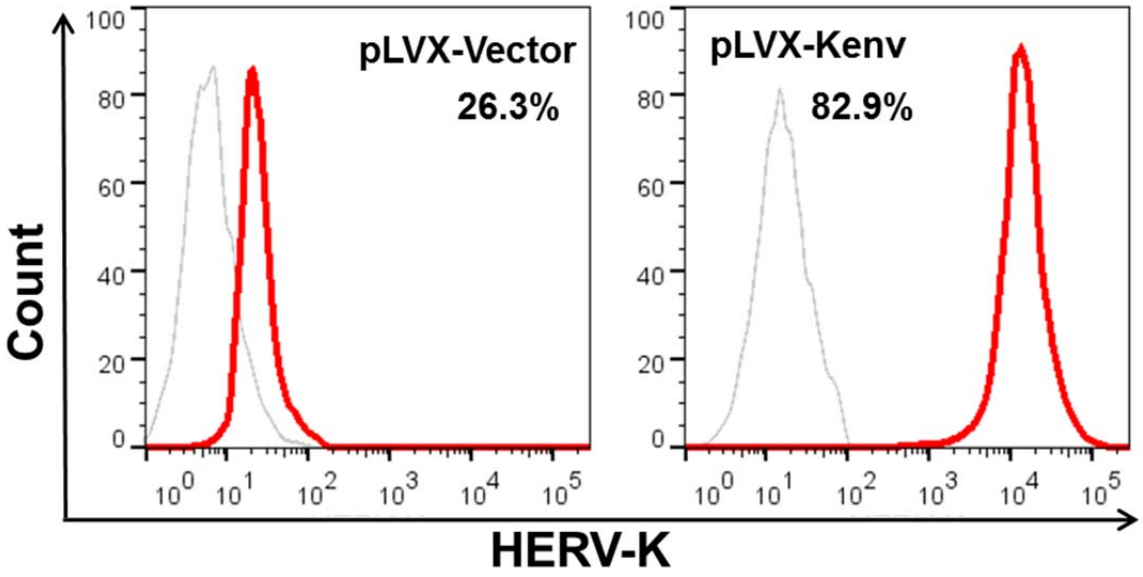

Fig. S2 Construction of K-CAR and artificial antigen present cells (aAPCs): A) An HERV-K-specific CAR was produced with 6H5 scFv to generate K-CAR. The schematic representation depicts the modular composition of the K-CAR used in this study, which includes a signal peptide (SP), 6H5 scFv as an extracellular domain, an Fc domain (IgG4), a transmembrane domain (CD28Tm and CD28Cyto), and an intracellular signal transduction domain CD3:ζ. K562 cells were transiently transduced with a pLVX-K env lentiviral vector (B) for the expression of HERV-K and used as aAPC cells. The expression of HERV-K in aAPCs was identified by RT-PCR (C), immunoblot (C) and FACS (D). K562 cells transiently transduced with the vector only were used as controls. The expression of HERV-K in aAPCs was increased approximately 4-fold in aAPCs compared with controls. T-cell populations underwent K-CAR-mediated numerical expansion on γ-ray irradiated HERV-K^+ aAPCs (100 Gy).

Fig. S3A

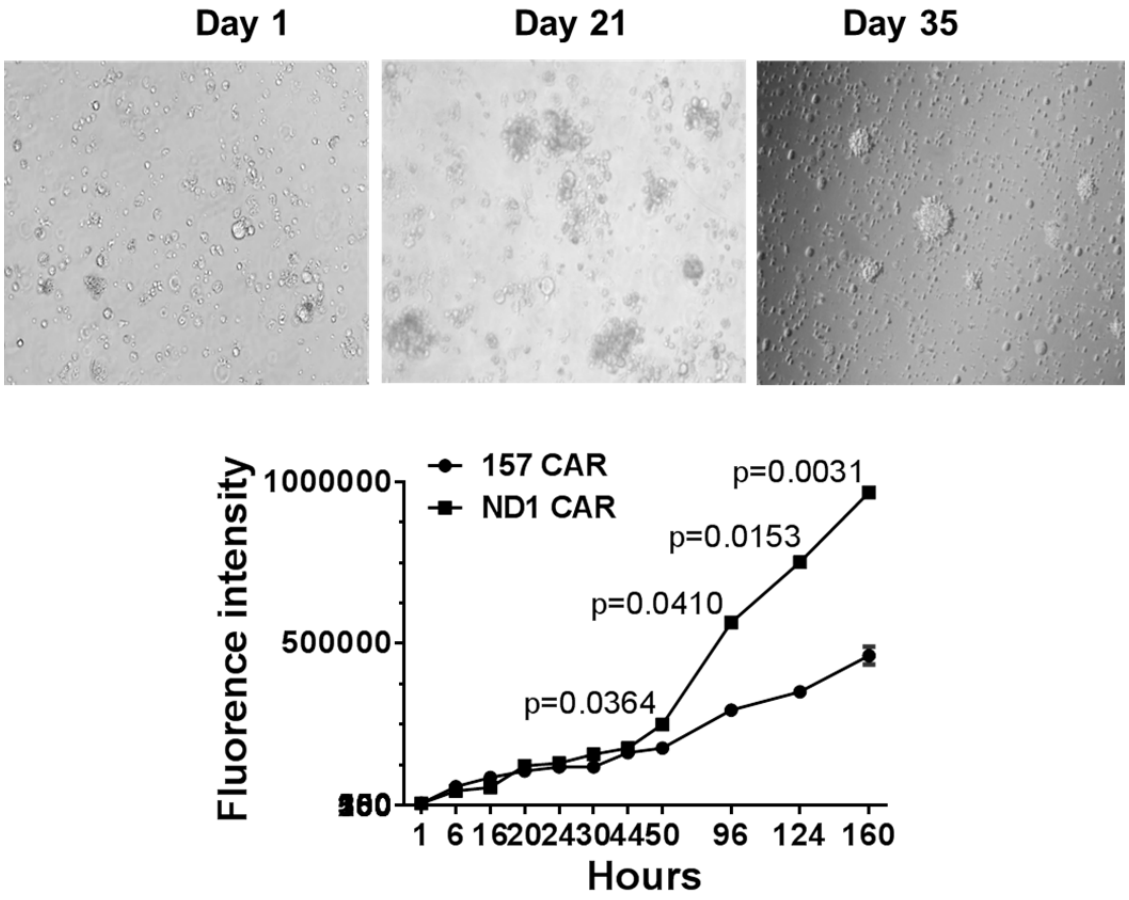

Fig. S3B

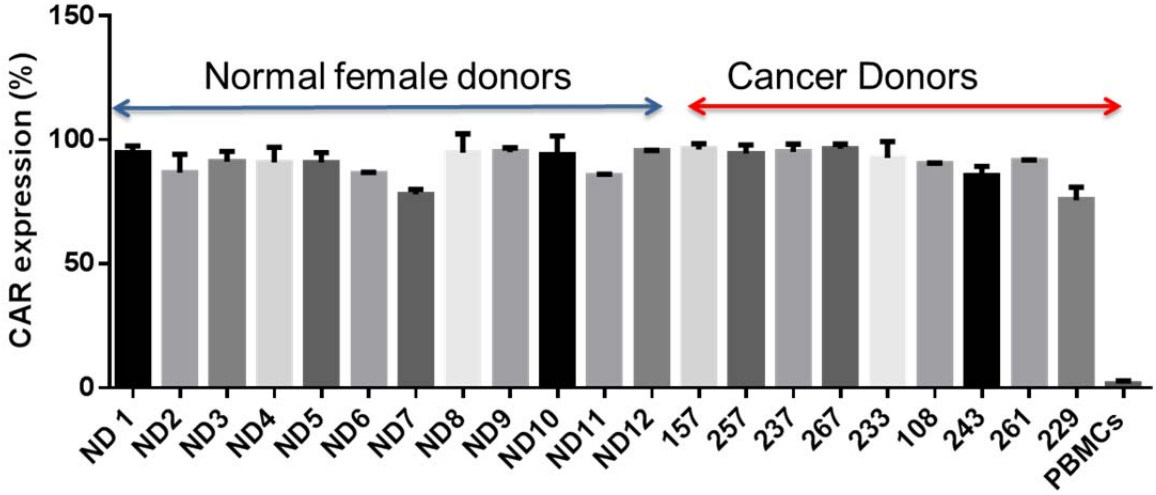

Fig. S3C

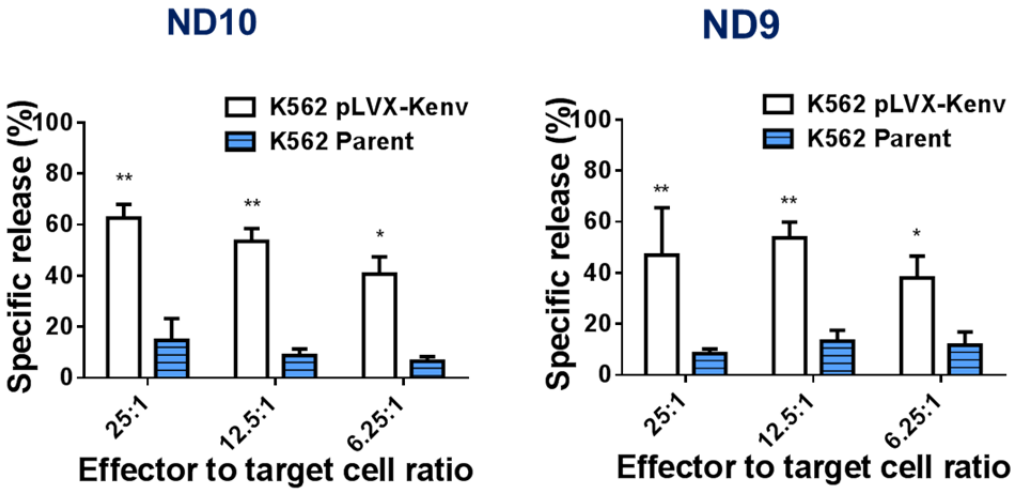

Fig. S3D

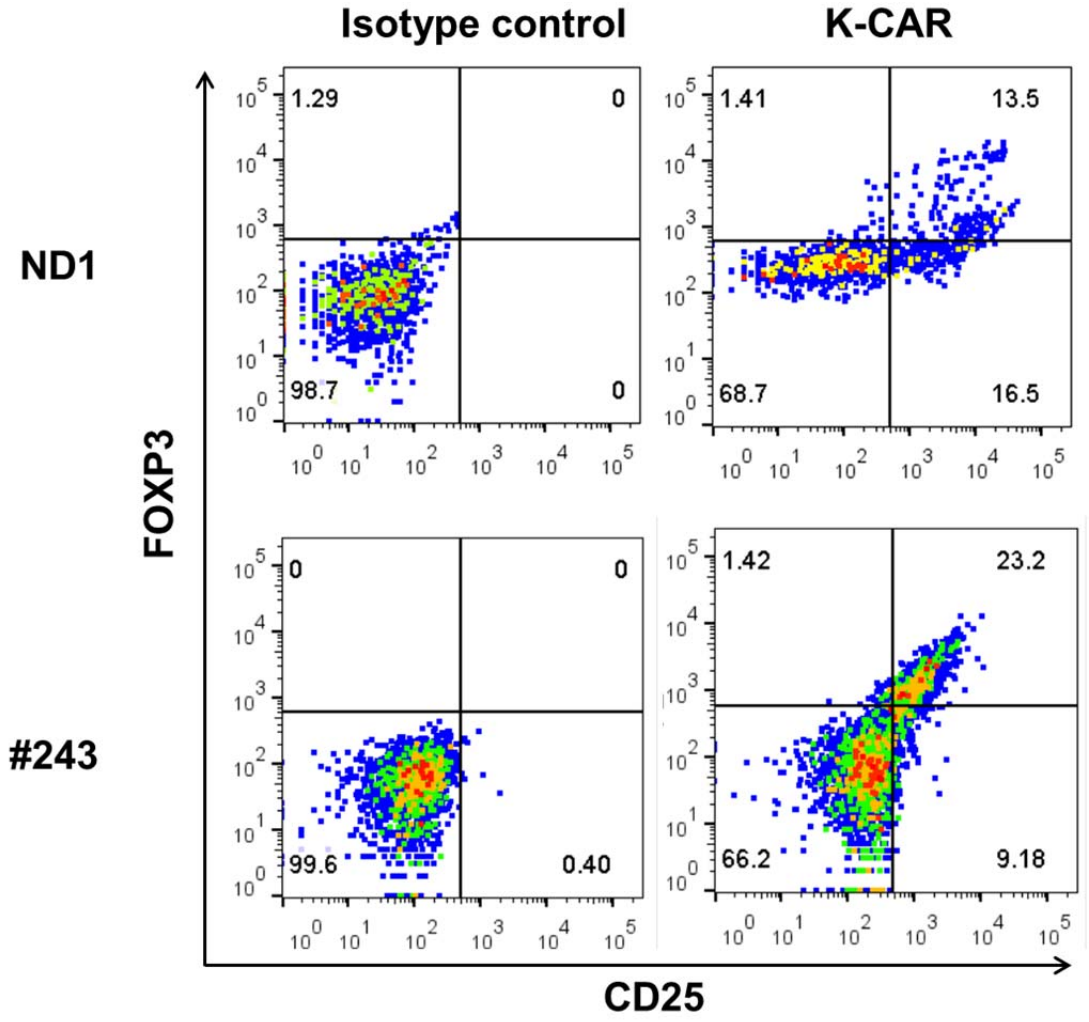

Fig. S3 Characterization of K-CAR T cells: A) The morphology of K-CAR T cells after growth for 1, 21 and 35 days (top panel). The proliferation rate of K-CAR T cells from patient 243 was significantly less than for ND1 control (bottom panel). B) The percentage of K-CAR^{+} T cells from 12 normal donors and 9 BC patients was compared on day 28 post-transduction with K-CAR constructs. C) A chromium release assay was used to determine the percentage of chromium released from aAPC cells compared with HERV-K^{-} kidney cells (HEK293 cells). D) Both FOXP3^{+} and CD25^{+} cell populations in K-CAR T cells obtained from ND1 and BC patient 157 were determined by FACS.

Fig. S4A

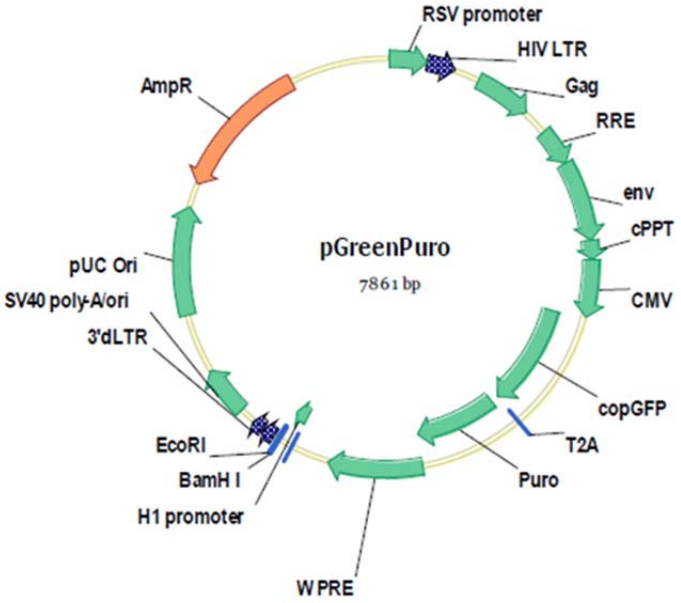

Fig. S4B

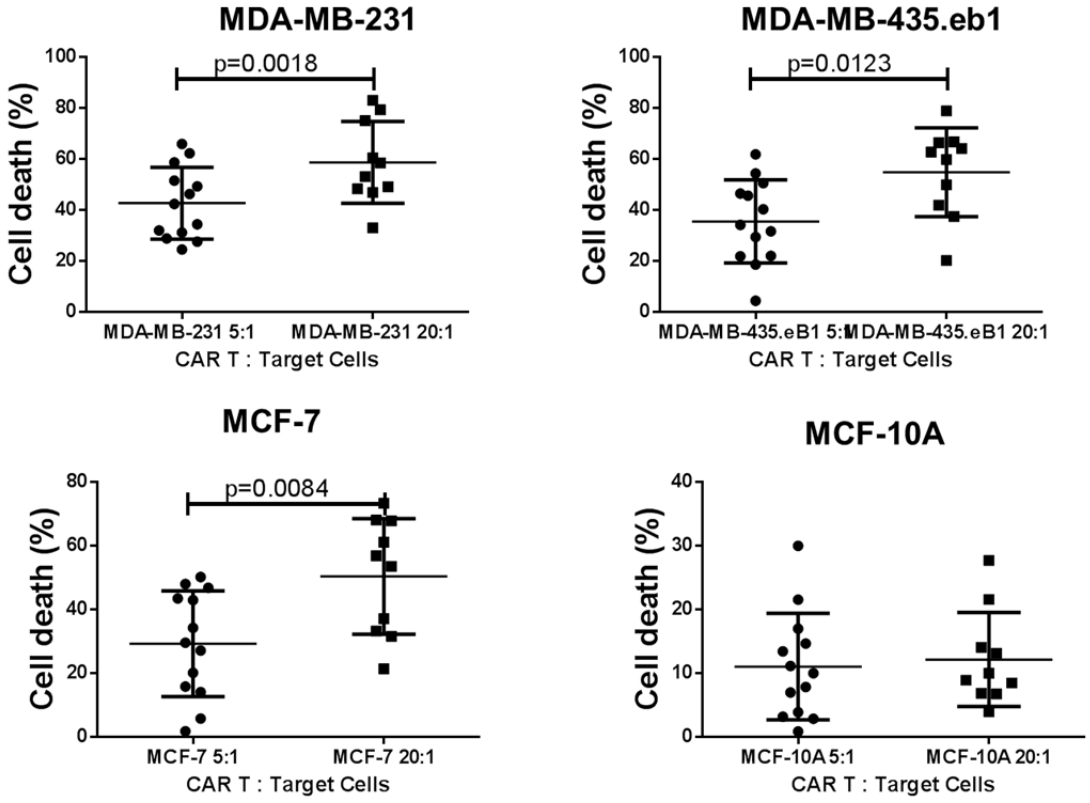

Fig. S4C

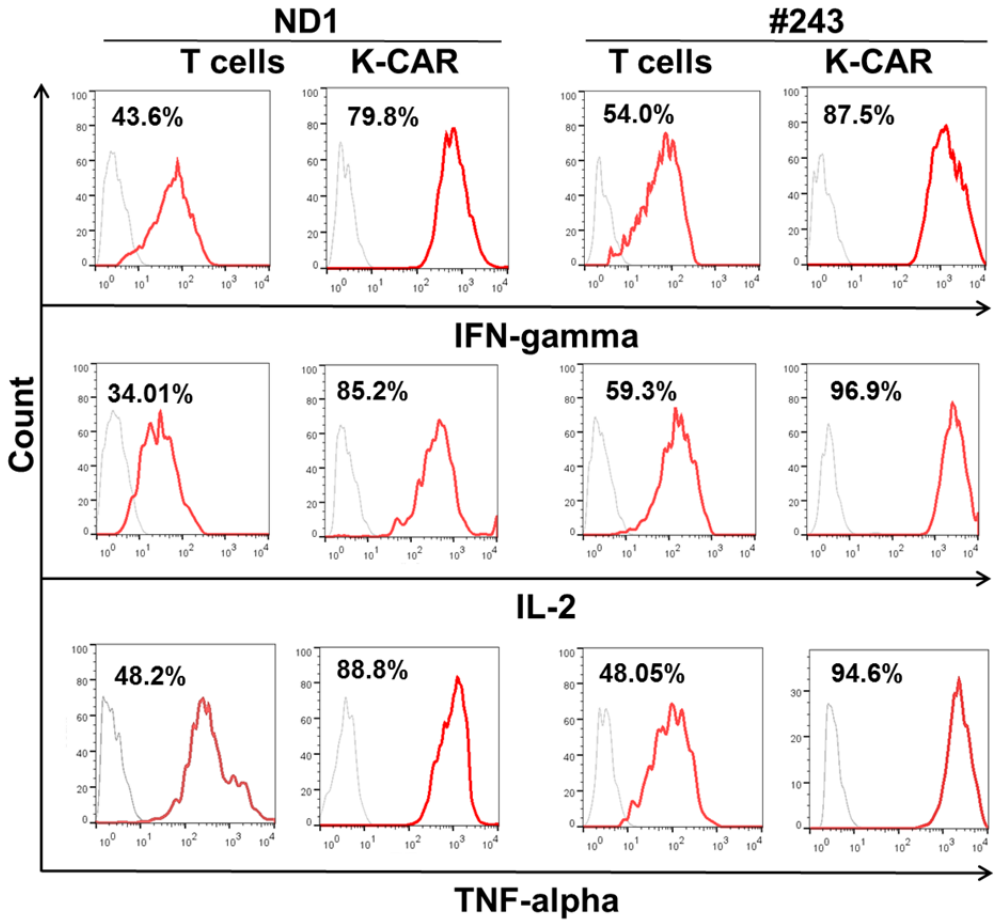
ND1
#243
T cells
K-CAR
T cells
K-CAR
43.6%
79.8%
54.0%
87.5%
IFN-gamma
Count
34.01%
85.2%
59.3%
96.9%
IL-2
48.2%
88.8%
48.05%
94.6%
TNF-alpha

Fig. S4D

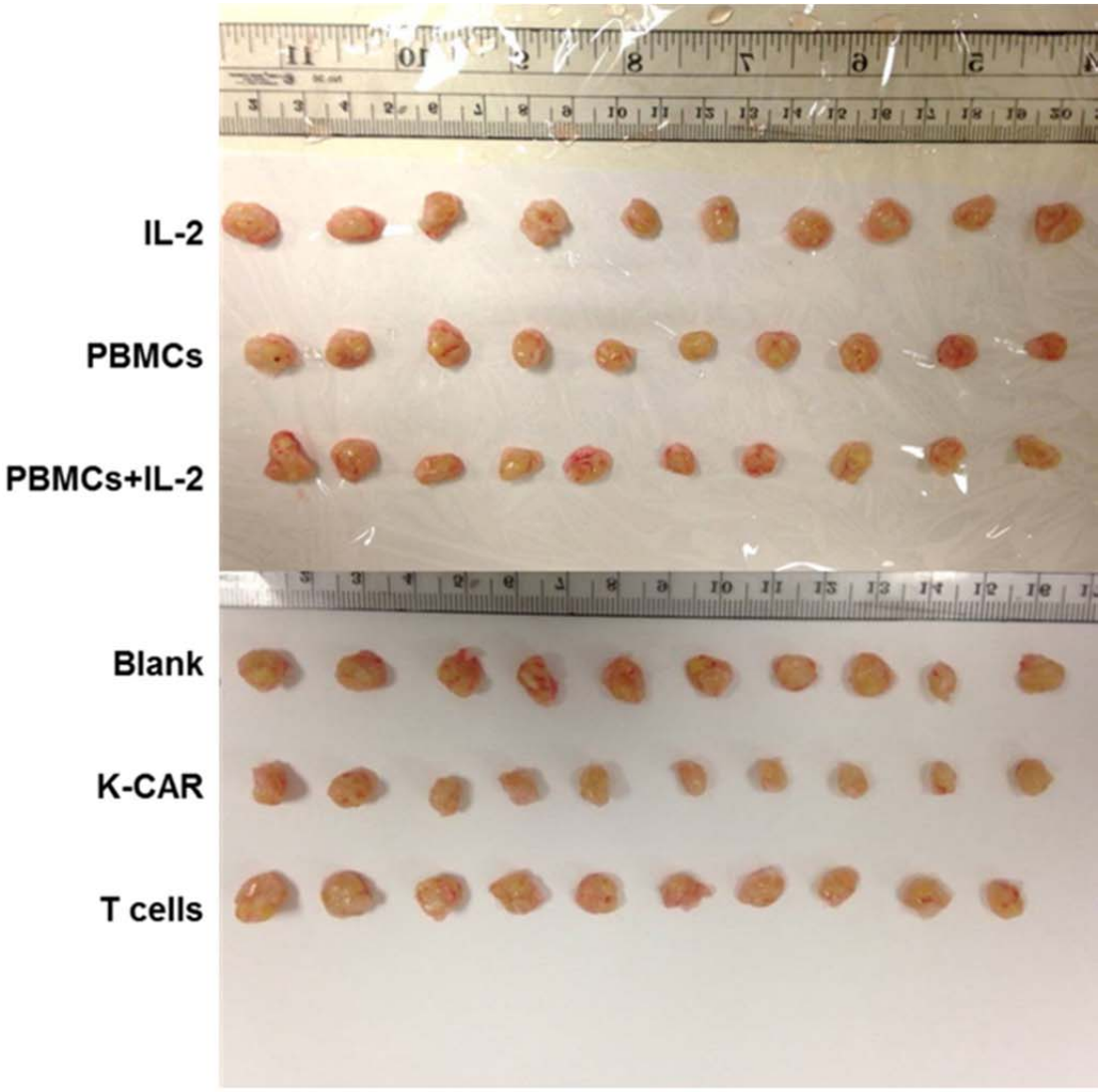
IL-2
PBMCs
PBMCs+IL-2
Blank
K-CAR
T cells

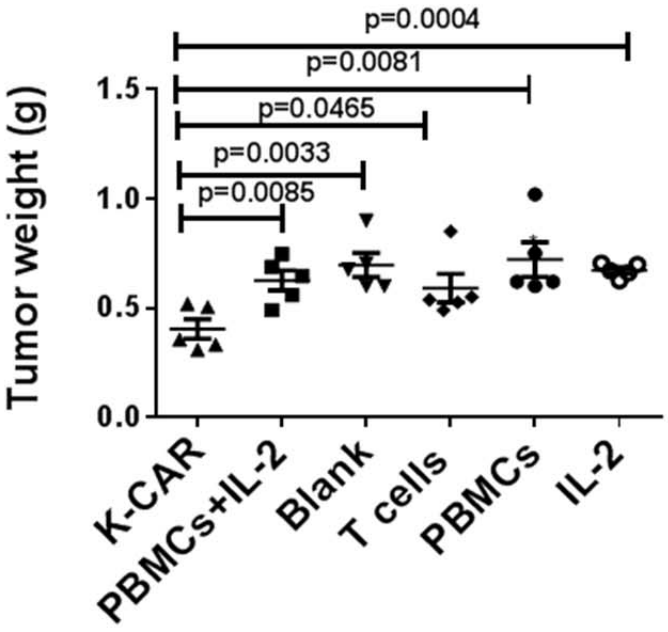
p=0.0004
p=0.0081
p=0.0465
p=0.0033
p=0.0085
Tumor weight (g)
1.5
1.0
0.5
0.0
K-CAR
PBMCs+IL-2
Blank
T cells
PBMCs
IL-2

Fig. S4 Characterization of K-CAR function in specific killing and cytokine production: A) K-CAR T cell killing of various target cell lines was compared, using a 5 to 1 ratio versus a 20 to 1 ratio of K-CAR T cells to target cells. Significantly enhanced target cell death was demonstrated in BC cell lines when the ratio of K-CAR T cells to target cells was increased. However, increased ratios of CAR to target did not increase killing of MCF-10A normal breast cells as it did for BC cells. B) Detection of release of IFN-γ, IL-2, and TNF-α cytokines in target cells treated with K-CAR T cells obtained from BC patient 243 or normal donor ND1. Higher cytokine release was observed in BC cells treated with control T cells or K-CAR T cells from the BC patient than from the control normal donor. C) Tumor sizes and weights were compared among treatment groups or a group with no treatment (blank).

Fig. S5A

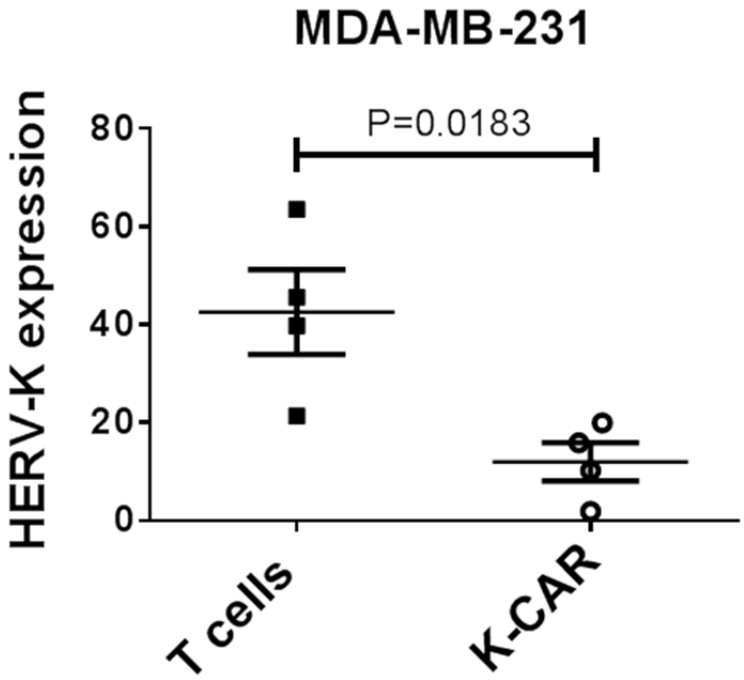

Fig. S5B

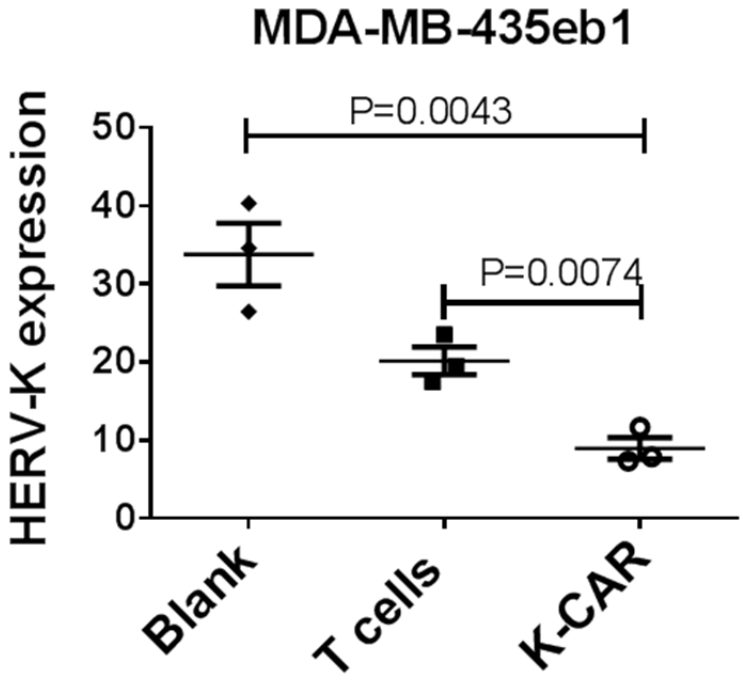

Fig. S5C

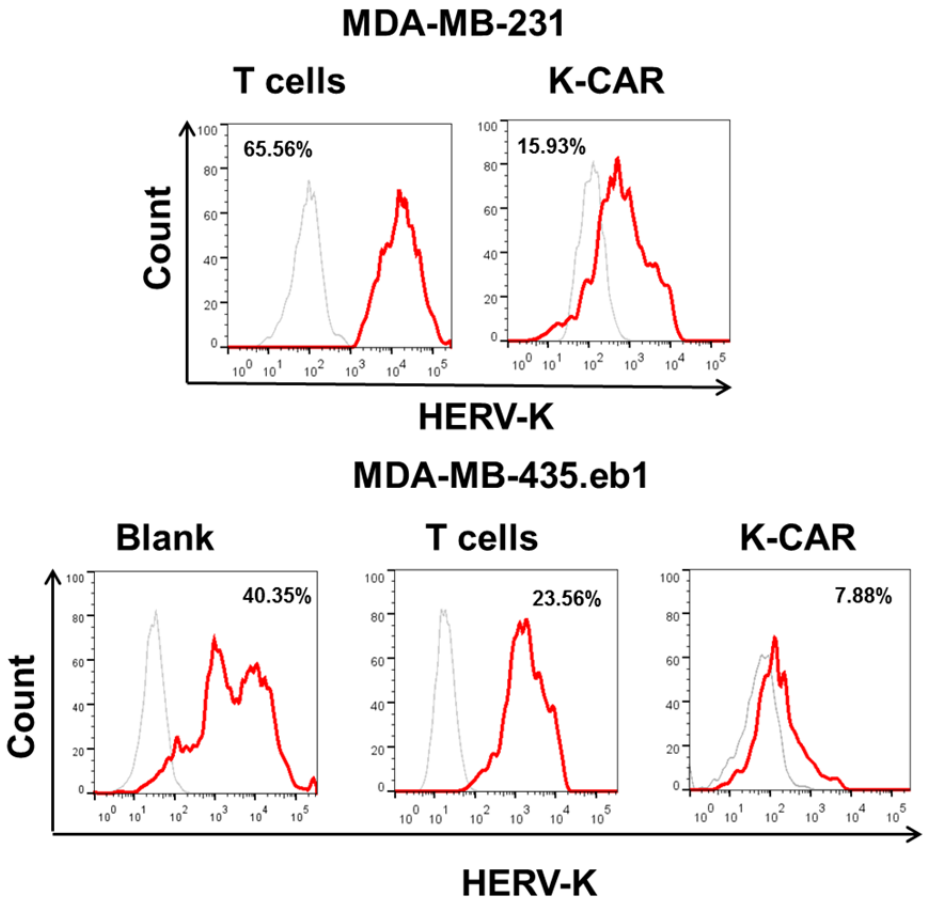

Fig. S5D

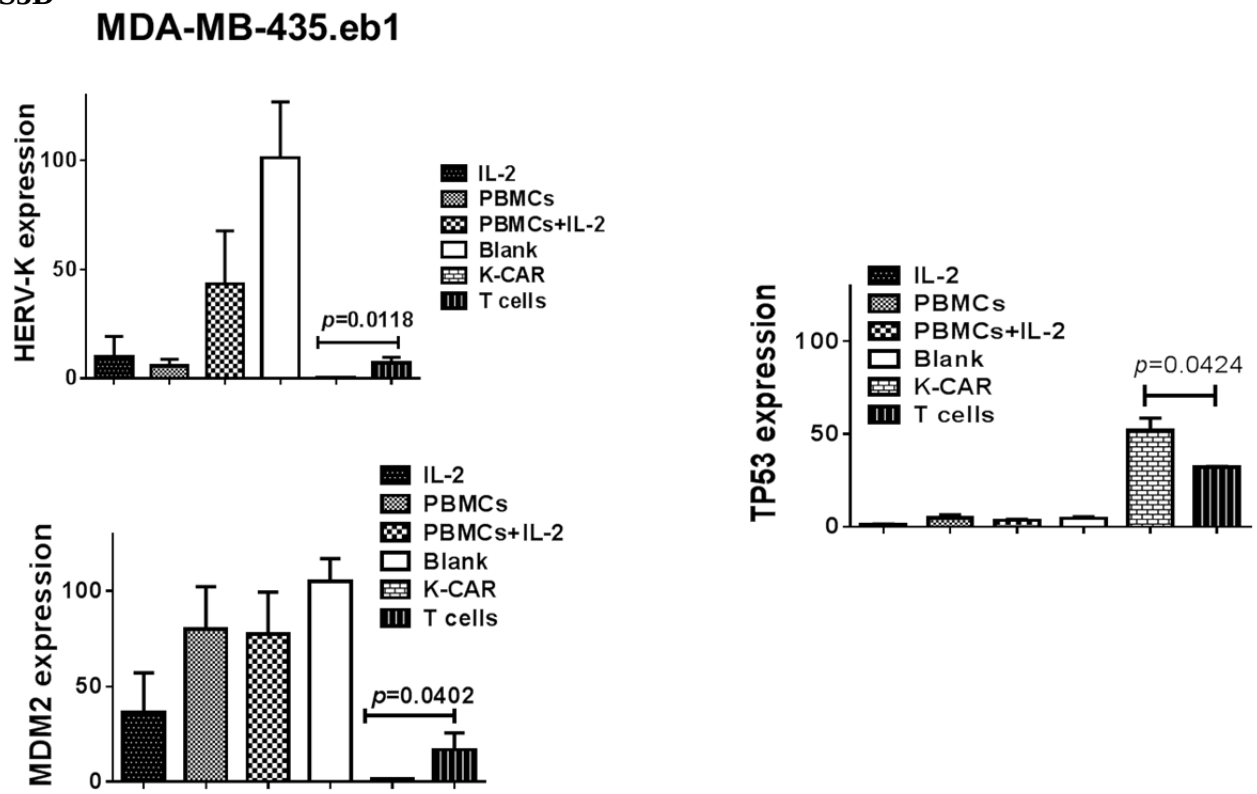

Fig. S5 Reprogramming of gene expression in tumor biopsies: FACS assay was used to determine the expression of HERV-K env protein in tumors obtained from mice treated with K-CAR or control T cells. Significantly decreased expression of HERV-K was demonstrated in MDA-MB-231 tumors (A) and MDA-MB-435.eB1 tumors (B) treated with K-CAR compared with T cell treatment or no treatment (blank). C) The expression of HERV-K env at the protein level was determined by FACS and reduced protein expression was observed in tumors treated with K-CAR compared with T cell treatment or no treatment (blank). D) Reprogramming of gene expression including upregulation of TP 53 and downregulation of MDM2 was associated with downregulation of HERV-K expression in tumor biopsies of mice treated with K-CAR, compared to all other treatments.

Fig. S6A

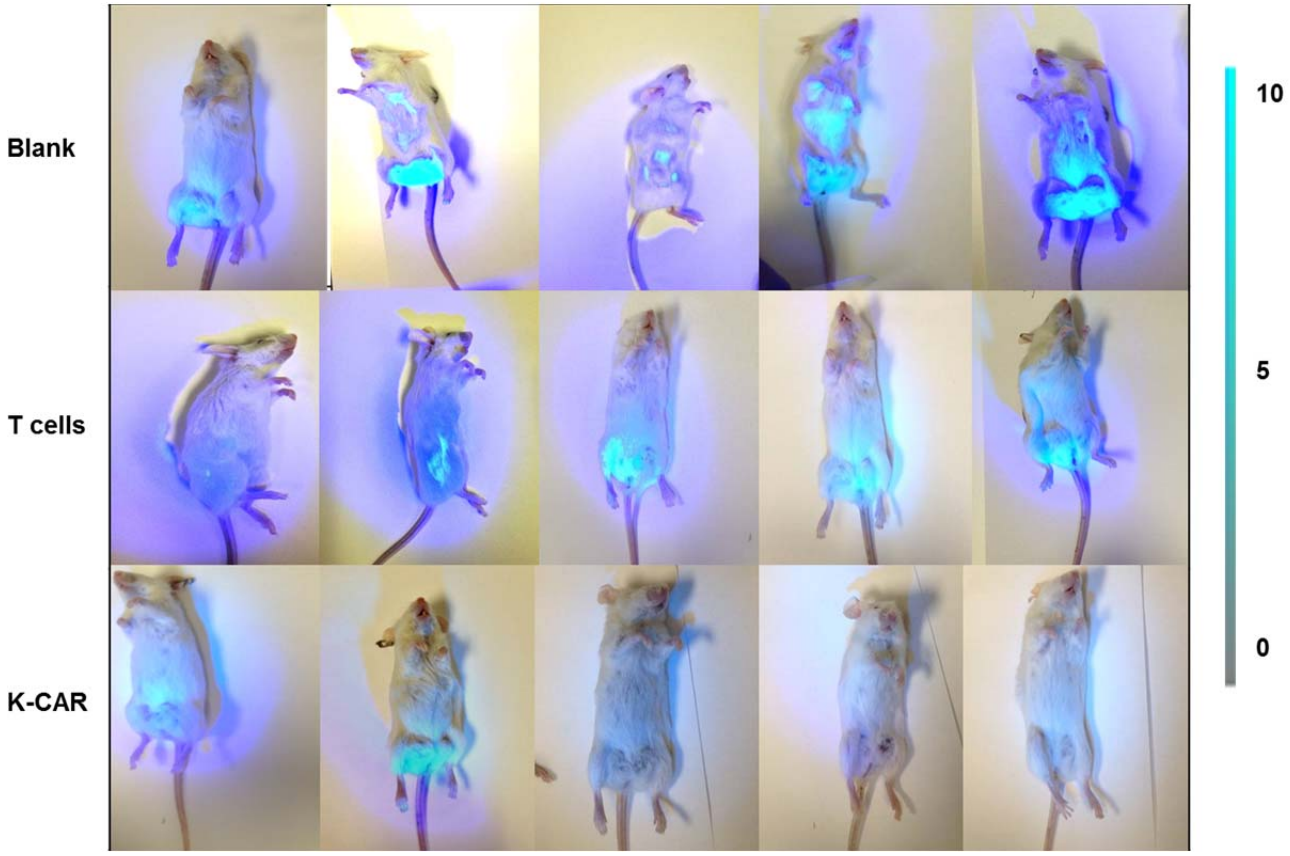

Fig. S6B

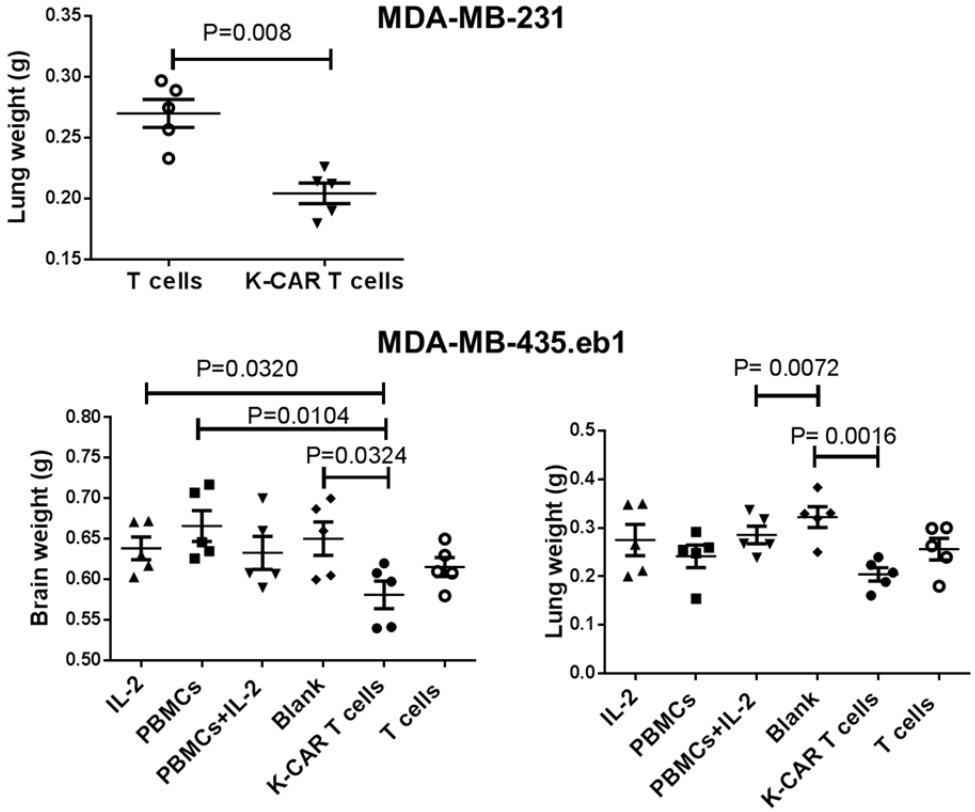

Fig. S6C

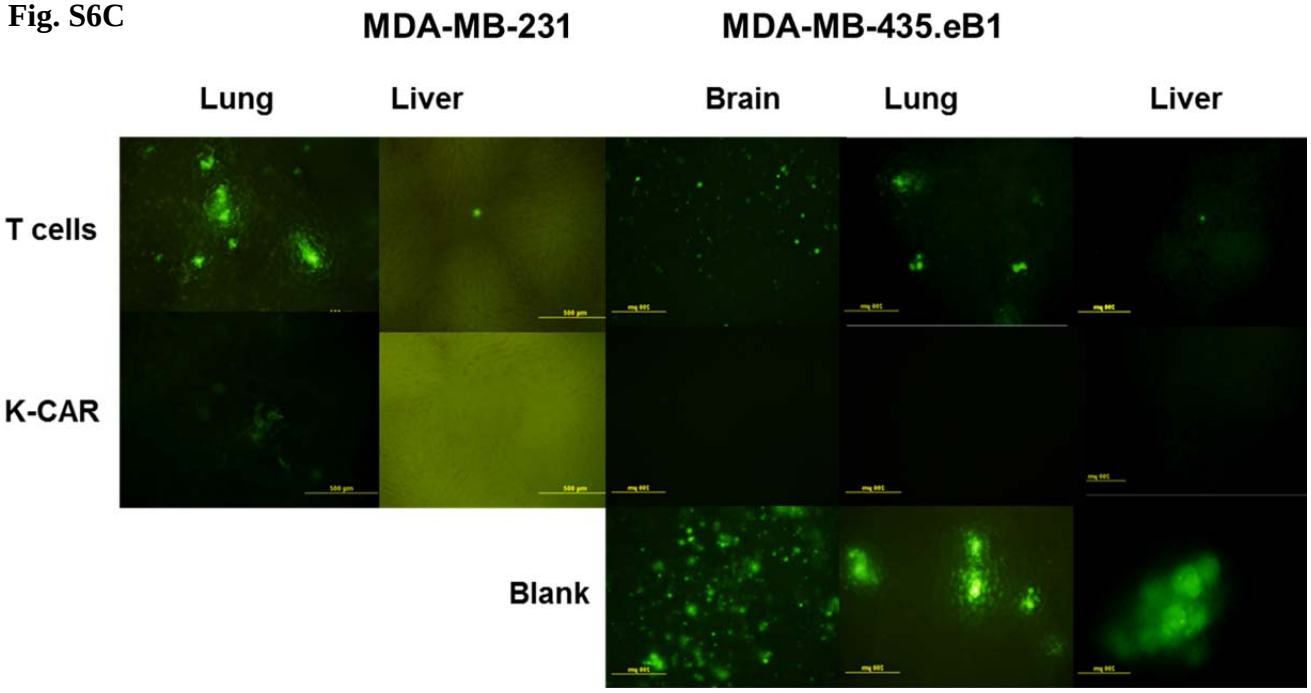
MDA-MB-231
MDA-MB-435.eB1
Lung
Liver
Brain
Lung
Liver
T cells
K-CAR
Blank

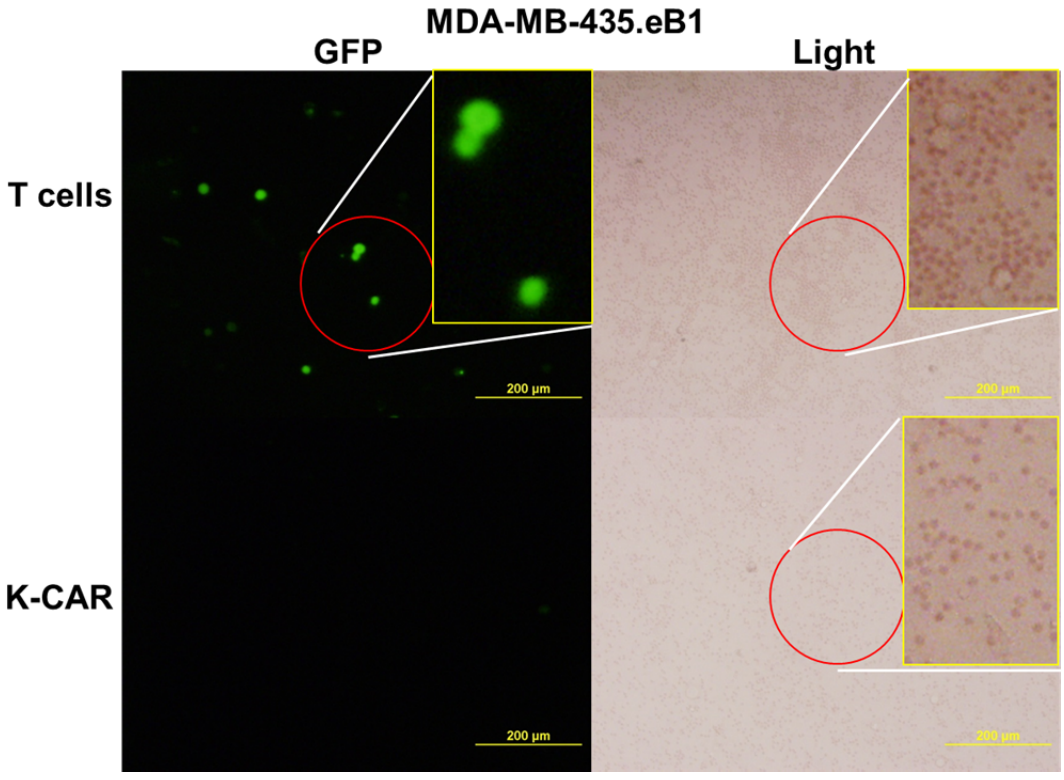
MDA-MB-435.eB1
GFP
Light
T cells
K-CAR
200 μm
200 μm
200 μm
200 μm

Fig. S6D

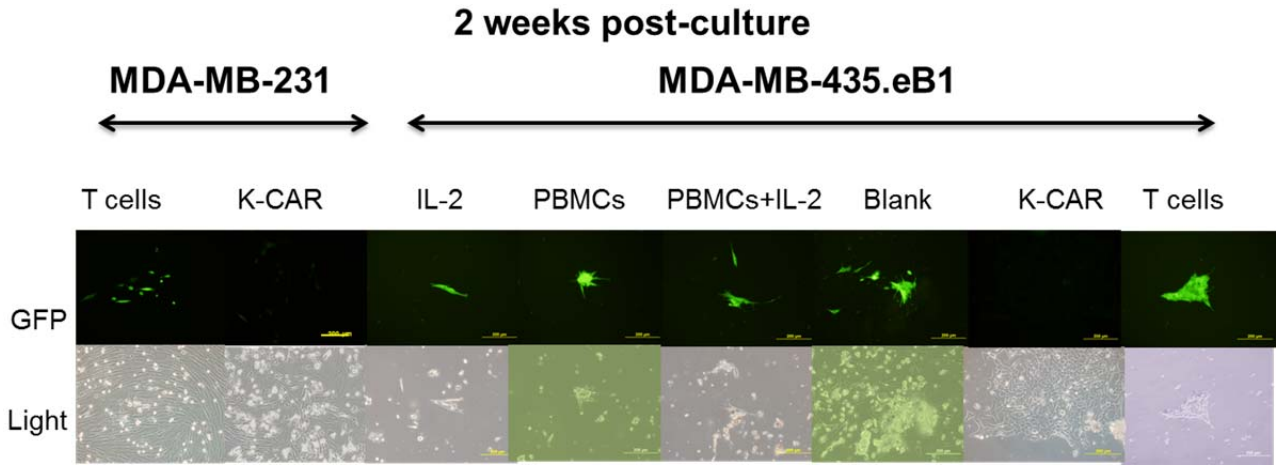

Fig. S6E

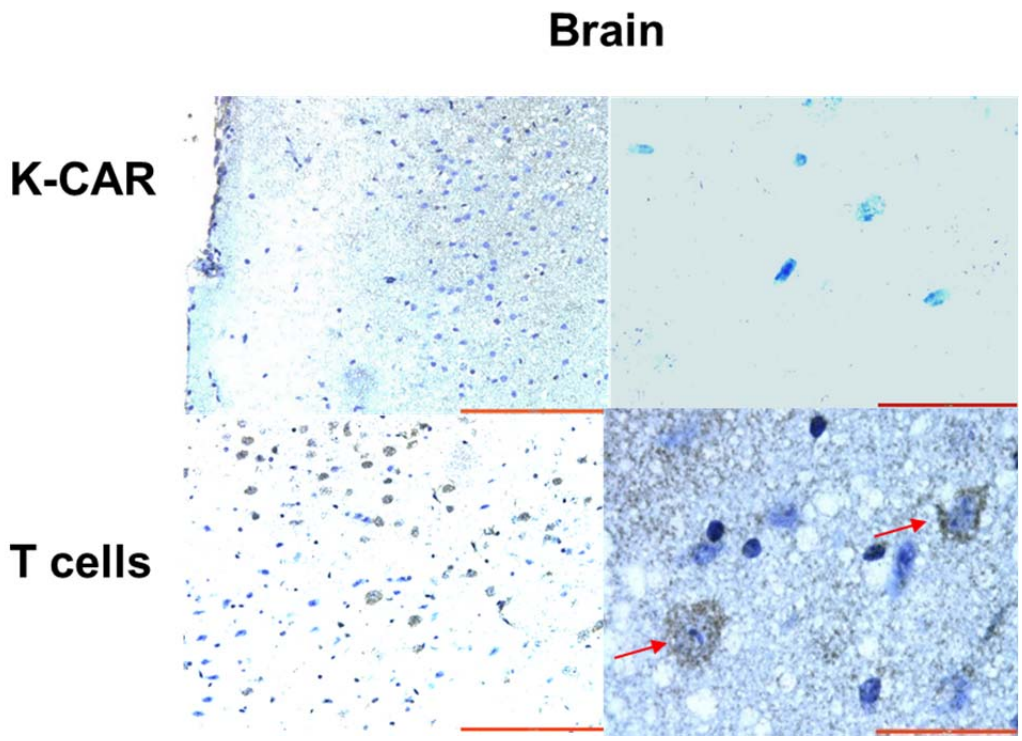

Fig. S6 Reduction of metastasis in mice treated with K-CAR: A) Green florescence was used to detect human cancer cell presence in mice treated with K-CAR or T cells, or untreated (blank). Greater fluorescence intensity indicates the presence of human cancer cells. B) Lung and brain tissue weights of mice treated with K-CAR or other treatments were compared. Significantly reduced lung weights were seen after K-CAR treatment of mice bearing MDA-MB-231 tumors, compared with T cell treatment. C) Green florescence was used to detect the human cancer cells in lung, liver and brain of mice treated with T cells, K-CAR, or untreated (blank) (top panel). Green florescent^{+} tissue pieces were observed in mice treated with T cells or untreated (blank), but not in K-CAR mice. Green florescent^{+} cells were also observed in pleural lavage fluid of mice treated with T cells, but not with K-CAR (bottom panel). D) Metastatic cancer cells were observed in cell cultures two weeks after cultures were initiated from minced green fluorescent^{+} tissue pieces. E) The expression of HERV-K was detected in brain tissues obtained from mice treated with T cells, but not K-CAR by IHC using 6H5 mAb.

Table 1 Demographic, medical, and independent variables measured at baseline of breast cancer

Acc.	Age/Race	Diagnosis	Stage	ER	PR	Her2	NG	Mastectomy	FAC	Neoadjuvant	Taxol	Radiation	Endocrinotherapy
108	55wf	mets IDC	IIIB	pos	pos	neg	3	Yes		Yes		Yes	Yes
157	59wf	DCIS	I	pos	pos	N/A	2	Yes					
229	54hf	IDC	I	neg	neg	neg	3	Yes	Yes		Yes		Yes
233	37hf	IDC	IIA	neg	neg	neg	3	Yes	Yes		Yes	Yes	
237	58af	DCIS	I	pos	pos	N/A	3	Yes					
243	56bf	DCIS	I	neg	neg	N/A	3	Yes					
257	69wf	ILC	IIA	pos	pos	pos	3	Yes					Yes
261	41wf	DCIS+IDC	IIA	pos	pos	neg	2	Yes	Yes		Yes	Yes	
267	57wf	ILC+IDC	IIA	pos	pos	neg	1	Yes	Yes		Yes		Yes
FAC=fluorouracil 500 mg/m^2, doxorubicin 50 mg/m^2, and cyclophosphamide 500 mg/m2													

IDC: Invasive ductal carcinoma
Mets IDC: Metastasis IDC
DCIS: Ductal carcinoma *in situ*
ILC: Invasive Lobular Carcinoma